

Ultracold Chemistry and its Reaction Kinetics

Der QUEST-Leibniz-Forschungsschule der
Gottfried Wilhelm Leibniz Universität Hannover
zur Erlangung des Grades
Doktor der Naturwissenschaften
Dr. rer. nat.

genehmigte Dissertation

von
Dipl.-Phys. Dipl.-Ing. Florian Richter
geboren am 02.05.1983 in Emden

Referent Prof. Dr. Tobias J. Osborne
Koreferentin Prof. Dr. Silke Ospelkaus
Tag der Promotion 19.08.2015

Abstract

Classically a chemical reaction occurs only when there are sufficient thermal fluctuations to overcome the Arrhenius activation energy. This makes chemistry close to the quantum ground state temperature seem paradoxical. However, nowadays there are many experimental techniques known to form ultracold molecules from ultracold atoms, e.g. via Feshbach resonance, which can be understood as a chemical process in an ultracold regime.

This thesis presents a framework for the description of the kinetics of ultracold chemical reactions and systematically investigates the occurring dynamical phenomena. We use the notion of order of reaction to classify two classes of ultracold bosonic reactions. The first class is given by linearly interacting quantum fields and allow for a compact analytical solution. Comparing these exact solutions to the corresponding dynamics of high-temperature kinetics shows the fundamental differences between classical and fully quantised reactions.

Chemical reactions belonging to the second class are modelled by non-linear interacting quantum field theories. Finding solutions for the dynamics of the non-linear systems turns out to be very hard, such that we have to rely on variational and perturbational techniques. Investigating the quantum dynamics of the most elementary example with non-linear interaction, the diatomic molecule formation, we find that quantum entanglement between the atomic and molecular modes plays a key role in driving the reaction towards a dynamical equilibrium. Moreover, we study the formation of solitons in the mean-field approximation of diatomic molecule formation. We find, by employing phase space methods, the emergent soliton pairs to be dynamically unstable. These results show the wide range of dynamical phenomena that occur for a single ultracold reaction.

As an extension to previous formulations of ultracold chemical reactions, our model allows us to consider concurrent reactions. We study the dynamics of a pair of reactions consisting of the diatomic molecule formation and a coupling of the atomic species to a particle reservoir. Choosing special values for the reaction constants, we find that chaos dominates the phase space dynamics in the mean-field approximation.

Key words: Ultracold quantum gases, Ultracold molecules, Entanglement

Kurzfassung

Bei Betrachtung der klassischen Sichtweise kann eine chemische Reaktion nur dann stattfinden, wenn genügend thermische Fluktuationen vorhanden sind, um die Arrhenius'sche Energiebarriere zu überwinden. Dieses Bild einer klassischen Reaktion lässt chemische Vorgänge in ultrakalten Umgebungen als etwas Paradoxes erscheinen. Heutzutage gibt es dennoch eine Vielzahl experimenteller Techniken um Moleküle aus ultrakalten Quantengasen zu erzeugen. Die dabei auftretenden Prozesse werden zusammenfassend als „ultrakalte Chemie“ bezeichnet.

Die vorliegende Arbeit stellt ein theoretisches Modell vor, das es ermöglicht, die Reaktionskinetik ultrakalter chemischer Reaktionen zu untersuchen. Hierfür wird der Begriff der Reaktionsordnung verwendet, um eine grundsätzliche Einteilung ultrakalter Reaktionen in zwei Klassen vorzunehmen. Die erste Klasse wird dabei durch linear wechselwirkende Quantenfeldtheorien beschrieben und kann analytisch gelöst werden. Die entstehenden analytischen Lösungen werden daraufhin mit den korrespondierenden Lösungen der klassischen Reaktionskinetik verglichen und, die durch den Vergleich herausgearbeiteten Unterschiede, dargestellt.

Die zweite Klasse ultrakalter chemischer Reaktionen wird hingegen durch nicht-linear wechselwirkende Quantenfeldtheorien beschrieben. Das Finden analytischer Ausdrücke für diese zweite Klasse ist nahezu unmöglich, so dass bei der Analyse dieser Systeme auf Näherungsverfahren zurückgegriffen werden muss. Das Hauptaugenmerk liegt auf der Betrachtung der Bildung eines zweiatomischen Moleküls, das das einfachste Beispiel einer nichtlinearen Reaktion darstellt. Bei der eingehenden Untersuchung dieser Reaktion wird festgestellt, dass das Phänomen der Verschränkung einen wesentlichen Einfluss auf die Dynamik hat. Darüber hinaus werden solitäre Lösungen der Molekularfeldnäherung der Reaktion betrachtet, wobei sich herausstellt, dass die gefundenen Lösungen dynamisch instabil sind.

Als eine Erweiterung der bisherigen theoretischen Modelle ultrakalter Reaktionen, ermöglicht das vorliegende Modell die Betrachtung mehrerer, gleichzeitig ablaufender, Reaktionen. Als lehrreiches Beispiel werden die Atome der Reaktion der Molekülbildung gleichzeitig an ein Reservoir gekoppelt. Für eine spezielle Wahl der Reaktionskonstanten wird gezeigt, dass die Phasenraumdynamik in der Molekularfeldnäherung des betrachteten Reaktionspaares chaotischer Dynamik folgt.

Schlagwörter: Ultrakalte Quantengase, Ultrakalte Moleküle, Verschränkung

Contents

1	Introduction	1
2	From classical kinetics to ultracold chemistry	3
2.1	Classical reaction kinetics	4
2.1.1	Rate equations	4
2.1.2	Reaction networks	8
2.1.3	Brusselator	9
2.2	Cold and ultracold chemistry	10
2.2.1	Classical reaction models	11
2.2.2	Quantum reactive scattering	16
2.2.3	Ultracold chemistry	20
3	Ultracold reaction kinetics	22
3.1	First quantisation	23
3.1.1	Dynamical embedding	24
3.1.2	Case-study	26
3.2	Second quantisation	31
3.3	Proposed framework	37
4	Elementary bosonic reactions	43
4.1	Conservation law	44
4.2	Low-order reactions	50
4.2.1	First-order reaction	51
4.2.2	Second-order reactions	55
5	Diatomic molecule formation	67
5.1	Mean-field approximation	68
5.1.1	Coherent states	68
5.1.2	Time-dependent variational principle	70
5.2	Two-mode model	73
5.2.1	Mean-field dynamics	75

5.2.2 Quantum phenomena	76
5.3 Molecule formation coupled to a bath	80
5.3.1 Perturbation theory	81
5.3.2 Chaos	84
6 Solitons in ultracold chemistry	89
6.1 Gross-Pitaevskii equation	89
6.1.1 Derivation as mean-field approximation	90
6.1.2 Bright and dark solitons	93
6.2 Solitons in diatomic molecule formation	98
7 Conclusion and outlook	103
Bibliography	105
Publications	112
Curriculum Vitae	113

CHAPTER 1

Introduction

A chemical reaction normally occurs at a few hundred kelvin between reagents involving large numbers of particles ($\sim 10^{23}$). This is because reactions are usually activated by *thermal fluctuations* which are only significant for large concentrations of particles with high momenta. The influence of the temperature on the emergent kinetics is often successfully described by Arrhenius' law [Arr89], which predicts the rate of a chemical reaction to exponentially decrease at smaller temperatures. Therefore, the possibility of a chemical reaction taking place in the dilute and ultracold ($T < 1 \mu\text{K}$) regime is somewhat counterintuitive.

However, this picture of a necessary activation energy breaks down, when the considered chemical reaction is *barrierless*, that is, the reaction takes place even if the relative translational energy between the reactants is small or equals zero. As soon as experimental cooling techniques were efficient enough to create a Bose-Einstein condensate (BEC) [Dav95], researchers began to investigate the creation of ultracold molecules by barrierless or low-barrier reactions from this new state of matter. The formation of ultracold molecules from atoms in a Bose-Einstein condensate was observed in [Wyn00]. This interaction of atoms and molecules close to the absolute zero of temperature has been referred to as *ultracold chemistry* [Hut10].

Nowadays, a variety of experimental techniques such as the coupling of atoms and molecules via magnetic Feshbach resonance [Don02; Reg03] have been successfully employed to achieve chemical bonding in an ultracold environment. For example, ultracold Potassium-Rubidium molecules [Osp10] have been investigated to analyse the quantum mechanical effects of particle statistics on molecular reactivity. The now ready experimental accessibility of chemical processes in the dilute ultracold regime strongly motivates us to develop a general physical understanding of their *reaction kinetics*.

A quantized description is required in order to study the dynamics of ultracold reactions, in order to fully account for the effects of quantum fluctuations and entanglement. Here we should replace the classical notion of a temperature-dependent

reaction with a coherent reversible Hamiltonian evolution. The first phenomenological steps toward such a description were taken in [Hei00], where a mean field ansatz was exploited to describe the coherent formation of diatomic molecules in a BEC. Since then a variety of extensions to this model, mainly focussed on adding quantum corrections to the original mean field ansatz, have been studied [Gór01; San06]. So far, a general and systematic investigation of the dynamics of ultracold reactions, analogous to the study of reaction kinetics for classical thermal reactions, has not yet been undertaken. Such an approach seems to be indispensable if one wants to study the role of quantum coherence and the production of quantum entanglement in ultracold chemical systems.

This thesis is organised as follows. In chapter 2 we introduce basic terminology and fundamental aspects of high-temperature kinetics. The terminology will help to understand our proposed framework of ultracold chemistry. Also included in this chapter is a short review of semi-classical descriptions for ultracold reactions. As a central aspect of the present thesis, chapter 3 contains the framework we subsequently use to formulate the reaction kinetics of ultracold chemistry. As motivation for formulating our proposal in the language of second quantisation, we also investigate the first quantisation of classical kinetics. Chapter 4 contains a systematic classification of the ensuing dynamics of elementary examples of ultracold reactions. We obtain the dynamical evolution in compact analytical form and compare it to the dynamics of the corresponding high-temperature reactions. Also included in this chapter is the identification of the overall number of quantum particles as conserved quantity. It turns out that this quantity can be thought of as quantum analogue of the classical principle of the conservation of mass. Chapter 5 is based on the work published in [Ric15], which was completed in collaboration with Daniel Becker, Cédric Bény, Torben Schulze, Silke Ospelkaus and Tobias Osborne. In this chapter we study the reaction kinetics of ultracold molecule formation, as an important instance of a non-linear interacting reaction within our theory. We find that, within the two-mode approximation, entanglement between the atomic and molecular mode plays an important role to the dynamics. Extending the molecule formation by a coupling of the participating atoms to a reservoir, we find that Hamiltonian chaos dominates the phase space dynamics of the mean-field approximation. Chapter 6 considers the existence and stability of solitary solutions in ultracold chemical reactions. We find a pair of bright solitons in diatomic molecule formation, which is unstable against small perturbations.

CHAPTER 2

From classical kinetics to ultracold chemistry

The study of chemical reaction kinetics dates back to the end of 18th century. At this time the experimental techniques in chemistry were so far developed, that scientists finally were able to investigate how the speed of a chemical reaction depends on the details of the experimental setting. The first important result in this field was obtained in 1864 with the formulation of the *law of mass action* [Gul64]. This law recognises that the chemical equilibrium of a reversible reaction is indeed a dynamical equilibrium in which the rate of the forward and reverse reaction balance each other. A subsequent result was given by Svantje Arrhenius in 1889. His famous equation identifies the temperature as decisive environmental factor of the rate constant [Arr89]; only when the temperature is beyond a certain threshold the reaction will occur.

In its modern form, the framework of chemical kinetics maps a chemical reaction, that is a stoichiometric reaction scheme and corresponding reaction constants, to a first-order differential system for the species' concentration. Depending on the complexity of the reaction it predicts numerous dynamical phenomena. Chemical kinetics is an *effective* theory. The reaction constants as dynamical parameters arise as quantities averaged over many different microscopic scenarios. The model of reaction kinetics is justified by its correct prediction of various amazing phenomena like pattern formation, chaotic oscillations, etc.

This chapter is organised as follows. We first introduce in section 2.1 the cornerstones of the theory of classical reaction kinetics. The clarity and effectiveness of this theory makes it an inspiring example for our later proposal of ultracold reaction kinetics. In section 2.2 we consider the microscopic foundations of classical reaction kinetics and how they are modified with decreasing temperature. This results in a first definition of ultracold chemistry. The material covered in 2.1 is well-known in the field of reaction kinetics and can be found in many textbooks and lecture notes. In particular we follow [Bro10; Con90].

2.1 Classical reaction kinetics

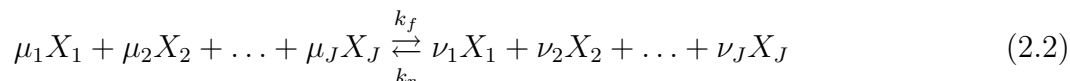
The subject of reaction kinetics covers a specific but important aspect of chemical reactions. While the study of chemical structures and chemical equilibrium considers stationary states, chemical kinetics focuses on the temporal evolution of the system. At a first glance kinetics seems to be very complicated, as it considers physical systems in which familiar concepts from thermodynamics like the minimisation of the Gibbs free energy fail. However, when a small number of physical requirements are satisfied, we are able to formulate an effective theory which predicts the dynamics of a certain class of chemical reactions with surprising accuracy.

2.1.1 Rate equations

In what follows, we will give a short introduction to the theory of reaction kinetics of classical chemical reactions. We focus on the notions and terminology which we refer to when proposing our scheme for ultracold reactions. For a thorough introduction to the topic we refer the reader to [Con90]. We start considering a volume V which contains a set of chemical species X_j with $j \in \{1, \dots, J\}$. Particles are not allowed to leave or enter the volume. We denote the number of particles of each species as N_{X_j} . This allows us to define the concentration

$$[X_j] := N_{X_j}/V. \quad (2.1)$$

A chemical reaction is some transformation between the species according to the scheme



The numbers μ_i and ν_j are referred to as *stoichiometric coefficients* with μ_i, ν_i as integers. In order to avoid ambiguity, we remove a possible factor of the coefficients in the chemical equation or consider the stoichiometric coefficients as the actual number of particles of a certain species required for a reactive collision to take place. The macroscopic quantities k_f and k_r are called *rate constants* of the forward or reverse reaction respectively. The species on the left-hand side of (2.2) side are called *reactants* whereas the right-hand side lists the *products*. In case of a reversible reaction we find both constants to be non-zero, whereas an irreversible reaction amounts to $k_r = 0$.

We start to derive the dynamics of (2.2) by first considering its equilibrium. It is a standard exercise in thermodynamics to derive the *law of mass action* [Sch06]

$$K = K(T, P) = \frac{[X_1]^{\mu_1} [X_2]^{\mu_2} \dots [X_N]^{\mu_N}}{[X_1]^{\nu_1} [X_2]^{\nu_2} \dots [X_N]^{\nu_N}}. \quad (2.3)$$

It relates the concentration of the species and the stoichiometric coefficients with an equilibrium constant K being a temperature T and pressure P dependent function¹. The crucial step to relate this static constant to dynamical quantities is now to assume that at the equilibrium state the forward and reverse reaction rates exactly balance each other

$$K(T,P) = \frac{k_r(T,P)}{k_f(T,P)}.$$

While the pressure dependence of the reaction constants is in general complicated to determine and depends on the particular reaction considered, the temperature dependence is often well described by Arrhenius' law

$$k(T) = A \exp\left(\frac{-E_A}{\kappa T}\right), \quad (2.4)$$

where A is referred to as pre-exponential factor. This empirical equation manifests a typical threshold law: If the weighted temperature κT (where κ denotes Boltzmann's constant) is smaller than the *activation energy* E_A , there are only few particles which possess enough energy to overcome the reaction barrier. However, if $\kappa T > E_A$, there is an exponential increase of the rate constant. However, for some chemical reactions we find that the rate of reaction decreases with increasing temperature. Some of these reactions still follow an exponential law, such that it is possible to fit a negative activation energy $E_A < 0$.

With these preliminaries it is now possible to infer the rate constants from equilibrium and assume their validity as reaction rates even outside equilibrium. The description non-equilibrium reactions requires the following properties [Kam92]:

- Homogeneity of the considered mixture of species
- The underlying velocity distribution (Maxwell) of a certain species is valid outside equilibrium
- The internal degrees of freedom of the molecules can be neglected during the reaction
- Temperature and pressure remain constant while the reaction takes place.

If these restrictions are fulfilled and if the reaction is *elementary*, that is there are no catalytic, intermediate, or concurrent reactions, the theory of classical reaction

¹ It is, in principle, possible to transform the inner variables to any other thermodynamic state variable, for instance the chemical potential μ . The preference for P and T stems from the fact that these quantities usually remain unchanged during a chemical reaction.

kinetics yields the *rate equations*

$$\frac{d[X_j]}{dt} = k_f(\nu_j - \mu_j) \prod_{k=1}^J [X_k]^{\mu_k} + k_r(\mu_j - \nu_j) \prod_{l=1}^J [X_l]^{\nu_l} \text{ with } j \in \{1, \dots, J\}. \quad (2.5)$$

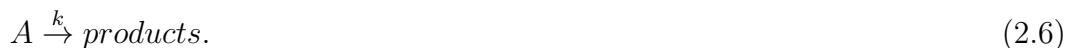
This means that the kinetics of chemical reactions are mathematically described by a—possibly nonlinear—system of first-order ordinary differential equations (ODE). It describes the time evolution of the concentrations outside equilibrium. This system is particularly easy to solve for elementary reactions as each rate equation in (2.5) is a multiple of the other:

$$\frac{1}{\mu_1 - \nu_1} \frac{d[X_1]}{dt} = \frac{1}{\mu_2 - \nu_2} \frac{d[X_2]}{dt} = \dots = \frac{1}{\mu_J - \nu_J} \frac{d[X_J]}{dt}$$

To confirm consistency of this framework, we find that the fixed point of (2.5), that is $\forall j : \frac{d[X_j]}{dt} = 0$, reproduces the law of mass action,

$$\frac{k_r}{k_f} = \frac{[X_1]^{\mu_1} [X_2]^{\mu_2} \dots [X_N]^{\mu_N}}{[X_1]^{\nu_1} [X_2]^{\nu_2} \dots [X_N]^{\nu_N}}.$$

To get a better intuition why the powers of the stoichiometric constants appear on the right-hand side in (2.5), we shortly sketch another way to derive the equations of motion. We do this exemplary for the concrete irreversible reaction



We consider the chemical reaction as Markov process, that is the combination of reactants (in this case only one) as a process without memory. The reaction constant k determines the probability of a *single* reactant to react. This means if (2.6) has initially one atom of species A , the probability of a reaction event in the time interval $[t, t + \Delta t]$ is $k\Delta t$, leading to an probability of reaction at time t given by

$$p(t) = ke^{kt}. \quad (2.7)$$

Now, suppose you consider n_A particles of species A as initial condition. How does this affect the probability of a reaction event? Since every of the n_A particles reacts independently of the other particles with reaction constant k , the overall probability of a reaction in the time interval $[t, t + \Delta t]$ is simply given by $n_A k \Delta t$.

In a next step, we connect this reaction probability with the time evolution of the concentration of particles. Every time a reaction occurs, the particle number is decreased by one and a small change in the particle concentration occurs. Therefore, we can write the following discrete time evolution for the probability distribution of

the particle concentration

$$P([A], t + \Delta t) = n_A k P([A] + \Delta[A], t) + (1 - n_A k) P([A], t). \quad (2.8)$$

Expanding this into a Taylor series yields

$$\begin{aligned} \frac{\partial P([A], t)}{\partial t} &= \frac{\Delta[A]}{\Delta t} n_A k \frac{\partial P([A], t)}{\partial [A]} \\ &= [A] k \frac{\partial P([A], t)}{\partial [A]}, \end{aligned} \quad (2.9)$$

where we choose the continuum limit $\Delta t \rightarrow 0$ and $\Delta[A] \rightarrow 0$ such that $\frac{\Delta[A]}{\Delta t} = \frac{1}{V}$. Identification of the deterministic particle concentration as expectation value of $P([A], t)$ yields the same equations of motion as classical reaction kinetics. The key point is that the probability of the reaction event divided by the volume occurs in the equations of motion. Suppose you consider the reaction



Then the probability of a reaction event in the time interval $[t, t + \Delta t]$ is $n_A n_B k \Delta t$, since the number of distinct reaction possibilities is $n_A n_B$. By extending this argumentation to more complex reactions, we obtain the same equations for the concentrations as provided by the law of mass action (2.5).

An important tool in reaction kinetics to classify the complexity of the occurring dynamics is the *reaction order*. Considering the rate equation of an elementary irreversible reaction ($k_r = 0$)

$$\frac{d[X_j]}{dt} = k_f (\nu_j - \mu_j) \prod_{k=1}^J [X_k]^{\mu_k}, \quad (2.11)$$

the the power μ_k is called the *order of reaction* with respect to species X_k . More important for our considerations is the *overall order* of this reaction, which is defined by

$$O_{cl} := \sum_k \mu_k. \quad (2.12)$$

Reactions with $O_{cl} \geq 2$ result in non-linear differential equations, which is a crucial prerequisite for many complex phenomena. However, in the realm of classical kinetics there are many non-elementary reactions whose rate equations are of different form

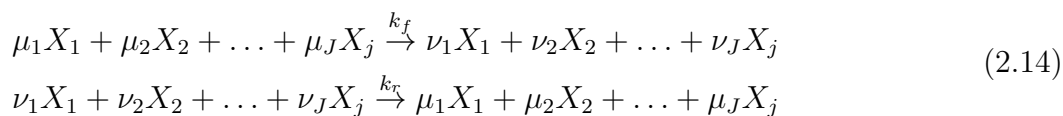
than (2.11). For instance, concentrations may appear in the denominator:

$$\frac{d[A]}{dt} = -k \frac{[A]^2}{[B]} \quad (2.13)$$

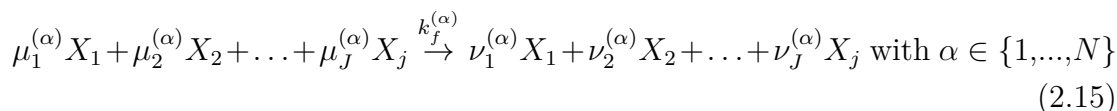
We can generalize the concept of reaction order to these kind of rate constants by allowing negative or even fractional values. However, the concept of overall order does not apply these kind of reactions, since the dynamics of (2.13) are more complicated than an elementary first order reaction. Throughout this thesis we will only consider elementary classical reactions. Therefore, if we use the term order of reaction we mean the overall order.

2.1.2 Reaction networks

So far, the presented framework provides the dynamic equations governing elementary reactions. Although describing elementary reactions is far from trivial, the more interesting dynamical effects occur in *reaction networks*, that is reactions where at least one reactant undergoes two or more concurrent chemical transformations¹. In order to define the kinematics for reaction networks, we note that any reversible reaction can be unfolded as a network of two concurrent irreversible reactions, e.g. (2.2) can be written as:



We therefore restrict our considerations to reaction networks of N irreversible reactions:



We introduce $v_i^{(\alpha)} := \nu_i^{(\alpha)} - \mu_i^{(\alpha)}$ as the difference of stoichiometric coefficients for the α -th reaction. The dynamical evolution of species $[X_j]$ is then a superposition of each reaction:

$$\frac{d[X_j]}{dt} = \sum_{\alpha=1}^N k^{(\alpha)} v_j^{(\alpha)} \prod_{i=1}^J [X_i]^{\mu_i^{(\alpha)}}. \quad (2.16)$$

¹ The standard chemical literature distinguishes more types of chemical reactions, e.g. consecutive or competitive reactions. For our purpose this distinction is not important as they can be considered as special cases of reaction networks.

All the assumptions we made on elementary reactions carry over to each of the reaction inside a reaction network. In addition it is assumed that each reaction only takes place when the reactants concentration are non-zero. It is clear that with growing complexity of the considered reaction networks the phenomenological description of classical reaction kinetics becomes inaccurate. This model of classical chemical reaction kinetics has been validated by its long term success in describing a wide range of astonishing phenomena from the oscillating Belousov-Zhabotinskii reaction [Bel59; Zha64] to deterministic chaos [Eps96].

2.1.3 Brusselator

As an instructive example of complex dynamics consider the Brusselator [Pri68]:



This one example of the class of Belousov-Zhabotinskii reactions, which is known to show chemical oscillations. A simplification of the model assumes the concentrations of species A, B, C and D to be constant during the reaction. For a closed system this is approximately true if the concentration of the respective species is much larger than the others. Applying scheme (2.16) yields the equations of motion:

$$\begin{aligned}
 \frac{d[X]}{dt} &= k_1[A] - k_2[B][X] + k_3[X]^2[Y] - k_4[X] \\
 \frac{d[Y]}{dt} &= k_2[B][X] - k_3[X]^2[Y].
 \end{aligned} \tag{2.18}$$

In order to reduce degrees of freedom, we introduce the following non-dimensional quantities:

$$\tau = k_4 t, \quad X = \frac{k_4}{k_1[A]} [X], \quad Y = \frac{k_4}{k_1[A]} [Y], \tag{2.19}$$

with free parameters

$$b = \frac{k_2}{k_4} [B], \quad a = \frac{k_3 k_1^2}{k_4^2} [A]^2. \tag{2.20}$$

This transforms (2.18) into

$$\begin{aligned}\frac{dX}{d\tau} &= 1 - (b+1)X + aX^2Y \\ \frac{dY}{d\tau} &= bX - aX^2Y.\end{aligned}\tag{2.21}$$

This system has been subject to thorough dynamical studies (see for example [Eps96]). The most interesting phenomenon is a Hopf bifurcation, that is the onset of a limit cycle in phase space when the fixed point $(1, \frac{b}{a})$ changes its stability. In figure (2.1), the shape of the limit cycle for different values of b .

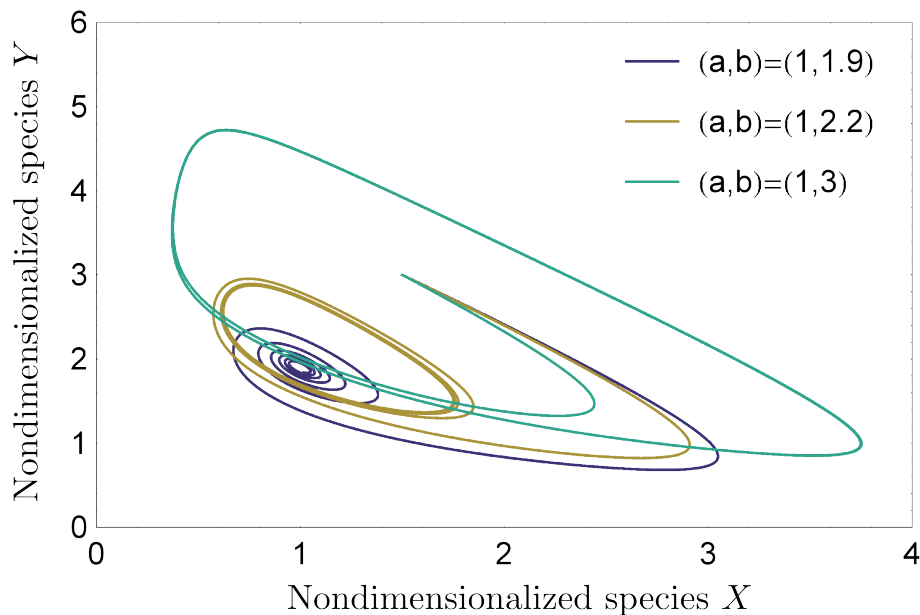


Figure 2.1: Phase space plot of the intermediate Brusselator species X and Y . A limit cycle occurs for $b > a + 1$. Starting from the initial nondimensionalized concentrations $(X_0, Y_0) = (1.5, 2)$, the trajectories either converge to the fix point $(1, \frac{b}{a})$ or drive towards the limit cycle.

We close this introductory example by mentioning that reaction kinetics of chemical networks is still an active field. The question of the existence of an equilibrium of reaction networks was only recently investigated in [Bae15].

2.2 Cold and ultracold chemistry

In the previous chapter we introduced an effective model for chemical reactions taking place in an environment that provides a large amount of thermal energy as well as

high densities of particles. However, in this thesis we want to present a framework for reaction kinetics under inherently different conditions. For example, the temperature of a Bose-Einstein condensate (BEC) is very close to absolute zero such that the application of Arrhenius' law would imply that no chemical reaction occurs at all. However, there is a wide range of environments between room temperature and a few nanokelvin in which chemical reactions occur, e.g. the lower parts of the stratosphere or interstellar clouds. For reactions in these environments, there are theoretical approaches to determine the rate and therefore the kinematics.

In order to get a better conceptual understanding of our proposed framework, we shortly review these theories. We start our review with a microscopical model of high-temperature reactions and subsequently decrease the temperature until quantum effects come into play. Eventually, we consider full quantum field descriptions for degenerate quantum gases on which our later proposal is based.

2.2.1 Classical reaction models

The previously introduced framework considers the temperature empirically via Arrhenius' law (2.4). In this section we introduce a microscopic account of chemical reactions referred to as a *capture model*. Loosely speaking, it assumes that all particles that can energetically overcome a certain barrier contribute to the chemical reaction.

The average speed of particles in a gas with roughly room temperature is about 500 m/s with a number of approximately 2.7×10^{19} particles per cm^3 . Therefore, the starting point of a microscopic theory of chemical kinetics is to investigate the scattering events between the species. For elastic collisions between two particles one considers the *cross section* σ , which can be inferred from the two-body interaction potential, to describe the likelihood for a scattering event. For collisions between two particles which may or may not chemically react, one extends this model to the *reactive cross-section* σ_R measuring the likelihood for a chemical reaction to take place. This quantity is in close relationship with the rate constant of a chemical reaction. By considering two particles that collide with fixed relative velocity v , the reaction rate is related to the reactive cross section via

$$k(v) = v\sigma_R(v). \quad (2.22)$$

In order to infer Arrhenius' law from the collision events, we need to average (2.22) over some thermal distribution of velocities $f(v,T)$:

$$k(T) = \int_0^\infty f(v,T)k(v)dv = \int_0^\infty f(v,T)v\sigma_R(v)dv. \quad (2.23)$$

What kind of distribution we choose for $f(v,T)$ depends sensitively on the physical context. Although there are counterexamples, for instance for photochemical reac-

tions, the relative velocity distribution in classical reaction kinetics will be essentially Maxwellian. Transforming to the center-of-mass frame we can express the velocity coordinate as a function of the collision energy:

$$E_T = \frac{\mu}{2}v^2, \quad (2.24)$$

where μ denotes the reduced mass. In case of Maxwell-Boltzmann distributed particles (2.23) takes the form

$$k(T) = \left(\frac{1}{\pi\mu}\right)^{\frac{1}{2}} \left(\frac{2}{\kappa T}\right)^{\frac{3}{2}} \int_0^\infty \exp\left[\frac{-E_T}{\kappa T}\right] E_T \sigma_R(E_T) dE_T. \quad (2.25)$$

The key is now to infer $\sigma_R(E_T)$ from the physical model of the scattering event. To introduce the standard terminology of scattering, in figure (2.2) we sketched a two-body collisional event. Using the center-of-mass frame, the impact parameter b labels the distance of the colliding particles perpendicular to their relative velocity v . We introduce the *opacity function* $P(b,v)$ as the probability that the collision with parameters b and v leads to reactive scattering. Using this terminology we are able to formulate an infinitesimal reactive cross-section $d\sigma_R$, that is, cross-sections where the impact parameter varies in the infinitesimal interval $[b, b + db]$

$$d\sigma_R = 2\pi b P(b,v) db. \quad (2.26)$$

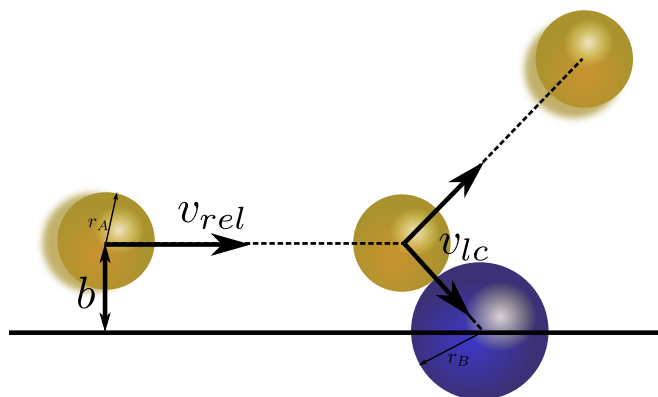


Figure 2.2: Depiction of line-of-centers model for impact parameter $b > b_{max}$ at fixed relative velocity v_{rel} . The reaction partners are modeled as hard spheres with radius r_A and r_B . The energy corresponding to the velocity in direction of the line of centers v_{lc} needs to be larger than E_0 for chemical reaction to take place. Otherwise, the particles merely scatter elastically. For the sake of simplicity, the sketch assumes that $m_B \gg m_A$ such that the center of mass is approximately in the middle of the blue particle.

A simple expression for the opacity function of a chemical reaction with energy threshold can be inferred from the line-of-centers model [Kup68]. The reaction partners are assumed to be hard spheres which form a molecule only if the collisional velocity v_{lc} along the line of centers is sufficient to overcome a certain threshold energy E_A . Therefore, this model provides a maximal impact parameter b_{max} for which the reaction occurs. The opacity function is thus of the form $P(b,v) = \Theta(b_{max}(v) - b)$ and the reactive cross section yields

$$\sigma_R(v) = 2\pi \int_0^\infty P(b,v) b db = \pi b_{max}^2(v). \quad (2.27)$$

Denoting the radii of the collisional particles as r_A and r_B , we readily obtain $b_{max}(v)$ from considering the collision velocity along the line of centers

$$v_{lc} = v \sqrt{1 - \frac{b^2}{(r_A + r_B)^2}}. \quad (2.28)$$

According to the model this quantity needs to be larger than the threshold $v_0 = \sqrt{\frac{2E_0}{\mu}}$ in order to amount to a reactive collision. This threshold translates to a maximal impact parameter as follows

$$b_{max}(v) = (r_A + r_B) \sqrt{\left(1 - \left(\frac{v_0}{v}\right)^2\right)}. \quad (2.29)$$

We may rewrite this in terms of the energy E_T and find the final expression for the reactive cross section:

$$\sigma_R(E_T) = \begin{cases} 0 & \text{if } E_T < 0 \\ \pi(r_A + r_B)^2 \left(1 - \frac{E_0}{E_T}\right) & \text{if } E_T \geq E_0 \end{cases} \quad (2.30)$$

Substituting this into (2.25) yields the reaction rate

$$k(T) = 2(r_A + r_B)^2 \sqrt{\frac{2\pi\kappa T}{\mu}} \exp\left[\frac{-E_0}{\kappa T}\right]. \quad (2.31)$$

This equation resembles Arrhenius' law (2.4) where we identify the macroscopical activation energy E_A with the microscopical threshold energy E_0 . Nevertheless, a difference between the models is that the pre-exponential factor A is now a function of the temperature. However, in actual chemical reactions this dependence is hard to measure as the growth of the exponential term is dominant for small temperature differences.

Evidently, Arrhenius' law fails to describe reactions at low temperatures as it predicts the reaction rate dropping quickly to zero when $\kappa T \ll E_0$. However, there is a class of *barrierless* reactions for which the rate can even increase at lower temperatures (e.g. ion-molecule reactions). The rate of these reactions is not dominated by the effect of the energy threshold $E_0 \approx 0$, but by the long-range shape of the interaction potential $V_{\text{int}}(R)$ between the particles. In order to derive a proper model for the rate constant of these reactions, we revise the motion of two colliding particles in terms of the participating energies:

$$E_{\text{tot}} = E_{\text{kin}} + E_{\text{pot}} = \frac{1}{2}\mu\dot{R} + \frac{l^2}{2\mu R^2} + V_{\text{int}}(R), \quad (2.32)$$

where R is the radial coordinate and l denotes the preserved angular momentum. Connecting this to the initial energy $E_T = \frac{1}{2}\mu v^2$ and impact parameter b yields

$$E_{\text{tot}} = \frac{1}{2}\mu\dot{R} + \underbrace{\frac{E_T b^2}{R^2} + V_{\text{int}}(R)}_{V_{\text{eff}}(R)}, \quad (2.33)$$

where we introduced the effective potential V_{eff} as the sum of the conserved part resulting from angular momentum $V_l = \frac{E_T b^2}{R^2}$ and interaction potential. The shape of the effective potential depends on the interaction forces between the molecules, but for most intermolecular potentials there is a unique maximum of $V_b = V_{\text{eff}}(R = R_{\text{max}})$ referred to as *centrifugal barrier* (see Fig. 2.3). The model assumes that all particles that can cross this barrier contribute to particle conversion. Using the fact that asymptotically the total energy E_{tot} equals E_T , we can write this condition as

$$\frac{1}{2}\mu\dot{R}^2|_{R=R_{\text{max}}} = \left(E_T - V_{\text{int}}(R) - \frac{E_T b^2}{R^2} \right)_{R=R_{\text{max}}} \geq 0. \quad (2.34)$$

Since this expression decreases as the impact parameter b increases, the maximal impact parameter b_{max} is implicitly given via

$$E_T - V_{\text{int}}(R_{\text{max}}) - \frac{E_T b_{\text{max}}^2}{R_{\text{max}}^2} = 0. \quad (2.35)$$

Solving this for $b_{\text{max}}(E_T)$ allows us to directly calculate σ_R via (2.27).

For the purpose of illustration we consider an example of a singly charged ion-molecule reaction, where we have a fourth-order power law:

$$V_{\text{int}}(R) = -\frac{C}{R^4}. \quad (2.36)$$

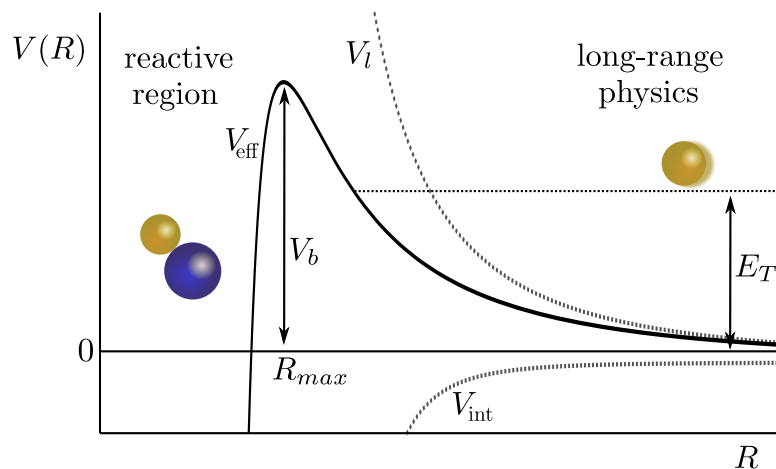


Figure 2.3: The effective potential V_{eff} as sum of centrifugal term V_l and interaction potential V_{int} . In the capture model the relative energy E_T of the particles needs to be larger than the centrifugal barrier V_b in order to form products. Treating the problem quantum mechanically also energies with $E_T < V_b$ contribute to the reaction through tunneling.

For an extensive discussion of other long-range potentials we refer to [Bro10]. Given the potential shape (2.36), the radius R_{max} follows from the condition:

$$\left. \frac{dV_{\text{eff}}}{dR} \right|_{R=R_{\text{max}}} = 0 \quad \Rightarrow \quad R_{\text{max}}(b) = \sqrt{\frac{4C}{2E_T b^2}}. \quad (2.37)$$

Applying this to (2.35) we obtain the maximum impact parameter

$$b_{\text{max}}^2(E_T) = \sqrt{\frac{4C}{E_T}}, \quad (2.38)$$

which yields the reactive cross section

$$\sigma_R(E_T) = \pi \sqrt{\frac{4C}{E_T}}. \quad (2.39)$$

Assuming a maxwellian distribution of relative energy, the reaction rate (2.25) becomes

$$k(T) = 2\pi \sqrt{\frac{2C}{\mu}}, \quad (2.40)$$

which is, in contrast to Arrhenius' law, independent of the temperature.

The models considered in this chapter show that, depending on the microscopical details of particle collisions, different types of rate laws can occur. However, one major problem of the introduced models is that this simple two-body point of view fails to describe *steric effects*: some orientations of colliding molecules may be more conducive to reaction than others. Nevertheless, the introduced simple models already show possible candidates for reactions at ultralow temperatures.

2.2.2 Quantum reactive scattering

Considering chemical reactions at lower and lower temperatures will inevitably introduce quantum mechanical effects to the setting. For example, the magnitude of the angular momentum is restricted to the values $|l| = \hbar\sqrt{l(l+1)}$ with $l \in \mathbb{N}_0$. Considering (2.23) we see two possible aspects of the previously introduced model, which can be extended to quantum mechanics straightforwardly. First, the probability distribution f over relative velocities can be adapted to quantum statistics, e.g. Bose-Einstein statistics for bosons or Fermi-Dirac statistics for fermions. Secondly, the reactive cross section σ_R can be inferred from a quantized description of the scattering process. In this chapter, we will shortly review the formalism of quantum scattering and its application in a simple quantum threshold model.

The formalism of elastic scattering, where the kinetic energy is conserved, is surely not suitable to describe reactive scattering. Therefore, we need to consider inelastic processes. We introduce a label n which collectively describes all the quantum degrees of freedom, except the inter-particle coordinate $\mathbf{r} = R\vec{r}$:

$$\psi(n, \mathbf{r}) = \sum_n |n\rangle \psi_n(\mathbf{r}). \quad (2.41)$$

Here the *channel functions* $|n\rangle$ label a basis of the inner degrees of freedom. For example, in the case of two scattering atoms with spin we have $|n\rangle = |s_1 m_1, s_2 m_2\rangle$, where s_i and m_i label the eigenstates of the corresponding irreducible representation. In quantum mechanics in the same way as in classical mechanics the collision of two particles is considered in the center-of-mass frame. A standard approach to scattering problems considers an incoming plane wave as flux of reactants in a quantum state $|n\rangle$ and expands this in terms of the spherical harmonics $Y_l^m(\vec{r})$. Let $\mathbf{k}_n = k_n \vec{k}$ be the wave vector of the incoming wave then we obtain

$$|n\rangle e^{i\mathbf{k}_n \mathbf{r}} = |n\rangle \sum_l i^l (2l+1) j_l(k_n R) P_l(\vec{k} \cdot \vec{r}) = 4\pi |n\rangle \sum_{l,m} i^l j_l(k_n R) Y_l^m(\vec{r}) Y_l^m(\vec{k})^*, \quad (2.42)$$

where P_l denotes a Legendre polynomial and j_l a spherical Bessel function [Sch05] and

for the second equality we used the spherical harmonic addition theorem. Considering a specific channel $|n\rangle$ the different values of l are referred to as *partial waves* of that channel. The asymptotic form of the Bessel function is

$$j_l(k_n R) \xrightarrow{R \rightarrow \infty} \frac{e^{i(k_n R - l\pi/2)} - e^{-i(k_n R + l\pi/2)}}{2ik_n R}, \quad (2.43)$$

such that for large R the plane wave can be written as combination of an incoming and outgoing spherical wave:

$$|n\rangle e^{i\mathbf{k}_n \mathbf{r}} \xrightarrow{R \rightarrow \infty} \frac{2\pi}{ik_n R} |n\rangle \sum_{l,m} Y_l^m(\vec{r}) [e^{i(k_n r - l\pi/2)} - e^{-i(k_n r + l\pi/2)}] i^l Y_l^m(\vec{k}). \quad (2.44)$$

Now, the S-matrix is the characteristic quantity which models the scattering process as a modification of the outgoing wave's amplitude, such that the overall wave function of the scattering problem can be written as:

$$\psi(\mathbf{k}_n, \mathbf{r}) \xrightarrow{R \rightarrow \infty} \frac{2\pi}{ik_n R} \sum_{n'} \sum_{l,m;l',m'} |n'\rangle Y_{l'}^{m'}(\vec{r}) \left[-e^{-i(k_n r - l'\pi/2)} \delta_{n,n'} \delta_{l,l'} \delta_{m,m'} + e^{i(k_n r - l'\pi/2)} S_{n',l',m';n,l,n} \right] i^l Y_l^m(\vec{k}) \quad (2.45)$$

When there is no interaction the S-matrix is equivalent to the identity matrix. Otherwise, the off-diagonal terms of the S-matrix measure how much is scattered into channels $|n'\rangle$ different from the incoming channel $|n\rangle$. This is more directly expressed by the related T-matrix, $T := \mathbf{1} - S$, with which we define the *scattering amplitude* $f_{n',n}$:

$$f_{n',n}(\vec{r}, \vec{k}) := -\frac{2\pi}{ik_n R} \sum_{l,m;l',m'} i^{l-l'} Y_{l'}^{m'}(\vec{r}) T_{n',l',m';n,l,m} Y_l^m(\vec{k})^* \quad (2.46)$$

This quantity is connected to the state-to-state integral cross section $\sigma_{n',n}$ for a particular incident direction \vec{k} by integration over the unit sphere:

$$\sigma_{n',n}(\vec{k}) = \int \int |f_{n',n}(\vec{r}, \vec{k})|^2 d\vec{r} \quad (2.47)$$

For an isotropically distributed scattering system we obtain the integral state-to-state cross section $\sigma_{n',n}$ by averaging over the incident directions:

$$\sigma_{n',n} = \frac{1}{4\pi} \int \int \sigma_{n',n}(\vec{k}) d\vec{k} = \frac{\pi}{k_n^2} \sum_{l,m;l',m'} |T_{n',l',m';n,l,m}|^2 \quad (2.48)$$

Let n_R label the reactive channels, then we obtain the reactive cross section σ_R from taking the sum of the contributing state-to-state integral cross sections:

$$\sigma_R = \sum_{n' \in n_R, n} \sigma_{n', n} \quad (2.49)$$

At this point we establish a link between the classical impact parameter b and the partial wave quantum number l . Due to the unitarity of the S-matrix we find an upper bound for the contribution of partial wave l for an initial state $|n\rangle$ to any of the output channels to be

$$\sigma_{n, l}^{max} = \frac{\pi}{k_n^2} (2l + 1), \quad (2.50)$$

where the factor $2l + 1$ stems from the summation over the possible m . Assuming that beyond some wave number l_{max} the partial waves become nonreactive, we obtain

$$\sigma_n^{max} = \sum_{l=0}^{l_{max}} \sigma_{n, l}^{max} = \frac{\pi}{k_n^2} (l_{max} + 1)^2. \quad (2.51)$$

Comparing this with the definition of the classical reactive cross section (2.27) leads us to conclude that

$$b_{max}^2 = \frac{(l_{max} + 1)^2}{k^2}. \quad (2.52)$$

Assuming the potential to have a maximal distance R_{max} at which particles interact yields

$$R_{max}^2 k^2 = (l_{max} + 1)^2. \quad (2.53)$$

This shows that when temperature decreases and k becomes smaller only a few partial waves contribute to the cross section. In case of ultracold temperatures the cross sections are often governed by partial waves with $l = 0$ (or s-waves) for bosons or distinguishable particles and $l = 1$ (or p-waves) for fermions.

Equation (2.48) shows that the T-matrix or equivalently the S-matrix are the key elements as they provide a direct way to derive reaction rates. Various methods have been developed to obtain the elements of these matrices, for example coupled channels theory [Hu06]. However, most of them are computationally demanding. Here we present an approach, referred to as quantum threshold model [Qué10] which modifies the results of the classical capture model by a simple quantum correction. We have already seen that for low-energy scattering only the smallest partial wave

contributes to the reactive cross section. The contributions of these waves in the limit of low energies follow the so-called Wigner threshold law [Wig48]

$$|T_{n',l';n,l}|^2 \propto k_n^{2l+1}, \quad (2.54)$$

implying the reactive cross section

$$\sigma_{n',l';n,l} \propto k_n^{2l-1}. \quad (2.55)$$

The quantum threshold model considers the classical effective potential (see figure 2.3) and assumes that for $E_T \geq V_b$ the entries of the T-matrix have modulus one, that is $|T_{l,m}|^2 = 1$, just as the probability for reaction in the classical capture model. However, for energies below the centrifugal barrier $E_T < V_b$ the reaction probability is not equal to zero but follows a threshold law,

$$|T_{l,m}|^2 = \left(\frac{E_T}{V_b} \right)^{l+1/2}. \quad (2.56)$$

This can be interpreted as the contribution to the reaction by tunnelling through the centrifugal barrier. Substituting this expression into (2.48) gives the reactive cross section

$$\sigma_R = \frac{\hbar^2 \pi}{2\mu V_b^{l+1/2}} E_T^{l-1/2}. \quad (2.57)$$

Note that this model does not apply to s-wave scattering due to the absence of the centrifugal barrier. However, assuming a Maxwell-Boltzmann distribution of the relative velocities and considering two fermionic molecules at ultracold temperatures we obtain a rate for the p-wave contribution that scales linearly with temperature. A considerable feature of this model is that it provides an analytical expression of the rate coefficient which scales with the height of the centrifugal barrier, which is in qualitative agreement with experiments. Moreover, one can easily introduce a fitting parameter to the barrier height or modify the reaction probability below the barrier by an overall factor to introduce flexibility.

To summarise, we have that the presented quantum treatment of scattering modifies the reaction constants of classical kinetics by important quantum effects. However, the resulting dynamical description is still dissipative as the quantum mechanically calculated reaction constants are simply used as parameters within the framework of classical kinetics.

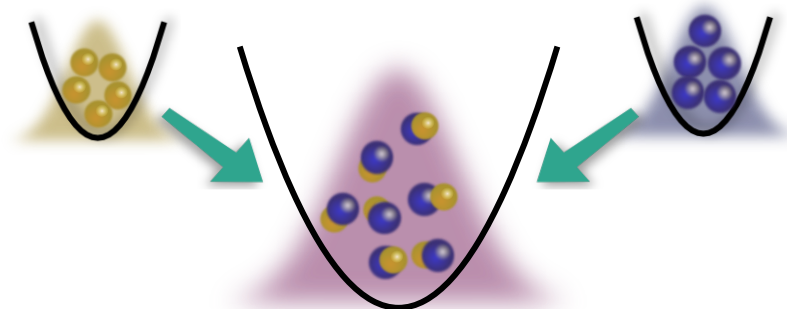


Figure 2.4: Depiction of an ultracold reaction resulting from the superposition or interaction of two BECs. Describing the creation of molecules by a two-body scattering model fails due to positional delocalization and indistinguishability of particles.

2.2.3 Ultracold chemistry

The ground-breaking experimental achievement of creating a Bose-Einstein condensate (BEC) of Sodium atoms [Dav95] spurred experimental as well as theoretical physicists to explore a wide range of questions around this new kind of matter. One aspect was the creation of a molecular BEC through coupling atomic BECs using photoassociation [Wyn00] or magnetic field Feshbach resonance [Don02] (sketched in Fig. 2.4). A natural question to ask is how a suitable framework for these ultracold particle conversions should look like. So far our determination of the reaction rate was based on the consideration of the two-particle reactive cross section σ_R . However, for chemical reactions taking place in the realm of BECs or degenerate quantum gases this picture necessarily fails; due to the spatial delocalization and indistinguishability of the particles throughout the condensate, the particles can only collectively "scatter", which requires a full quantum description of the many body system.

The first theoretical proposal to effectively describe the coherent creation of molecules inside a BEC completely within the quantum framework was made in [Dru98]. The authors described the atoms as well as the molecules by three-dimensional quantum fields interacting through

$$\hat{H}_{int} = \int d^3x \frac{\chi}{2} \left[\hat{\phi}^2 \hat{\psi}^\dagger + \hat{\phi}^{\dagger 2} \hat{\psi} \right], \quad (2.58)$$

where $\hat{\phi}$ labels the atomic and $\hat{\psi}$ the dimer species. The coupling constant χ represents the s-wave scattering limit of the dimer formation rate, effectively modeling process photoassociation as well as magnetoassociation. At the same time a similar approach was described in [Jav99], whereas the authors derive the coupling parameter from the matrix dipole moment in photoassociation.

A first step to describe the proposed theories as a new kind of chemistry was undertaken in [Hei00]. In this publication the authors coined the term *superchemistry* as ‘the coherent stimulation of chemical reactions via macroscopic occupation of a quantum state by a bosonic chemical species’. The authors point out that the resulting kinetics are fundamentally different from Arrhenius’ type of dynamics. However, the authors miss to present a complete scheme or method to describe the reaction kinetics of more complex reactions as well as a fundamental categorization of the occurring dynamical regimes. Subsequent work [Hop01; Oli04] extended the specific model of diatomic molecule formation correcting previous predictions of the system dynamics. In [Moo02] the authors consider the dissociation of triatomic molecules, assuming two open rearrangement channels. It is found that a small change in the coupling constants to the rearrangement channels has dramatic effects on the dynamics. A short review article considering certain aspects of superchemistry can be found in [Jin11].

In this thesis we extend the notion of superchemistry to *ultracold chemistry* by two major aspects: First, we allow the participating species to be fermions. Although mentioned by the authors in [Hei00], they miss to provide possible explicit interaction Hamiltonians to describe a fermionic reactions. And secondly, we do not restrict ourselves to elementary reactions. Our proposed model allows to describe ultracold reaction networks, that is an arbitrary number of concurrent reactions. Consequently, we define ultracold chemistry as *chemical reactions driven by the coherent interaction of quantum degenerate Fermi or Bose gases*.

CHAPTER 3

Ultracold reaction kinetics

The main objective of this thesis is to set up a framework that provides a comprehensive description of ultracold reaction kinetics and allows for a systematic classification of the occurring phenomena. As a template we consider the theory of classical reaction kinetics, which successfully finds a trade-off between a not too complex description of an open thermodynamic system and still capturing the important physical aspects to predict experimental interesting phenomena. A promising route to follow is to consider the equations of motion of classical reaction kinetics as some kind of classical limit of the proposed quantum framework. This can be achieved by employing the method of *first quantisation* [Dir25]. This method takes the classical equations of motion as a starting point and proposes a class of related quantum systems. First quantisation is validated by its enormous success in predicting fundamental quantum phenomena like discrete energy levels, tunnelling and uncertainty principles. However, within the framework of first quantisation it is not possible to model creation and annihilation of particles. Considering a chemical reaction, it is an appealing interpretation to understand the transformation process between chemical species as annihilation of the reactant species and creation of the product species. Therefore, the formalism of *second quantisation*, which is capable of modelling creation and annihilation of particles, provides another promising approach to model ultracold chemical reactions. Second quantisation describes many-particle quantum systems in terms of occupation numbers of a complete set of single particle states. This method is used as a framework for quantum field theories and therefore validated by the successful description of numerous physical systems ranging from superconductors to particle physics. However, as second quantisation usually begins with the quantisation of a classical field theory, it is not clear how classical reaction kinetics should appear as classical limit.

This chapter is organised as follows. In section 3.1 we review the method of first quantisation. The method has a classical Hamiltonian system as starting point. Therefore, we present a way to embed the dissipative dynamics of classical kinetics

into a Hamiltonian description. We first quantise the embedded systems and discuss the validity of this approach. In section 3.2 we introduce the basic concepts of second quantisation. We focus on certain aspects which will help to understand the formulation of the proposed framework. In section 3.3 we present a proposal, which starts with the stoichiometric scheme of an arbitrary chemical reaction and yields a second quantised Hamiltonian description. This proposal is a central aspect of the thesis as we study the following chapters instructive examples of second quantised kinetics.

3.1 First quantisation

First quantisation of classical systems has a long and successful history of applications. The idea of describing particles or other physical objects by ‘wave functions’ goes back to the early days of quantum mechanics [Dir25]. In translating a classical Hamiltonian description into the framework of single-particle wave functions, it succeeded in describing fundamental quantum phenomena. Besides the explicitly single particle aspects, it also successfully explained even many-body systems, for example the occurrence of energy gaps in semiconductors. The starting point of first quantisation of a classical Hamiltonian system is to replace the Poisson brackets by commutator relations

$$\{x,p\} \mapsto i [\hat{x},\hat{p}]. \quad (3.1)$$

This maps the dynamics from a finite-dimensional phase space to an infinite dimensional Hilbert space. However, first quantisation does not provide a unique connection between quantum and classical systems; the quantisation of canonically equivalent classical systems leads to non-equivalent quantum systems. In this sense, first quantisation can only give us an indication of which quantum systems we should investigate, given its classical limit.

Inspired by the success of first quantisation in predicting phenomena for quantised classical systems, we attempt to apply this method to classical reaction kinetics. Keeping in mind that a chemical reaction is inherently a many particle problem, we assume the resulting description to be approximate. Nevertheless, we hope to gain insights, from first quantisation, into the qualitative behaviour of chemical reactions at ultracold temperatures. Clearly, this requires a valid Hamiltonian description of the system under consideration, which brings us to the first problem: The dynamic of high-temperature kinetics 2.16 is in general of dissipative nature, that is, there is neither a time-reversal symmetry nor a preservation of the state space volume during time evolution. Moreover, the conservation of energy is a central aspect of closed Hamiltonian systems. However, we know that dissipative terms effectively model the interaction a system with an environment, for example a heat reservoir in thermodynamics. Therefore, by enlarging the system to include

environment, we obtain an energy-conserving model. However, in case of classical chemical reactions this seems to be a hopeless endeavour as this would require including all particles taking part in the reaction. Consequently, we try to find an effective Hamiltonian description which on the one hand reproduces the dissipative dynamics when considered on a subsystem, and on the other hand is not too complex to be suitable for a first quantisation.

In what follows, we present a efficient way of embedding a dissipative system into a Hamiltonian description. We apply this embedding to a classical first-order reaction and first-quantise different equivalent descriptions of the resulting Hamiltonian system. We compare the dynamics of the different quantised systems with the dynamics of classical reaction kinetics.

3.1.1 Dynamical embedding

Before we can quantise classical reaction kinetics, we need to find a suitable Hamiltonian description of it. By ‘suitable’ we mean that the original dissipative dynamics should be reproduced by some kind of natural restriction within the Hamiltonian system. We employ a method which we refer to as *dynamical embedding*. The key idea of this method is to set up a Hamiltonian system of twice the dimension¹ of the dissipative system, in such way that we obtain the dissipative trajectories as a projection onto a subspace. To be more precise, we define a Hamiltonian system to be a triple consisting of a $2N$ -dimensional phase space with coordinates

$$(\mathbf{x}, \mathbf{p}) = ((x_1, p_1), (x_2, p_2), \dots, (x_N, p_N)), \quad (3.2)$$

a Hamilton function $H = H(\mathbf{x}, \mathbf{p})$ and a set of observables $\{A_i(\mathbf{x}, \mathbf{p})\}_{i=1}^k$ evolving in time according to

$$\frac{dA_i(\mathbf{x}, \mathbf{p})}{dt} = \sum_{j=1}^N \frac{\partial A_i(\mathbf{x}, \mathbf{p})}{\partial x_j} \frac{\partial H(\mathbf{x}, \mathbf{p})}{\partial p_j} - \frac{\partial H(\mathbf{x}, \mathbf{p})}{\partial x_j} \frac{\partial A_i(\mathbf{x}, \mathbf{p})}{\partial p_j} \quad i = 1, 2, \dots, k. \quad (3.3)$$

Note that for the sake of simplicity we restrict our considerations to quantities which are not explicitly time-dependent. A dynamical first-order system consists of a state space (z_1, z_2, \dots, z_n) and an ODE-system

$$\frac{dz_i}{dt} = f_i(z_1, \dots, z_n) \quad i = 1, 2, \dots, n, \quad (3.4)$$

where f_i is a smooth function for each i . We say a dynamical first-order system is *dynamically embedded* into a Hamiltonian system if we can find a set of observables

¹ Considered as vector space, not as symplectic space.

A_i for the Hamiltonian system whose time-evolution coincides with (3.4).

In what follows we show that, although the existence of a dynamical embedding for any finite dimensional first-order dynamical system is guaranteed, it is not unique. In fact, we can find infinitely many Hamiltonian systems reproducing the proper dissipative dynamics on a subsystem. To see this, we identify the state space coordinates (z_1, z_2, \dots, z_n) as position variables of a n -dimensional phase space, that is $z_i = x_i$. Substituting this ansatz into 3.3 yields

$$\frac{dx_i}{dt} = \frac{\partial H(\mathbf{x}, \mathbf{p})}{\partial p_i} \stackrel{!}{=} f_i(\mathbf{x}), \quad (3.5)$$

as a constraint on possible Hamilton functions. Equation (3.5) is an underdetermined system as it merely determines the partial derivatives of H with respect to the canonical momenta. We see that any Hamiltonian of the form

$$H = \sum_{i=1}^n f_i(\mathbf{x})p_i + \sum_{i=1}^n g_i(\mathbf{x}) = \sum_{i=1}^n f_i(\mathbf{x})p_i + g(\mathbf{x}), \quad (3.6)$$

induces the desired equations on the subspace spanned by (x_1, x_2, \dots, x_n) , for any smooth function g . The freedom of choosing an arbitrary g has a large impact on the dynamics of the conjugate variables (p_1, \dots, p_n) ,

$$\frac{dp_j}{dt} = -\frac{\partial H(\mathbf{x}, \mathbf{p})}{\partial x_j} = -\left(\sum_{i=1}^n p_i \frac{\partial f_i(\mathbf{x})}{\partial x_j} + \sum_{i=1}^n \frac{\partial g_i(\mathbf{x})}{\partial x_j} \right). \quad (3.7)$$

However, this seemingly large degree of freedom may be reduced by the fact that different embeddings may describe the same physical system in different coordinates. In this case Hamiltonian dynamics tells us that there exists a canonical transformation [Gol65] between the systems. This transformation maps the position and momentum coordinates of a given Hamiltonian system to new coordinates while preserving Hamilton's equation of motion. However, the particular canonical transformation relating two systems may, in general, be very hard to find. At this point, we content ourselves by formulating a sufficient condition for the existence of a canonical transformation between two different embeddings. This condition relies on the fact that every canonical transformation is induced by some generating function. Bearing in mind that there are different types of generating functions, we assume here that the generating function depends on the old and new position coordinates, that is $F = F(\mathbf{x}, \tilde{\mathbf{x}})$. This implies the following equations for the respective momentum

coordinates:

$$\begin{aligned} p_i &= \frac{\partial F(\mathbf{x}, \tilde{\mathbf{x}})}{\partial x_i} \\ \tilde{p}_i &= \frac{\partial F(\mathbf{x}, \tilde{\mathbf{x}})}{\partial \tilde{x}_i}. \end{aligned} \tag{3.8}$$

By inserting (3.8) into (3.6), we find that two of dynamical embeddings, determined by distinct g_1 and g_2 in (3.6), describe the same physical system if the partial differential equation

$$\sum_i f_i(\tilde{\mathbf{x}}) \frac{\partial F(\mathbf{x}, \tilde{\mathbf{x}})}{\partial \tilde{x}_i} + \sum_i f_i(\mathbf{x}) \frac{\partial F(\mathbf{x}, \tilde{\mathbf{x}})}{\partial x_i} = g_1(\tilde{\mathbf{x}}) - g_2(\mathbf{x}) \tag{3.9}$$

has a non-trivial solution in $F(\mathbf{x}, \tilde{\mathbf{x}})$. We emphasize again that this is merely a sufficient condition and the class of equivalent descriptions may be much larger.

Summarising this method, we see we can obtain a compact canonical description of a dissipative system. Within this description the dissipative dynamics emerge naturally from the physical restriction of only having access to a subspace of the full phase space. Naively applied, this method comes with a large degree of freedom, making it difficult to decide which embeddings might be the right for the subsequent quantisation. We might be able to mitigate this effect by identifying equivalent embeddings through canonical transformations. However, as long as we have no full classification of the different embeddings, we can merely pick out certain examples and investigate the consistency between the quantised and classical systems.

3.1.2 Case-study

As an example of a dynamical embedding and of the predicted dynamics of the corresponding first quantised system, let us consider the elementary reaction



For the sake of clarity, we henceforth omit the embracing brackets $[\cdot]$ of the particle concentration. The dynamical equation for species A can be inferred from (2.16) to be

$$\frac{dA}{dt} = -kA, \tag{3.11}$$

which is solved by an exponential decay

$$A = A_0 e^{-kt}, \tag{3.12}$$

with A_0 as initial particle number. Considering the concentration A as a canonical variable x of some Hamiltonian system results in the following equation determining the Hamiltonian:

$$\frac{dx}{dt} = \frac{\partial H}{\partial p} = -kx \quad (3.13)$$

This is solved by the set of Hamilton functions

$$H(x,p) = -kxp + g(x), \quad (3.14)$$

with g as smooth function. As already mentioned, the choice of a particular g seems to result in different physical systems. However, let us evaluate our sufficient criterion for canonical equivalence (3.9):

$$\tilde{x} \frac{\partial F}{\partial \tilde{x}} + x \frac{\partial F}{\partial x} = g(x), \quad (3.15)$$

where we set $g_1(\tilde{x}) = 0$ and $g_2(x) = g(x)$. This equation is analytically solvable by the method of characteristics (see for example in [Cou66]). The generating function can be determined to be

$$F(x,\tilde{x}) = \int_0^x dx' \frac{g(x')}{x'} + h\left(\frac{\tilde{x}}{x}\right), \quad (3.16)$$

where h can be any non-zero smooth function. This result is surprising as it means that for all possible embeddings given by g_2 , we can find a generating function F inducing a transformation to the embedding with $g = 0$. In mathematical terms we say that all possible embeddings belong to the same equivalence class.

Motivated by this result, let us further investigate the dynamical embedding with $g = 0$, that is

$$H_0(x,p) = -kxp. \quad (3.17)$$

This physics described by this system can be understood if we canonically transform it to coordinates

$$\begin{pmatrix} x \\ p \end{pmatrix} = \frac{1}{\sqrt{2}} \begin{pmatrix} 1 & -1 \\ 1 & 1 \end{pmatrix} \begin{pmatrix} \tilde{x} \\ \tilde{p} \end{pmatrix} \quad (3.18)$$

The Hamiltonian then yields

$$H_1 = \frac{k}{2}(\tilde{p}^2 - \tilde{x}^2). \quad (3.19)$$

This Hamiltonian represents a physical system consisting of a particle moving in the inverted harmonic potential $V(x) = -\frac{k}{2}x^2$. This system therefore has one unstable fixed point at $x = p = 0$. Trajectories starting with $x \neq 0$ only move to this fixed point when the initial kinetic energy is equal to minus the potential energy. Therefore, most of the trajectories will diverge to infinity. Similar systems occur in the path integral framework of quantum field theory as result of Wick rotation [Das93]. The original dissipative dynamics are reproduced by following the observable $A = \frac{1}{\sqrt{2}}(\tilde{x} - \tilde{p})$.

Having understood the physical model of the dynamical embedding of the chemical reaction, we now apply first quantisation to the system. Let us consider, as an example, the classical equivalent systems (3.19) and (3.17). Replacing the classical phase space variables with operators yields

$$\hat{H}_0 = -k\hat{x}\hat{p}, \quad (3.20)$$

and

$$\hat{H}_1 = \frac{k}{2}(\hat{p}^2 - \hat{x}^2). \quad (3.21)$$

The first problem we immediately see is that (3.20) is not self-adjoint. This can be resolved by rewriting the classical term xp as $\frac{xp+px}{2}$ resulting in the operator

$$\hat{H}_0 = -\frac{k}{2}(\hat{x}\hat{p} + \hat{p}x). \quad (3.22)$$

To reach a more intuitive understanding we rewrite \hat{H}_0 and \hat{H}_1 in terms of the ladder operators of the harmonic oscillator, that is

$$\hat{a} = \frac{\hat{x} + i\hat{p}}{\sqrt{2}} \quad (3.23)$$

and

$$\hat{a}^\dagger = \frac{\hat{x} - i\hat{p}}{\sqrt{2}}. \quad (3.24)$$

Substituting these identities into 3.22 yields

$$\begin{aligned} \hat{H}_0 &= -\frac{k}{2}(\hat{x}\hat{p} + \hat{p}x) = -\frac{ik}{4}((\hat{a} + \hat{a}^\dagger)(\hat{a}^\dagger - \hat{a}) + (\hat{a}^\dagger - \hat{a})(\hat{a} + \hat{a}^\dagger)) \\ &= -\frac{ik}{2}(\hat{a}^\dagger\hat{a}^\dagger - \hat{a}\hat{a}). \end{aligned} \quad (3.25)$$

The quantised particle concentration in case of \hat{H}_0 is

$$\hat{A}_0 = \hat{x} = \frac{1}{\sqrt{2}} (\hat{a}^\dagger + \hat{a}). \quad (3.26)$$

Similarly, we obtain for 3.21 the expression

$$\begin{aligned} \hat{H}_1 &= \frac{k}{2} (\hat{p}^2 - \hat{x}^2) = \frac{k}{2} \left(-\frac{1}{2} (\hat{a}^\dagger - \hat{a})^2 + \frac{1}{2} (\hat{a}^\dagger + \hat{a})^2 \right) \\ &= -\frac{k}{2} (\hat{a}^\dagger \hat{a}^\dagger + \hat{a} \hat{a}), \end{aligned} \quad (3.27)$$

with quantised observable

$$\hat{A}_1 = \frac{1}{\sqrt{2}} (\hat{x} - \hat{p}) = \frac{1-i}{2} \hat{a}^\dagger + \frac{1+i}{2} \hat{a}. \quad (3.28)$$

We see that first quantisation has led us to two seemingly different quantum descriptions of equivalent classical models. We mention here, that besides the observables that result directly from the quantisation, we also consider the expectation value of the particle number operator

$$\langle \hat{N} \rangle = \langle \hat{a}^\dagger \hat{a} \rangle, \quad (3.29)$$

as a possible candidate for a dynamical observable. This is due to its great success in quantum optics, where it successfully establishes a duality between the classical particle and quantum wave view. To make the quantum framework complete, we assume that the Hamiltonian induces the dynamics via the time-dependent Schrödinger equation (TSDE)

$$|\psi(t)\rangle = e^{-i\hat{H}t} |\psi(0)\rangle. \quad (3.30)$$

Within this framework, we find by substituting (3.25) and (3.27) into (3.30) that the time evolution is represented by two different instances of *squeeze* operators [Ger05]:

$$\hat{S}(s, \theta) = e^{\frac{1}{2}s(e^{-i\theta}\hat{a}\hat{a} - e^{i\theta}\hat{a}^\dagger\hat{a}^\dagger)}, \quad (3.31)$$

with $\theta = 0$ for \hat{H}_0 and $\theta = \frac{3}{2}\pi$ for \hat{H}_1 and $s = kt$ for both. To obtain an analytical expression for the temporal evolution of observables, we use the identities [Lou00]

$$\begin{aligned} \hat{S}^\dagger \hat{a} \hat{S} &= \hat{a} \cosh(s) - \hat{a}^\dagger e^{-i\theta} \sinh(s) \\ \hat{S}^\dagger \hat{a}^\dagger \hat{S} &= \hat{a}^\dagger \cosh(s) - \hat{a} e^{i\theta} \sinh(s). \end{aligned} \quad (3.32)$$

In what follows, we compare the resulting quantum trajectory with the classical trajectory. To make this comparison as feasible as possible, we choose the quantum systems to be initially in a coherent state labelled by $|\alpha\rangle$. These states are to some extent the most classical states (see details in 5.1.1).

Let us start our investigation by considering the expectation value of the observable A_0 :

$$\begin{aligned}\langle \hat{A}_0(t) \rangle &= \frac{1}{\sqrt{2}} \langle \alpha | \hat{a} \cosh(kt) - \hat{a}^\dagger \sinh(kt) + \hat{a}^\dagger \cosh(kt) - \hat{a} \sinh(kt) | \alpha \rangle \\ &= \sqrt{2} \operatorname{Re}(\alpha) (\cosh(kt) - \sinh(kt)) = 2 \operatorname{Re}(\alpha) e^{-kt}.\end{aligned}\quad (3.33)$$

Surprisingly, this exactly reproduces the classical trajectory if we identify $A_0 = \sqrt{2} \operatorname{Re}(\alpha)$. This gives us an intuition concerning how to find a classical limit of this system resulting in the expected classical dynamics, namely, a limit where the fluctuations around the expectation value become negligibly small. As a second system we consider \hat{H}_1 with observable \hat{A}_1 :

$$\begin{aligned}\langle \hat{A}_1(t) \rangle &= \frac{1}{2} \langle \alpha | (1 - i) (\hat{a}^\dagger \cosh(kt) + i \hat{a} \sinh(kt)) | \alpha \rangle \\ &\quad + \frac{1}{2} \langle \alpha | (1 + i) (\hat{a} \cosh(kt) - i \hat{a}^\dagger \sinh(kt)) | \alpha \rangle \\ &= (\operatorname{Re}(\alpha) - \operatorname{Im}(\alpha)) e^{kt}\end{aligned}\quad (3.34)$$

Its dynamics are fundamentally different from the classical ones. Depending on the choice of real and imaginary part of α the expectation value goes to plus or minus infinity. Therefore, it is not possible to interpret this observable as pendant of the classical particle number. In the last step, we consider the expectation value of the number operator,

$$\begin{aligned}\langle \hat{N}(t) \rangle &= \langle \alpha | \hat{a}^\dagger \hat{a} \cosh^2(kt) - \hat{a}^\dagger \hat{a}^\dagger e^{i\theta} \cosh(kt) \sinh(kt) | \alpha \rangle \\ &\quad + \langle \alpha | -\hat{a} \hat{a} e^{-i\theta} \sinh(kt) \cosh(kt) + (\hat{a}^\dagger \hat{a} + 1) \sinh^2(kt) | \alpha \rangle \\ &= |\alpha|^2 \cosh(2kt) - \operatorname{Re}(\alpha^2 e^{-i\theta}) \sinh(2kt) + \sinh^2(kt) \\ &= \left(|\alpha|^2 + \frac{1}{2} \right) \cosh(2kt) - \operatorname{Re}(\alpha^2 e^{-i\theta}) \sinh(2kt) - \frac{1}{2}.\end{aligned}\quad (3.35)$$

Here we keep θ as a parameter so we may compare the different time evolutions induced by \hat{H}_0 and \hat{H}_1 . However, for large times the difference between the systems vanishes and the particle number is dominated by an exponential increase

$$\langle \hat{N}(t) \rangle \xrightarrow{t \gg 1} A e^{2kt}, \quad (3.36)$$

where A is a constant depending on the initial state.

Comparing the trajectories of the different systems, we see that A_0 evolves in time like the classical trajectory, whereas the others strongly deviate from the classical solution. This seems to be a good starting point as it means we have found a quantum description which recovers the classical kinetics in the limit of vanishing fluctuations around the mean value. However, further investigations of (3.25) reveal some problems for it as candidate for the description of ultracold reactions: For a general coherent state the expectation value of \hat{H}_0 is given by

$$\langle \alpha | \hat{H}_0 | \alpha \rangle = -\frac{ik}{2} (\bar{\alpha}^2 - \alpha^2) = -k\text{Im}(\alpha^2). \quad (3.37)$$

Since there are no restrictions on the imaginary part of α^2 , we find that the operator \hat{H}_0 is neither bounded from below nor from above. This shows that the system described by \hat{H}_0 cannot be subject to thermal investigations as the ground state is not well defined. The same reasoning can be applied to \hat{H}_1 . Moreover, the fact that \hat{H}_0 and \hat{H}_1 model squeezing hints at another problem: In quantum optics the squeezing operator results from an approximate description of parametric down conversion [Wu86], that is the recombination of two photons into one of double energy. However, this recombination scheme would correspond to a second-order reaction, whereas our classical example is a first order reaction.

To summarise, we have successfully embedded the dissipative dynamics of a classical first-order reaction into a Hamiltonian framework. By comparing different quantisations of canonically equivalent systems, we found that the resulting systems predict different dynamics. Although we found a promising candidate reproducing the dissipative dynamics on a subspace, the resulting Hamiltonian systems are "unphysical" in the sense that they violate essential properties we demand from a proper quantum description. Besides these issues, it is completely unclear how important aspects like the distinction between fermionic and bosonic reactions should enter a first quantised description. Altogether, we consider the obtained insights not promising enough warrant following this route further.

3.2 Second quantisation

A chemical reaction can be considered as a result of two or more scattering particles that form particles of inherently different structure. This implies that a full quantum description of this process needs to take the different structure of reactants and products as well as variable particle numbers into account. The resulting formalism should, in particular, be capable of describing the change of the statistics of the particles, which can have an important impact on the dynamics of the reaction. The formalism of second quantisation has the required properties and, moreover, provides a compact route for the formulation of our proposed framework. As such, we review

here the basic notions and terminology of second quantisation. In the sequel, we closely follow [Sch05].

We start our introduction of second quantisation by considering a single-particle quantum system with $\{\psi_j(\mathbf{x})\}_{j=1}^{\infty}$ as a complete orthogonal basis of wave functions. Here \mathbf{x} does not merely denote the position of the particle, but also other degrees of freedom, e.g. spin. According to the rules of quantum mechanics the wave function of N copies of this particle will be an element of the N -fold tensor product:

$$\Psi(\mathbf{x}_1, \dots, \mathbf{x}_N, t) = \sum_{i_1, \dots, i_N} c_{i_1, \dots, i_N}(t) \psi_{i_1}(\mathbf{x}_1) \dots \psi_{i_N}(\mathbf{x}_N). \quad (3.38)$$

A typical Hamiltonian many-body system consists of kinetic energy and an interaction potential:

$$\hat{H} = \sum_{k=1}^N \hat{T}(\mathbf{x}_k) + \frac{1}{2} \sum_{\substack{(k,l)=1 \\ k \neq l}}^N \hat{V}(\mathbf{x}_l, \mathbf{x}_k). \quad (3.39)$$

Considering the time-dependent Schrödinger equation, this problem is equivalent to an infinite number of coupled differential equations in $c_{i_1, \dots, i_N}(t)$. A basic principle in many-body quantum mechanics is that identical particles are indistinguishable in the following sense: The permutation of two particles in the wave function does not result in observable consequences. Let P_{jk} denote the operator that exchanges the labels of the particles j and k . Then, the indistinguishability condition can be written as

$$\hat{P}_{jk} \Psi(\mathbf{x}_1, \dots, \mathbf{x}_j, \dots, \mathbf{x}_k, \dots, \mathbf{x}_N) = e^{i\phi_{jk}} \Psi(\mathbf{x}_1, \dots, \mathbf{x}_j, \dots, \mathbf{x}_k, \dots, \mathbf{x}_N), \quad (3.40)$$

that is the permuted wave function merely changes by a phase. It is intuitive to demand that applying the exchange operator $P_{j,k}$ twice yields the original wave function¹. This implies that any phase $\phi_{j,k}$ is either 0 or π or, equivalently, the wave function is either even or odd under permutations. Particles with an even parity are called *bosons* whereas an odd parity corresponds to fermions. To ensure the right properties of the wave function the coefficients in (3.38) must satisfy

$$c_{i_1, \dots, i_k, \dots, i_j, \dots, i_N}(t) = \pm c_{i_1, \dots, i_j, \dots, i_k, \dots, i_N}(t), \quad (3.41)$$

where $+$ holds in the bosonic and $-$ for the fermionic case. The bosonic symmetry makes it convenient to rewrite the wave function in a symmetrised basis. Let n_1

¹ For excitations in certain two-dimensional systems, e.g. the toric code, this condition is indeed violated. These particle-like quantities are referred to as anyons

denote the number of particles which are in state ψ_1 , n_2 the number of particles in state ψ_2 and so on. We refer to (n_1, n_2, \dots) as occupation numbers which in the bosonic case, can take values between zero and N . Using this terminology we can write a complete set of symmetrised functions as

$$\phi_{n_1, n_2, \dots}(\mathbf{x}_1, \dots, \mathbf{x}_N) := \sqrt{\frac{n_1! n_2! \dots}{N!}} \sum_{\substack{i_1, \dots, i_N \\ (n_1, n_2, \dots)}} \psi_{i_1}(\mathbf{x}_1) \dots \psi_{i_N}(\mathbf{x}_N), \quad (3.42)$$

where the summation runs over all i_1, \dots, i_N that satisfy a pattern of (n_1, n_2, \dots) . Moreover, for a fixed particle number N we find that the pattern of occupation numbers needs to satisfy $\sum_i n_i = N$. Expressing the wave function in this basis yields

$$\Psi(\mathbf{x}_1, \dots, \mathbf{x}_N, t) = \sum_{\substack{n_1, n_2, \dots \\ \sum_i n_i = N}} f_{n_1, n_2, \dots}(t) \cdot \phi_{n_1, n_2, \dots}(\mathbf{x}_1, \dots, \mathbf{x}_N), \quad (3.43)$$

where $f_{n_1, n_2, \dots}$ labels the coefficients in this basis. The same reformulation for the basis can be done for fermions, with the differences that the antisymmetry of the wave function restricts the occupation numbers to be either zero or one $n_i \in \{0, 1\}$ and that an extra sign appears in (3.42) according to the parity of the wave function.

While the representation introduced allows us to correctly write down the time evolution of the many-body wave function of a system with fixed particle number, particularly in chemical systems we need to be able to describe number-changing processes. In what follows, we introduce a more compact notation of the previous concepts that in addition keeps track of the underlying statistics and allows us to express particle-number-changing Hamiltonians. To this end, we rewrite (3.42) in bra-ket notation,

$$|n_1, n_2, \dots\rangle := \phi_{n_1, n_2, \dots}(\mathbf{x}_1, \dots, \mathbf{x}_N). \quad (3.44)$$

We define the n -particle sector as the linear span of all states with particle number N ,

$$\mathcal{F}_N := \text{span}\{|n_1, n_2, \dots\rangle, \sum_i n_i = N\} \quad (3.45)$$

and consider the direct sum of the spaces with all possible particle numbers N , that is the *Fock space*:

$$\mathcal{F} = \bigoplus_{i=0}^{\infty} \mathcal{F}_N. \quad (3.46)$$

Inside this Hilbert space it is now possible to define operator which change the overall particle number of the state, for example the *creation operators* $\hat{a}_i^\dagger : \mathcal{F}_N \mapsto \mathcal{F}_{N+1}$, which creates a particle in state ψ_i as

$$\hat{a}_i^\dagger |n_1, \dots, n_i, \dots\rangle = \sqrt{n_i + 1} \eta^{s_i} |n_1, \dots, n_i + 1, \dots\rangle, \quad (3.47)$$

where $\eta = 1$ for bosonic and $\eta = -1$ for fermionic systems and $s_i = \sum_{j=1}^{i-1} n_j$. Note that for fermionic particles the occupation numbers are restricted to 0 and 1, that is the application of a_i^\dagger to a state with $n_i = 1$ maps this state to zero. Defining the vacuum state as the state where no particles are present, that is $|0\rangle := |0, 0, \dots\rangle$, allows us to obtain every basis state of \mathcal{F} by repeated application of \hat{a}_i^\dagger ,

$$|n_1, n_2, \dots\rangle = \prod_i \frac{1}{\sqrt{n_i!}} \left(\hat{a}_i^\dagger\right)^{n_i} |0\rangle. \quad (3.48)$$

The completeness of the occupation number basis allows us to derive further properties of the creation operator. From (3.47) we find

$$\left(\hat{a}_i^\dagger \hat{a}_j^\dagger - \eta \hat{a}_j^\dagger \hat{a}_i^\dagger\right) |n_1, n_2, \dots\rangle = 0. \quad (3.49)$$

Since this is true for every basis vector, this is equivalent to

$$\hat{a}_i^\dagger \hat{a}_j^\dagger - \eta \hat{a}_j^\dagger \hat{a}_i^\dagger = 0. \quad (3.50)$$

The action of the adjoint of the creation operator $\left(a_i^\dagger\right)^\dagger = a_i$ can be inferred to be

$$\hat{a}_i |n_1, \dots, n_i, \dots\rangle = \sqrt{n_i} \eta^{s_i} |n_1, \dots, n_i - 1, \dots\rangle, \quad (3.51)$$

that is it takes states from \mathcal{F}_N to \mathcal{F}_{N-1} and is consequently called an *annihilation operator*. The adjoint of (3.50) shows that it obeys the same relations as the creation operator. Combining (3.47) and (3.51) amounts to the following between annihilation and creation operator:

$$\hat{a}_i \hat{a}_j^\dagger - \eta \hat{a}_j^\dagger \hat{a}_i = \delta_{i,j}. \quad (3.52)$$

In case of bosons these results are referred to as *canonical commutation relations* (CCR):

$$[\hat{a}_i, \hat{a}_j^\dagger] = \delta_{i,j} \quad \text{and} \quad [\hat{a}_i, \hat{a}_j] = [\hat{a}_i^\dagger, \hat{a}_j^\dagger] = 0. \quad (3.53)$$

In case of fermionic systems we have the *canonical anticommutation relations* (CAR):

$$\{\hat{a}_i, \hat{a}_j^\dagger\} = \delta_{i,j} \quad \text{and} \quad \{\hat{a}_i, \hat{a}_j\} = \{\hat{a}_i^\dagger, \hat{a}_j^\dagger\} = 0, \quad (3.54)$$

where $\{\hat{A}, \hat{B}\} := \hat{A}\hat{B} + \hat{B}\hat{A}$ denotes the anticommutator¹.

This formalism provides a very compact notation for many-body operators in terms of the single particle wave function and creation and annihilation operators. Let us illustrate this by considering the kinetic operator in (3.39). Due to the indistinguishability of the particles, we can write it as a sum of identical single-particle operators

$$\hat{T} = \sum_k \hat{T}_k = \sum_{i,j,k} \langle i | \hat{T}_k | j \rangle |i\rangle_k \langle j|_k, \quad (3.55)$$

where k labels a single-particle Hilbert space. Our aim is to express \hat{T} in terms of creation and annihilation operators. We consider its action on an arbitrary state of the form (3.44). Suppose $j \neq i$, then

$$\begin{aligned} & \left(\sum_k |i\rangle_k \langle j|_k \right) |\dots, n_i, \dots, n_j, \dots\rangle \\ &= \left(\sum_k |i\rangle_k \langle j|_k \right) \sqrt{\frac{\dots, n_i, \dots, n_j, \dots}{N!}} \sum_{\substack{i_1, \dots, i_N \\ (\dots, n_i, \dots, n_j, \dots)}} |i_1, i_2, \dots, i_N\rangle. \end{aligned} \quad (3.56)$$

The expression on the right-hand side can now be evaluated as follows: The n_j positions which are in state $|j\rangle$ will be replaced by state $|i\rangle$. This leads to n_j states with occupation numbers $n_j + 1$ and $n_i - 1$,

$$\begin{aligned} &= n_j \sqrt{n_i + 1} \frac{1}{\sqrt{n_j}} |\dots, n_i + 1, \dots, n_j - 1, \dots\rangle \\ &= \hat{a}_i^\dagger \hat{a}_j |\dots, n_i, \dots, n_j, \dots\rangle. \end{aligned} \quad (3.57)$$

For $i = j$ the evaluation is straightforward

$$\left(\sum_k |i\rangle_k \langle j|_k \right) |\dots, n_i, \dots\rangle = n_i |\dots, n_i, \dots\rangle = \hat{a}_i^\dagger \hat{a}_i |\dots, n_i, \dots\rangle. \quad (3.58)$$

¹ Note that in the context of canonical quantisation of relativistic field theories the commutation relations are multiplied by the complex number i on the rhs

Hence we can write (3.55) in terms of creation and annihilation operators

$$\hat{T} = \sum_{i,j} \langle i | \hat{T}_k | j \rangle \hat{a}_i^\dagger \hat{a}_j. \quad (3.59)$$

This can be generalized to two-body operators. For example, the interaction potential in (3.39) can be rewritten as

$$\begin{aligned} \frac{1}{2} \sum_{k \neq l} \hat{V}(\mathbf{x}_l, \mathbf{x}_k) &= \frac{1}{2} \sum_{k \neq l} \sum_{\substack{ij \\ mn}} \langle i, j | \hat{V} | m, n \rangle |i\rangle_k |j\rangle_l \langle m|_k \langle n|_l \\ &= \frac{1}{2} \sum_{\substack{ij \\ mn}} \langle i, j | \hat{V} | m, n \rangle \hat{a}_i^\dagger \hat{a}_j^\dagger \hat{a}_m \hat{a}_n. \end{aligned} \quad (3.60)$$

Using the above, we may write Hamiltonian (3.39) in second quantised form

$$\hat{H} = \sum_{i,j} \hat{a}_i^\dagger \langle i | \hat{T} | j \rangle \hat{a}_j + \sum_{i,j,k,l} \hat{a}_i^\dagger \hat{a}_j^\dagger \langle ij | \hat{V} | kl \rangle \hat{a}_k \hat{a}_l. \quad (3.61)$$

A nice interpretation of this expression is to say that the kinetic operator T removes a particle in state ψ_j and adds one in state ψ_i weighted by its single particle matrix element $T_{i,j}$. The same applies to the interaction term V with the difference that it removes and adds two particles. This form of the Hamiltonian is generally referred to as *second quantised* form.

Let us close this short introduction by considering what happens to (3.61) if we change the single particle basis $\{|j\rangle\}$ to another $\{|\mu\rangle\}$. Using the completeness of both bases we can write

$$\hat{a}_\mu^\dagger |0\rangle = |\mu\rangle = \underbrace{\left(\sum_j |j\rangle \langle j| \right)}_{=1} |\mu\rangle = \sum_j \langle j | \mu \rangle \hat{a}_j^\dagger |0\rangle. \quad (3.62)$$

From this we obtain the transformation rule for the creation operators:

$$\hat{a}_\mu^\dagger = \sum_j \langle j | \mu \rangle \hat{a}_j^\dagger. \quad (3.63)$$

A useful basis for the description of single-particle problems is the position basis $\{|x\rangle\}$. Transformation of a countable basis $\{|i\rangle\}$ into this basis yields the *field operators*,

$$\hat{\psi}^\dagger(x) := \sum_i \langle i | x \rangle \hat{a}_i^\dagger = \sum_i \phi(x) \hat{a}_i^\dagger \quad \text{and} \quad \hat{\psi}(x) = \sum_i \phi_i(x) \hat{a}_i. \quad (3.64)$$

The completeness of the single particle basis implies the commutation relations

$$\left[\hat{\psi}(x), \hat{\psi}^\dagger(y) \right] = \sum_i \psi_i(y) \overline{\psi_i(x)} = \delta(x - y), \quad (3.65)$$

and

$$\left[\hat{\psi}^\dagger(x), \hat{\psi}^\dagger(y) \right] = \left[\hat{\psi}(x), \hat{\psi}(y) \right] = 0. \quad (3.66)$$

We can interpret the action of the field operators as creating or removing a particle at position x . In case of fermions analogous identities follow for the anticommutator. The Hamiltonian (3.61) transforms in terms of field operators into

$$\hat{H} = \int dx \hat{\psi}^\dagger(x) \hat{T} \hat{\psi}(x) + \frac{1}{2} \int dx dy \hat{\psi}^\dagger(x) \hat{\psi}^\dagger(y) V(x, y) \hat{\psi}(x) \hat{\psi}(y). \quad (3.67)$$

Our proposal for an effective theory of ultracold chemical reactions will use second quantised Hamiltonians of similar form in position representation.

3.3 Proposed framework

In this section we present a framework providing an effective description of ultracold chemical reaction kinetics. Following our definition of ultracold chemistry as 'chemical reactions driven by the coherent interaction of quantum degenerate Fermi or Bose gases', we resort to the language of second quantisation to formulate a framework for the corresponding reaction kinetics. Second quantisation in connection with ultracold quantum gases is validated by its success in describing phenomena like superfluidity in case of bosons [Bog47] and superconductivity in case of fermions [Bar57]. Moreover, in contrast to a first quantised description, the incorporation of creation and annihilation of particles as it happens in a chemical transformation is easy to implement in the description of second quantised operators.

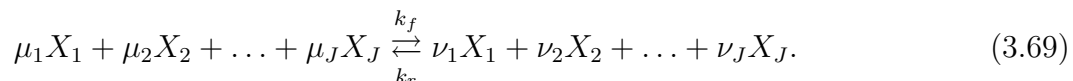
The standard approaches to constructing a second-quantised field theory, the path integral formalism and canonical quantisation, consider a classical Lagrangian field theory as a starting point. A possible ansatz would thus be to look for a classical field theory that is in some sense related to the equations of classical reaction kinetics. Indeed, the theory of reaction kinetics can be extended to incorporate positional degrees of freedom, resulting in *reaction-diffusion* systems [Nic77]. However, the results obtained in 3.1 hint that it might be very difficult to find a Hamiltonian or Lagrangian field density that reproduces the proper dynamics on a subspace. Therefore we take another route here and consider the set of single-particle quantum states as a starting point. These quantum states describe a single bosonic or fermionic particle in the context of a degenerate quantum gas. Following the second quantisation procedure considered in the previous section then results in a second-quantised version

of Schrödinger's equation

$$i \frac{\partial |\psi(t)\rangle}{\partial t} = \hat{H} |\psi(t)\rangle, \quad (3.68)$$

where $|\psi(t)\rangle$ is an abstract state vector of an underlying Fock space. Following this approach, the central problem is to determine a suitable Hamilton operator, which effectively describes an ultracold chemical reaction between the degenerate quantum gases. One important aspect of using (3.68) to describe a chemical reaction is that this elementary quantum description amounts to coherent, energy-conserving and time-reversal-invariant dynamics. This seems to be contradictory as we know that the dissipation resulting from energy gain or loss is the driving force of classical chemical reactions. We argue here in two ways: First, there is no reason why particle conversion in the ultracold regime such as molecule production should be inherently connected to an energy gain or loss. A prominent counterexample is spontaneous parametric down-conversion of photons in quantum optics [Bur70]. And secondly, we know from various physical models (e.g. quenched systems [Sch13]) that even closed quantum systems can be 'driven' to equilibrium due to growth of entanglement. The question remains how we can obtain classical reaction kinetics as a classical limit if the proposed Hamiltonian does not result from quantisation of the classical system. Here we argue that the model we are going to propose can readily be extended to incorporate possible environmental effects such as energy gains or losses. By successively incorporating more and more environmental effects, we eventually expect to reproduce high-temperature kinetics.

We start to present our proposal by recapitulating the cornerstones of classical reaction kinetics for a general elementary chemical equation



The important quantities determining the time evolution of each species density $[X_j]$ are the stoichiometric coefficients (μ_j, ν_j) and the rate constants k_i and k_f . Classical kinetics maps these parameters to a coupled first-order ODE system. Solving this for given initial conditions provides the dynamical evolution of the species concentration.

Translating scheme (3.69) into a framework of interacting quantum fields, we first assign every reacting species X_j to a corresponding set of quantum field operators $\{\hat{\psi}_{X_j}(x)\}_{x \in \mathbb{R}}$ (see (3.64)), that is a d -dimensional quantum field $\hat{\psi}_{X_j}$. For the sake of simplicity, and since we are interested in basic phenomena, we will focus throughout this thesis on the case $d = 1$. We assume the quantum field to be contained inside in a (1-dimensional) box with length L and periodic boundary conditions. The

underlying Hilbert space is given by the tensor product of each species Fock space

$$\mathcal{H} = \bigotimes_{j=0}^J \mathcal{F}_{X_j}. \quad (3.70)$$

Representing a classical system, all possible observables in classical reaction kinetics can be measured jointly. However, proposing a quantum field theoretical description for chemical reactions, we are confronted with the typical quantum situation of incompatible observables. A common interpretation of quantum field theory is that particles are considered as excitations of the quantum field. Therefore the particle number operator

$$\hat{N}_{X_j} = \int dx \hat{\psi}_{X_j}^\dagger(x) \hat{\psi}_{X_j}(x), \quad (3.71)$$

should count the overall number of particles of species X_j . The number of particles seems to be a natural candidate to replace the role of the classical particle concentration, and is even directly related to it when we divide the number of particles by the size of the considered volume V . To make direct comparison between classical and quantised kinetics possible, we consider the trajectories of the *expectation value* of the particle number operator as the quantum counterpart of the classical trajectory.

The crucial part of our proposal is now the choice of the Hamilton operator \hat{H} describing the ultracold chemical reaction. For the sake of clarity, we split the Hamiltonian into two parts

$$\hat{H} = \hat{H}_0 + \hat{H}_{\text{int}}. \quad (3.72)$$

The first part H_0 is a non-interacting part and models the standard kinetic and potential terms of each species. This part should dominate in the absence of a chemical reaction in the system. This situation occurs if the degenerate condensates are spatially separated. Expressing the standard terms in position basis yields

$$\hat{H}_0 = \int dx \sum_{j=0}^J \left(\hat{\psi}_{X_j}^\dagger(x) \left(\hat{T}_{X_j} + V_{X_j}(x) \right) \hat{\psi}_{X_j}(x) \right). \quad (3.73)$$

Here the potential term $V_{X_j}(x)$ models the trapping potential of the ultracold degenerate gas. In a next step, we define a suitable interaction term \hat{H}_{int} describing the chemical reaction, that is, the conversion of particles between the species. Similarly as in [Dru98], we take guidance from the successful description of photon conversion by quantum fields in non-linear optics. In the quantum optical setting the interactions between the modes of the quantum field are modelled by non-linear interaction terms

resulting from a canonical quantisation of the electromagnetic field in a non-linear crystal [Wal07]. Analogously, considering the nonlinear terms in the equations of motion in classical kinetics, we propose the following interaction Hamiltonian for the elementary reaction (3.69)

$$\hat{H}_{\text{int}} = \int dx \left(k_f \prod_{j=0}^J \left(\hat{\psi}_{X_j}^\dagger(x) \right)^{\nu_j} \left(\hat{\psi}_{X_j}(x) \right)^{\mu_j} + k_r \prod_{j=0}^J \left(\hat{\psi}_{X_j}^\dagger(x) \right)^{\mu_j} \left(\hat{\psi}_{X_j}(x) \right)^{\nu_j} \right), \quad (3.74)$$

where the $\hat{\psi}_{X_j}$ obey the canonical commutation relations (CCR) or canonical anti-commutation relations (CAR) according to particle type of the species. This proposal extends the previous approaches in different ways. Whereas previous work focuses on bosonic diatomic molecule formation [Gór01; Hop01; Oli04], our proposal allows the reaction to have an arbitrary order. Higher orders will merely lead to an increase of the degree of the monomial of field operators in (3.74). The reaction can consist of bosons and fermions and undergo a change of statistics, for instance the formation of bosonic molecules from pairs of fermionic particles. Note that due to symmetry requirements for fermionic particles without any inner degree of freedom the stoichiometric coefficients are restricted to $\mu_i, \nu_i \in \{0,1\}$. To circumvent this issue, we can add degrees of freedom to the model, e.g. a spin coordinate for each species $\Psi_{X_j}(x) \mapsto \Psi_{X_j}(x, \sigma)$. Alternatively, we can assume the formation of particles to not occur exactly at position x , but instead at an infinitesimally shifted position $x + dx$.

As a next step, let us discuss the role of the reaction constants in the proposed model. In contrast to previous approaches, the reaction constants of forward and reverse reaction can be different. Considering the overall Hamiltonian (3.72), the reaction constants represent the coupling strength between the quantum fields and, in contrast to classical reaction kinetics, can take complex values. This includes negative reaction constants, which makes the comparison to the classical interpretation, as rate or probability with which the particles react, difficult. However, in previous work the reaction constants were real valued as they resulted from a description of concrete physical setting. For instance, they might represent the limit of dipole matrix elements in photoassociation [Kos00] or the S-wave limit of interparticle scattering [Dru98]. Assuming complex reaction constants, we immediately infer the following constraint from the hermiticity of \hat{H}_{int} :

$$k_f = \bar{k}_r. \quad (3.75)$$

This implies that it is not possible to model non-trivial irreversible reactions within the framework of our proposal. This is a consequence of the fact that our system is

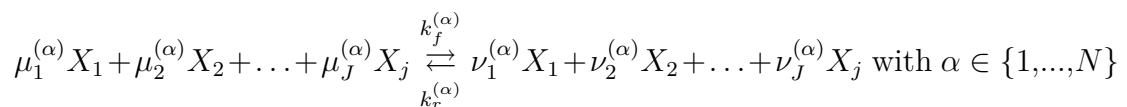
closed. Nevertheless, we want to introduce the concept of *overall reaction order* as a useful tool for the classification of the complexity of the resulting reaction dynamics. Remember, in classical kinetics the overall order of the reaction is defined as the sum of the stoichiometric coefficients of the reactant species (2.12), or equivalently, the sum of all exponents in the rate equation. The definition is restricted to irreversible reactions, since for reversible reactions terms appear in the denominator of (2.11), making the classification by the overall order ambiguous. However, according to our proposal the reversible part of the reaction is expressed by creation operators in the forward and annihilation operators in the backward part of \hat{H}_{int} . Therefore the backward and forward reaction parts contribute in the same way to the interaction Hamiltonian. Considering the overall order as sum of the exponents, we can generalise the concept to the ultracold setting by defining

$$O_{uc} := \sum_j \nu_j + \sum_j \mu_j. \quad (3.76)$$

This means that the order of the chemical reaction corresponds to the order of the monomial of field operators inside the Hamiltonian. As a simple consequence, in case of spinless fermions we need a minimum number of participating species J for a given order

$$J \geq \left\lceil \frac{O_{uc}}{2} \right\rceil. \quad (3.77)$$

The study of elementary ultracold reactions seems already very promising as the quantum optical analog, quantum field theory of nonlinear optics, shows a rich structure of phenomena ranging from solitary waves in crystals to the generation of squeezed states of light [Dru14]. However, similarly to classical reaction kinetics, we expect even more interesting phenomena to appear, if we consider a *network* of ultracold reactions. In order to define the interaction Hamiltonian describing an ultracold reaction network, we take guidance from the classical setting, which simply superposes the equations of motion for each reaction. Therefore we propose, for a network of N ultracold reactions



to take the sum of each of the interaction Hamiltonians $\hat{H}_{\text{int}} = \sum_{\alpha=1}^N \hat{H}_{\text{int}}^{(\alpha)}$ as the Hamiltonian describing the overall system. This superposition of each system should be valid as long the reactions are sufficiently decoupled from each other. Finally, we mention that, similar to the classical case, the treatment of multiple concurrent

reactions will increase the complexity of the considered system and therefore impede the finding of analytical and numerical solutions.

Let us close the section with a first discussion of our proposed model. In contrast to the result of first quantisation, our proposed model contains a non-interacting term, representing the system in absence of chemical reactions. The non-existence of this term in the first quantised examples stems from the fact that the dynamical equations of classical kinetics do not cover the ‘non-interacting’ scenario. However, this term is of major importance in the ultracold setting. We learn from the theory of interacting Bose gases that changing the external potential can lead to entirely different behaviour of the condensate [Bag87]. Considering the proposed interaction Hamiltonian (3.74), it is clear that such an effective description can only occur after various approximations of a real physical model. However, we know from dilute interacting Bose gases that exactly local interactions can arise as the low-temperature limit of some complex shaped interaction potential. Also the nonlinear terms in case of high-order reactions, like the formation of diatomic molecules, have been successfully applied in quantum optics. The fact that the rate constants are complex valued in the ultracold setting seems to impede the comparison to the rate constants of classical kinetics. However, so far we have not specified in which way classical reaction kinetics appears as classical of our framework. Hence there is no need at this point for consistency of the descriptions.

CHAPTER 4

Elementary bosonic reactions

High-temperature kinetics show that the dynamics of classical low-order reactions have a compact solution. The corresponding dynamical systems can be solved in analytical form, making it possible to explicitly calculate characteristic values in terms of the rate constant and initial conditions. For example, the half-life of a first-order reaction is the natural logarithm of two divided by the reaction constant [Con90]. These results of classical kinetics inspire us to investigate ultracold low-order reactions. Table 4.1 shows interaction Hamiltonians for elementary reactions according to our proposal. Throughout this chapter we restrict ourselves to consider real valued reaction constants. This makes it possible to compare the ultracold reactions to classical reactions. The zeroth-order reaction is just listed for the sake of completeness; some reaction constant added to the Hamiltonian has no impact on the dynamics. We see that elementary ultracold chemical reactions with order $O_{uc} \geq 3$ describe interacting field theories implying that it is not possible to find a

Table 4.1: The proposed interaction Hamiltonians for low-order reactions, assuming a real-valued reaction constant k . The single-mode approximation refers to the case where we expand the field operator in a single-particle basis and merely retain the first term of the expansion.

Order O_{uc}	Reaction	Proposed \hat{H}_{int}	One-mode approx.
0.	—	k	k
1.	$\boxed{\text{bath}} \xrightleftharpoons{k} A$	$k \int dx \left(\hat{\psi}_A^\dagger + \hat{\psi}_A \right)$	$k(\hat{a}_A^\dagger + \hat{a}_A)$
2.	$A \xrightleftharpoons{k} B$	$k \int dx \left(\hat{\psi}_A \hat{\psi}_B^\dagger + \text{h.c.} \right)$	$k(\hat{a}_A \hat{a}_B^\dagger + \text{h.c.})$
3.	$A + B \xrightleftharpoons{k} C$	$k \int dx \left(\hat{\psi}_A \hat{\psi}_B \hat{\psi}_C^\dagger + \text{h.c.} \right)$	$k(\hat{a}_A \hat{a}_B \hat{a}_C^\dagger + \text{h.c.})$
4.	$A + B \xrightleftharpoons{k} C + D$	$k \int dx \left(\hat{\psi}_A \hat{\psi}_B \hat{\psi}_C^\dagger \hat{\psi}_D^\dagger + \text{h.c.} \right)$	$k(\hat{a}_A \hat{a}_B \hat{a}_C^\dagger \hat{a}_D^\dagger + \text{h.c.})$

compact solution to these reactions. In contrast, reactions with $O_{uc} \leq 2$ describe ‘free’ or ‘quasi-free’ systems. These systems are known to be analytically solvable. However, we will see that even for low order reactions we can find dynamical regimes, which can not be transformed to normal modes.

The conservation of mass in closed chemical system is a frequently used fact in the dynamical analysis of chemical reactions. In particular for elementary reactions the mass balance equations give rise to a conserved quantity and therefore restrict the temporal evolution to a subspace of the full state space. Since conserved quantities also simplify the analysis of quantum systems, we investigate how the conservation of mass translates into our proposed framework.

This chapter is organised as follows. In section 4.1 we establish the existence of a conserved quantity in the case of an elementary bosonic reaction of any order. Starting from elementary reactions with distinct reactant and product species, we extend the conservation law to autocatalytic reactions. In section 4.2 we investigate the dynamics of elementary low-order reactions. Due to the fact that low-order reactions result in free field theories, we find analytical solutions for the occurring dynamics. This gives us the possibility to discuss the impact of the reaction constant as dynamical parameter. Moreover, we compare the dynamics of ultracold reactions to the dynamics of classical reactions of the same order.

4.1 Conservation law

The principle of mass conservation in chemical reactions results in a conserved quantity that facilitates the investigations in classical reaction kinetics. In this section we will show how the mass conservation carries over to the ultracold setting. We find that any elementary ultracold reaction in a closed system has a non-trivial constant of motion different from the energy. To get a better overview, let us first consider reactions which are not autocatalytic:



where we divided the participating species into reactants X_a and products X_b . Due to the fact that our framework merely allows for reversible reactions in which the roles of reactants and products can be interchanged, this distinction is somewhat artificial. Therefore we expect our results to be symmetric with respect to this partition. Nevertheless, using this notation, the property of being non-autocatalytic reads $A \cap B = \emptyset$. Moreover, the reaction is not allowed to couple to a bath, that is at least one of the μ_a and one of the ν_b is not equal zero. To ease the notation, we will label the quantum fields corresponding to some species by a small index, that is X_a by $\hat{\psi}_a$, etc. Applying our proposal to (4.1) results in the Hamiltonian $\hat{H} = \hat{H}_0 + \hat{H}_{int}$,

where

$$\begin{aligned} \hat{H}_0 = \hat{H}_{0,a} + \hat{H}_{0,b} &= \int dx \sum_a \left(\hat{\psi}_a^\dagger(x) \left(\hat{T}_a + V_a(x) \right) \hat{\psi}_a(x) \right) \\ &+ \int dx \sum_b \left(\hat{\psi}_b^\dagger(x) \left(\hat{T}_b + V_b(x) \right) \hat{\psi}_b(x) \right) \end{aligned} \quad (4.2)$$

and

$$\hat{H}_{\text{int}} = \int dx \underbrace{\prod_{a,b} k_f \left(\hat{\psi}_a^\dagger(x) \right)^{\mu_a} \left(\hat{\psi}_b(x) \right)^{\nu_b}}_{\hat{H}_{\text{int},f}} + \underbrace{\prod_{a,b} k_r \left(\hat{\psi}_a(x) \right)^{\mu_a} \left(\hat{\psi}_b^\dagger(x) \right)^{\nu_b}}_{\hat{H}_{\text{int},r}}, \quad (4.3)$$

where $\hat{H}_{\text{int},f}$ and $\hat{H}_{\text{int},r}$ describe the forward and reverse part of the reaction respectively. Given this notation, we will show that conservation of mass in classical systems translates to the conservation of the weighted *overall particle number* of the system

$$\hat{N}_{\text{tot}} := \left(\sum_b \nu_b \right) \sum_a \hat{N}_a + \left(\sum_a \mu_a \right) \sum_b \hat{N}_b, \quad (4.4)$$

where \hat{N}_a, \hat{N}_b denote the particle number operators (3.71) of the respective reactants and products. To ease the notation further, we write $M := \sum_a \mu_a$ and $K := \sum_b \nu_b$ for the sum of the stoichiometric coefficients. Due to the fact that the time evolution is induced by the Schrödinger equation, a sufficient criterion for \hat{N}_{tot} to be conserved is a vanishing commutator with the Hamiltonian of the overall system:

$$\left[\hat{H}, \hat{N}_{\text{tot}} \right] = \left[\hat{H}_0, \hat{N}_{\text{tot}} \right] + \left[\hat{H}_{\text{int}}, \hat{N}_{\text{tot}} \right] = 0. \quad (4.5)$$

In a first step, we focus on the commutator of the non interacting part, that is

$$\begin{aligned} \left[\hat{H}_0, \hat{N}_{\text{tot}} \right] &= \left[\sum_a \hat{H}_{0,a} + \sum_b \hat{H}_{0,b}, K \sum_a \hat{N}_a + M \sum_j \hat{N}_b \right] \\ &= K \sum_a \left[\hat{H}_{0,a}, \hat{N}_a \right] + M \sum_b \left[\hat{H}_{0,b}, \hat{N}_b \right]. \end{aligned} \quad (4.6)$$

Therefore, it suffices to show that for each species X_a, X_b the number operator \hat{N}_a, \hat{N}_b commutes with the standard kinetic and potential term. This is best illustrated by expanding the operators in a countable single particle basis $\{|j\rangle\}$. Let us pick an

arbitrary reactant species and consider the commutator

$$\begin{aligned}
\left[\hat{H}_{0,a}, \hat{N}_a \right] &= \left[\int dx \left(\hat{\psi}_a^\dagger(x) \left(\hat{T}_a + V_a(x) \right) \hat{\psi}_a(x) \right), \int dx \hat{\psi}_{A_i}^\dagger(x) \hat{\psi}_{A_i}(x) \right] \\
&= \left[\sum_{i,j,k} \langle i | \hat{T}_a + \hat{V}_a | j \rangle \hat{a}_i^\dagger \hat{a}_j, \hat{a}_k^\dagger \hat{a}_k \right] \\
&= \sum_{i,j,k} \langle i | \hat{T}_a + \hat{V}_a | j \rangle \left(\hat{a}_i^\dagger \underbrace{[\hat{a}_j, \hat{a}_k^\dagger \hat{a}_k]}_{\delta_{jk} \hat{a}_j} + \underbrace{[\hat{a}_i^\dagger, \hat{a}_k^\dagger \hat{a}_k]}_{-\delta_{ik} \hat{a}_i^\dagger} \hat{a}_j \right) \\
&= \sum_k \langle k | \hat{T}_a + \hat{V}_a | k \rangle \left(\hat{a}_k^\dagger \hat{a}_k - \hat{a}_k^\dagger \hat{a}_k \right) = 0.
\end{aligned} \tag{4.7}$$

Since this calculations also apply to product species, it shows that $\left[\hat{H}_0, \hat{N}_{\text{tot}} \right]$ in 4.5 vanishes. To prove that the commutator with the interacting part vanishes as well, we shall use the following identities [Sch05]:

$$\begin{aligned}
\left[\hat{N}_{a'}, \int dx \prod_a \left(\hat{\psi}_a^\dagger(x) \right)^{\mu_a} \right] &= \mu_{a'} \int dx \prod_a \left(\hat{\psi}_a^\dagger(x) \right)^{\mu_a} \\
\left[\hat{N}_{b'}, \int dx \prod_b \left(\hat{\psi}_b(x) \right)^{\nu_b} \right] &= -\nu_{b'} \int dx \prod_b \left(\hat{\psi}_b^\dagger(x) \right)^{\nu_b}.
\end{aligned} \tag{4.8}$$

Applying these identities for a sum of number operators of the reactants \hat{N}_a yields

$$\begin{aligned}
\left[\sum_{a'} \hat{N}_{a'}, \hat{H}_{\text{int},f} \right] &= \left[\sum_{a'} \hat{N}_{a'}, \int dx \prod_{a,b} k_f \left(\hat{\psi}_a^\dagger(x) \right)^{\mu_a} \left(\hat{\psi}_b(x) \right)^{\nu_b} \right] \\
&= \left(\sum_{a'} \mu_{a'} \right) \int dx \prod_{a,b} k_f \left(\hat{\psi}_a^\dagger(x) \right)^{\mu_a} \left(\hat{\psi}_b(x) \right)^{\nu_b} \\
&= M \hat{H}_{\text{int},f}.
\end{aligned} \tag{4.9}$$

Similarly, for the product species \hat{N}_b :

$$\begin{aligned} \left[\sum_{b'} \hat{N}_{b'}, \hat{H}_{\text{int},f} \right] &= \left[\sum_b \hat{N}_b, \int dx \prod_{a,b} k_f \left(\hat{\psi}_a^\dagger(x) \right)^{\mu_a} \left(\hat{\psi}_b(x) \right)^{\nu_b} \right] \\ &= - \left(\sum_{b'} \nu_{b'} \right) \int dx \prod_{a,b} k_f \left(\hat{\psi}_a^\dagger(x) \right)^{\mu_a} \left(\hat{\psi}_b(x) \right)^{\nu_b} \\ &= -K \hat{H}_{\text{int},f}. \end{aligned} \quad (4.10)$$

Now, with the previous results we can readily show that the commutator between \hat{N}_{tot} and $\hat{H}_{\text{int},f}$ vanishes:

$$\begin{aligned} \left[\hat{N}_{\text{tot}}, \hat{H}_{\text{int},f} \right] &= \left[K \left(\sum_a \hat{N}_a \right) + M \left(\sum_b \hat{N}_b \right), \hat{H}_{\text{int},f} \right] \\ &= (KM - MK) \hat{H}_{\text{int},f} = 0. \end{aligned} \quad (4.11)$$

Since the part of the interaction Hamiltonian modelling the reverse reaction is the adjoint of the forward part, it follows that

$$\left[\hat{N}_{\text{tot}}, \hat{H}_{\text{int},r} \right] = 0 \quad (4.12)$$

Altogether, this shows the validity of (4.5) and therefore the conservation of \hat{N}_{tot} . As we expected, we found that \hat{N}_{tot} is symmetric under the change of reactants and products: Interchanging the indices a and b amounts to the same conserved quantity.

The connection of \hat{N}_{tot} with the classical conservation of mass is best illustrated by an example. Consider the elementary fourth-order reaction



Due to the fact that classical kinetics assumes homogeneous concentrations, we neglect positional degrees of freedom in the quantum system by restricting ourselves to the ground state approximation of the proposed Hamiltonian

$$\hat{H} = E_A \hat{a}^\dagger \hat{a} + E_B \hat{b}^\dagger \hat{b} + k \left(\hat{a}^\dagger \hat{a}^\dagger \hat{b} \hat{b} + \hat{a} \hat{a} \hat{b}^\dagger \hat{b}^\dagger \right). \quad (4.14)$$

Within this approximation the overall particle number (4.4) for the reaction is given by

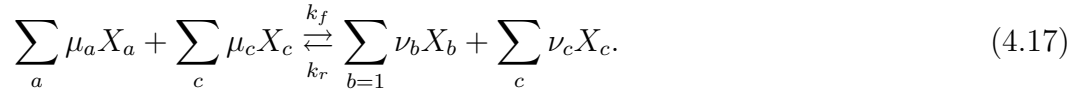
$$\hat{N}_{\text{tot}} = 2\hat{a}^\dagger \hat{a} + 2\hat{b}^\dagger \hat{b}. \quad (4.15)$$

To see the consequences of this conserved quantity for the dynamics, we consider the underlying Hilbert space in the occupation number bases $|n_A, n_B\rangle$. Furthermore, we assume the system to start in an eigenstate of \hat{N}_{tot} with eigenvalue N_{tot} . Instead of evolving through the whole Hilbert space, the dynamics is restricted to the subspace

$$\mathcal{H}_{N_{\text{tot}}} = \text{span} \left\{ |n_A, \frac{N_{\text{tot}} - 2n_A}{2n_B}\rangle : n_a \in \{0, 2, \dots, N_{\text{tot}}\} \right\}. \quad (4.16)$$

This reduces the solution of (4.14) to a finite dimensional problem as the dimension of the subspace is $N_{\text{tot}}/2$. Fig. 4.1 illustrates the evolution within the subspace for initially six particles in the system. Considering the evolution of the classical analogue of (4.13) in the classical state space, the conservation of mass results in exactly the same restrictions, if we replace the occupation numbers in the Fock states by the number of classical particles [Kam92]. Therefore, we can say that the conservation of \hat{N}_{tot} is the quantum analogue of the conservation of mass in classical chemistry.

In a next step, we extend the considered class of reactions and allow species X_c on both sides of the chemical equation:



This means that according to our proposal the forward part of the autocatalytic interaction Hamiltonian is

$$\hat{H}_{\text{int},f}^{(ac)} = \int dx \prod_{a,b,c} k_f \left(\hat{\psi}_a^\dagger(x) \right)^{\mu_a} \left(\hat{\psi}_b(x) \right)^{\nu_b} \left(\hat{\psi}_c^\dagger(x) \right)^{\mu_c} \left(\hat{\psi}_c(x) \right)^{\nu_c}. \quad (4.18)$$

Note that most of the reasoning from the non-autocatalytic case be translated into this setting. In particular, the quantity (4.4) remains an non-trivial constant of motion on the subsystem of species X_a and X_b . The problem is to figure out the weight of autocatalytic number operators \hat{N}_c in the contribution to \hat{N}_{tot} such that it commutes with (4.18). For this purpose, we consider the commutator between $\hat{N}_{c'}$ and the part of (4.18) which models the autocatalytic contribution:

$$\begin{aligned} & \left[\hat{N}_{c'}, \int dx \left(\hat{\psi}_c^\dagger(x) \right)^{\mu_c} \left(\hat{\psi}_c(x) \right)^{\nu_c} \right] \\ &= \int dx \left(\hat{\psi}_c^\dagger(x) \right)^{\mu_c} \left[\hat{N}_{c'}, \left(\hat{\psi}_c(x) \right)^{\nu_c} \right] + \left[\hat{N}_{c'}, \int dx \left(\hat{\psi}_c^\dagger(x) \right)^{\mu_c} \right] \left(\hat{\psi}_c(x) \right)^{\nu_c} \\ &= (\mu_{c'} - \nu_{c'}) \int dx \left(\hat{\psi}_c^\dagger(x) \right)^{\mu_c} \left(\hat{\psi}_c(x) \right)^{\nu_c}. \end{aligned} \quad (4.19)$$

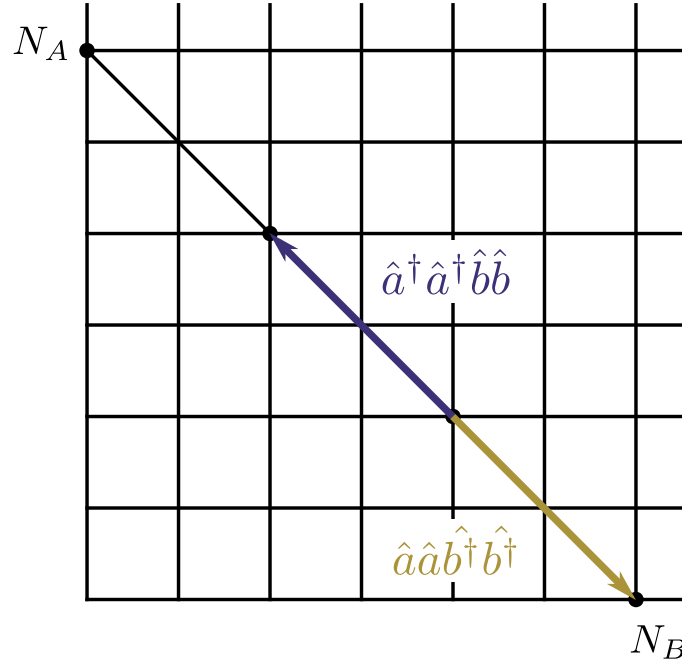


Figure 4.1: Illustration of subspace (4.16) for the case of six particles in the system. Each point where the grid-lines intersect represents a possible state in Fock space. Starting in the state $|4,2\rangle$, the dynamics is restricted to the states marked by a dot. This can be understood by considering the interaction part of (4.14). While the non-interacting part does not convert between the species, the interaction part either creates or annihilates two particles of species A and B correspondingly. The same kind of restriction of the state space can be found for the classical kinetics of reaction (4.13), if we replace the occupation number of Fock modes with the classical particle number.

Therefore, introducing $L := \sum_c (\mu_c - \nu_c)$ we find

$$\left[\sum_{a,b,c} \hat{N}_a + \hat{N}_b + \hat{N}_c, \hat{H}_{\text{int},f}^{(ac)} \right] = (M + L - K) \hat{H}_{\text{int},f}^{(ac)}, \quad (4.20)$$

and eventually the conserved quantity

$$\hat{N}_{\text{tot}}^{(ac)} = K \left(\sum_a \hat{N}_a \right) + K \left(\sum_c \hat{N}_c \right) + (M + L) \left(\sum_b \hat{N}_b \right). \quad (4.21)$$

The conservation of the overall particle number reduces the degree of freedom for elementary reactions by one. This will be useful in particular when we deal with high-order elementary reactions, like the diatomic molecule formation. Considering this conservation law as the quantum analogue of the conservation of mass, we expect

this law to carry over in a modified form to the case of concurrent reactions. However, if the considered system is coupled to some environment, this conservation law is immediately violated.

4.2 Low-order reactions

Solutions to the equations of motion of classical low-order reactions can be given in closed analytical form [Upa07]. This results in detailed knowledge of the system's behaviour under the change of experimental parameters, making it possible to identify dynamically interesting phenomena. Motivated by this systematic classification we consider ultracold low-order reactions. As shown in Table 4.1, ultracold reactions with order less than or equal two amount to non-interacting quantum fields. These are known to be exactly solvable via a transformation to normal modes. The physical systems we will encounter are reminiscent of typical models in quantum optics. This fact lets us hope that we obtain compact solutions to the dynamics of ultracold reactions. In what follows we study the dynamics of low-order reactions and compare the results to the kinetics of the analogous classical reactions.

A useful operation that we will frequently use to study the dynamics of chemical reactions is the so called *operator mode expansion*. As we mentioned in section 3.2, we can rewrite the field operators in terms of an arbitrary orthonormal single-particle basis $\{|i\rangle\}$ as follows

$$\hat{\psi}(x) := \sum_i \langle i|x\rangle \hat{a}_i = \sum_i \phi_i(x) \hat{a}_i. \quad (4.22)$$

Which one of the possible single-particle bases is the most suitable to study the proposed Hamiltonian depends on the physical situation. Assuming that the particles are confined in a finite box with periodic boundary conditions and without external potential, plane waves are a promising candidate:

$$\hat{\psi}(x) = \frac{1}{\sqrt{L}} \sum_n e^{-i\omega_n x} \hat{a}_n, \quad (4.23)$$

with $\omega_n = \frac{2\pi}{L}n$ and $n \in \mathbb{Z}$ labelling the modes of the free particle. Given the free-particle situation, the non-interacting part of the Hamiltonian is diagonal in this basis. An important advantage of this operator mode expansion is that it allows us to readily implement approximations into our model. For instance, if we assume all species to be in the ground state during the reaction, we speak of the *one-mode approximation* and merely retain the $\omega_n = 0$ term. Another step that simplifies the problem is to perform a momentum cut-off and fix a maximal n_{max} after which we stop the expansion.

4.2.1 First-order reaction

A first-order reaction is not a chemical reaction per se, due to the absence of any interaction of different species. It can be rather understood as a connection of the considered species to some reservoir:



Within our framework this corresponds to the Hamiltonian

$$\hat{H} = \int dx \left(\hat{\psi}_A^\dagger(x) \left(\hat{T}_A + V_A(x) \right) \hat{\psi}_A(x) \right) + k \int dx \left(\hat{\psi}_A^\dagger(x) + \hat{\psi}_A(x) \right). \quad (4.25)$$

Let us first put our attention to the interacting part of the Hamiltonian. This part determines the dynamics if the coupling strength k is much larger than other energies in the system. If the dynamics are dominated by \hat{H}_{int} , we refer to this situation as *strong coupling regime*. The operator mode expansion yields for a general single-particle basis $\{\phi_i(x)\}$

$$\begin{aligned} \hat{H}_{\text{int}} &= k \int dx \left(\hat{\psi}_A^\dagger(x) + \hat{\psi}_A(x) \right) \\ &= k \sum_i \int dx \left(\overline{\phi_i(x)} \hat{a}_i^\dagger + \phi_i(x) \hat{a}_i \right), \end{aligned} \quad (4.26)$$

and in particular for the plane waves as single-particle basis.

$$\begin{aligned} \hat{H}_{\text{int}} &= \frac{k}{\sqrt{L}} \int_0^L dx \left(\sum_n e^{i\omega_n x} \hat{a}_n^\dagger + \sum_m e^{-i\omega_m x} \hat{a}_m \right) \\ &= k\sqrt{L} \left(\hat{a}_0^\dagger + \hat{a}_0 \right). \end{aligned} \quad (4.27)$$

We see that the created and annihilated particles all have zero momentum. The generated dynamics of the ground state mode can be solved analytically. This solution can be obtained intuitively, if we rewrite (4.27) in terms of the position operator $\hat{x} = \frac{\hat{a}_0^\dagger + \hat{a}_0}{\sqrt{2}}$:

$$\hat{H}_{\text{int}} = k\sqrt{L} \left(\hat{a}_0^\dagger + \hat{a}_0 \right) = \underbrace{k\sqrt{2L}}_{\tilde{k}:=} \hat{x}_0 \quad (4.28)$$

Position operators are the displacement generators in momentum space:

$$\begin{aligned}\frac{d\langle\hat{p}_0\rangle}{dt} &= i\tilde{k}\langle[\hat{x}_0,\hat{p}_0]\rangle = -\tilde{k} \\ \frac{d\langle\hat{p}_0^2\rangle}{dt} &= i\tilde{k}\langle[\hat{x}_0,\hat{p}_0^2]\rangle = -2\tilde{k}\langle\hat{p}_0\rangle\end{aligned}\tag{4.29}$$

Solving these equations results in a quadratic scaling of the average particle number in the ground state mode $\langle\hat{n}_0(t)\rangle \propto t^2$:

$$\begin{aligned}\langle\hat{n}_0(t)\rangle &= \frac{1}{2}(\langle\hat{x}_0^2\rangle(t) + \langle\hat{p}_0^2\rangle(t) - 1) \\ &= \frac{1}{2}(\langle x_0^2(0)\rangle + \langle p_0^2(0)\rangle + \tilde{k}^2 t^2 - 2\tilde{k}\langle p_0(0)\rangle t - 1),\end{aligned}\tag{4.30}$$

where $\langle x_0^2(0)\rangle$, $\langle p_0^2(0)\rangle$ and $\langle p_0(0)\rangle$ denote the initial expectation of the respective operators. Assuming the modes with momentum $k \neq 0$ to be initially depleted, all particles of species A will have zero momentum and therefore $\langle\hat{n}_A(t)\rangle = \langle\hat{n}_0(t)\rangle$. An alternative account to understand the dynamics induced by the interaction Hamiltonian is to identify (4.27) as the generator of a displacement operator for coherent states (5.2). As the time increases the operator displaces the coherent state linearly into a certain direction of the phase spaces. Since the number of particles within a coherent state is given by the magnitude squared of the complex number labelling the state, the linear displacement leads to a quadratic increase of the ground state mode.

In what follows, we describe a possible physical situation where the first-order interaction follows as a natural approximation. Consider the second-order reaction



This models a simple particle conversion and occurs for example in quantum optics modelling linear interactions [Wal07]. For the sake of a clear notation, we label in the following the creation and annihilation operators according to the name of the species, that is \hat{a} represents species A and \hat{b} labels B . Considering the plane wave

expansion of the proposed interaction Hamiltonian leads to

$$\begin{aligned}
\hat{H}_{int} &= k \int dx \left(\hat{\psi}_A(x) \hat{\psi}_B^\dagger(x) + \hat{\psi}_A^\dagger(x) \hat{\psi}_B(x) \right) \\
&= \frac{k}{L} \int_0^L dx \left(\sum_{n,n'} e^{i(\omega_n - \omega_{n'})x} \hat{a}_n^\dagger \hat{b}_{n'} + \sum_{m,m'} e^{-i(\omega_m - \omega_{m'})x} \hat{a}_m \hat{b}_{m'}^\dagger \right) \\
&= k \left(\sum_n \hat{a}_n^\dagger \hat{b}_n + \sum_m \hat{a}_m \hat{b}_m^\dagger \right)
\end{aligned} \tag{4.32}$$

Now, the crucial step to obtain the first-order reaction as approximation is to assume, that for both species only the ground state mode is occupied. This is a valid assumption for a condensate of ultracold particles. Furthermore, the particle number of the ground state mode of species B shall be much larger than the particle number of the ground state mode of species A . In this case we can employ the Bogoliubov approximation [Lie05],

$$b_0 = b_0^\dagger = \sqrt{N_{0,B}} \in \mathbb{R}, \tag{4.33}$$

where $N_{0,B}$ labels the occupation number of the ground state. Substituting this approximation into 4.32 yields

$$\hat{H}_{int} = k \sqrt{N_{0,B}} \left(\hat{a}_0^\dagger + \hat{a}_0 \right), \tag{4.34}$$

which is identical to the interaction Hamiltonian of the first-order reaction (4.27), where we identify $\sqrt{L} = \sqrt{N_{0,B}}$.

After solving the interaction Hamiltonian, we now incorporate the non-interacting term to obtain the full description of the reaction. In the case of no external potential, the plane wave expansions yields

$$\begin{aligned}
\hat{H}_0 + \hat{H}_{int} &= \sum_p \frac{p^2}{2m_A} \hat{a}_p^\dagger \hat{a}_p + \underbrace{k\sqrt{L}}_{\tilde{k}} \left(\hat{a}_0^\dagger + \hat{a}_0 \right) \\
&= \sum_{p \neq 0} \frac{p^2}{2m_A} \hat{a}_p^\dagger \hat{a}_p + \tilde{k} \left(\hat{a}_0^\dagger + \hat{a}_0 \right),
\end{aligned} \tag{4.35}$$

which means that the number of particles in the ground state mode evolves according to (4.30), while the number of particles in the other modes stays constant. Let us further extend our studies to a non-vanishing potential $V_A(x)$. In this case, we find

that \hat{H}_0 couples the plane wave modes,

$$\hat{H}_0 + \hat{H}_{\text{int}} = \sum_{n,m} \underbrace{\langle n | \left(\hat{T}_A + V_A(x) \right) | m \rangle}_{C_{n,m} :=} \hat{a}_n^\dagger \hat{a}_m + \tilde{k} \left(\hat{a}_0^\dagger + \hat{a}_0 \right). \quad (4.36)$$

The introduced coefficient matrix C is by definition hermitian and we denote U as the diagonalising transformation. Note at this point that unitary transformations on modes $\hat{b}_j = \sum_i U_{ji} \hat{a}_i$ preserve the CCR:

$$\left[\hat{b}_j, \hat{b}_k^\dagger \right] = \left[\sum_i U_{ji} \hat{a}_i, \sum_l \bar{U}_{lk} \hat{a}_l^\dagger \right] = \sum_{il} U_{ji} \bar{U}_{lk} \left[\hat{a}_i, \hat{a}_l^\dagger \right] = \sum_i U_{ji} \bar{U}_{ik} = \delta_{ik} \quad (4.37)$$

Applying the diagonalising transformation, we can rephrase the Hamiltonian in terms of other modes $\hat{a}_n = \sum_m U_{nm} \hat{c}_m$, yielding the decoupled system

$$\begin{aligned} \hat{H} &= \sum_{\substack{n,m \\ k,l}} \bar{U}_{k,n} C_{n,m} U_{m,l} \hat{c}_k^\dagger \hat{c}_l + \tilde{k} \sum_l \left(\bar{U}_{l,0} \hat{c}_l^\dagger + U_{0,l} \hat{c}_l \right) \\ &= \sum_l \lambda_l \hat{c}_l^\dagger \hat{c}_l + \tilde{k} \sum_l \left(\bar{U}_l' \hat{c}_l^\dagger + U_l' \hat{c}_l \right) = \sum_l \hat{H}^{(l)}, \end{aligned} \quad (4.38)$$

where λ_l labels the eigenvalues of C and $U_l' = U_{0,l}$. In a next step, we can neglect the phase factors \bar{U}_l' and U_l' due to the fact that they have no effect to the dynamics. This leads to

$$\hat{H}^{(l)} = \lambda_l \hat{c}_l^\dagger \hat{c}_l + \tilde{k} (\hat{c}_l^\dagger + \hat{c}_l) \quad (4.39)$$

as Hamiltonian which induces the dynamics of the first-order reaction in an external potential. This system represents a shifted harmonic oscillator as we see by the transformation $\hat{c}_l + \frac{\tilde{k}}{\lambda_l} = \hat{d}_l$:

$$\begin{aligned} \hat{H}^{(l)} &= \lambda_l \left(\hat{d}_l^\dagger - \frac{\tilde{k}}{\lambda_l} \right) \left(\hat{d}_l - \frac{\tilde{k}}{\lambda_l} \right) + \tilde{k} \left(\hat{d}_l^\dagger - \frac{\tilde{k}}{\lambda_l} \right) + \tilde{k} \left(\hat{d}_l - \frac{\tilde{k}}{\lambda_l} \right) \\ &= \lambda_l \hat{d}_l^\dagger \hat{d}_l - \frac{\tilde{k}^2}{\lambda_l}, \end{aligned} \quad (4.40)$$

where the \hat{d}_l obey by definition the CCR. Assuming the vacuum as initial state, the expectation value of the number operator of each mode evolves according to

$$\left\langle \hat{N}^{(l)}(t) \right\rangle = \left(\frac{\sqrt{2\tilde{k}}}{\lambda_l} \right)^2 (1 - \cos \lambda_l t) = \left(\frac{\sqrt{2k}}{\lambda_l} \right)^2 N_{0,B} (1 - \cos \lambda_l t), \quad (4.41)$$

where for the last equality we identified $\sqrt{L} = \sqrt{N_{0,B}}$, meaning we consider the first-order reaction as an effective approximation of a second-order reaction. The closed analytical form in (4.41) allows us to identify the role of the energies λ_l and \tilde{k} for the ultracold reaction: The amplitude of the oscillations is determined through the ratio between the coupling constant and energy. However, the frequency of the oscillations solely depends on the eigenenergies.

Motivated by this result, let us draw comparison to the classical analogue of (4.24). Applying the scheme of classical reaction kinetics to 4.24, we obtain

$$\frac{d[A]}{dt} = -k[A] + kN_0 \quad (4.42)$$

as resulting equation of motion for the particle concentration. N_0 denotes here the concentration of the bath species which remains constant during the time evolution. Equation 4.42 has the solution

$$[A](t) = N_0(1 - e^{-kt}), \quad (4.43)$$

if we choose $[A]_0 = 0$ as initial condition. To complete the comparison, we also consider the case where $N_0 \gg [A]$ effectively making the first term in 4.42 negligibly small, which is the classical analogue to the situation that the coupling energy k is much larger than the other energies in the system. In this situation the concentration linearly increases in time according to

$$[A](t) = kN_0t. \quad (4.44)$$

Comparing the quantum to the classical trajectories (see Fig. 4.2), we see that the classical particle concentration relaxes to the particle number of the bath, whereas the quantum occupation number in the case of a non-vanishing potential is oscillating between bath and species. However, the case of a strong coupling constant k or a vanishing external potential the average particle number increases quadratically, whereas the classical case of a large reservoir, that is $N_0 \gg [A]$, results in a linear increase of the particle concentration. We see that at some point the strong coupling limit breaks down, because the particle number in the ground state mode becomes larger than the number of particles in the reservoir. However, for small times the evolutions of the strong coupling approximation and the particles in an external potential coincide.

4.2.2 Second-order reactions

The class of elementary second-order reactions can be divided in two different sets which we expect to show fundamentally different dynamics. The first set consists of the reaction , which models particle conversion between two species. Due to the fact

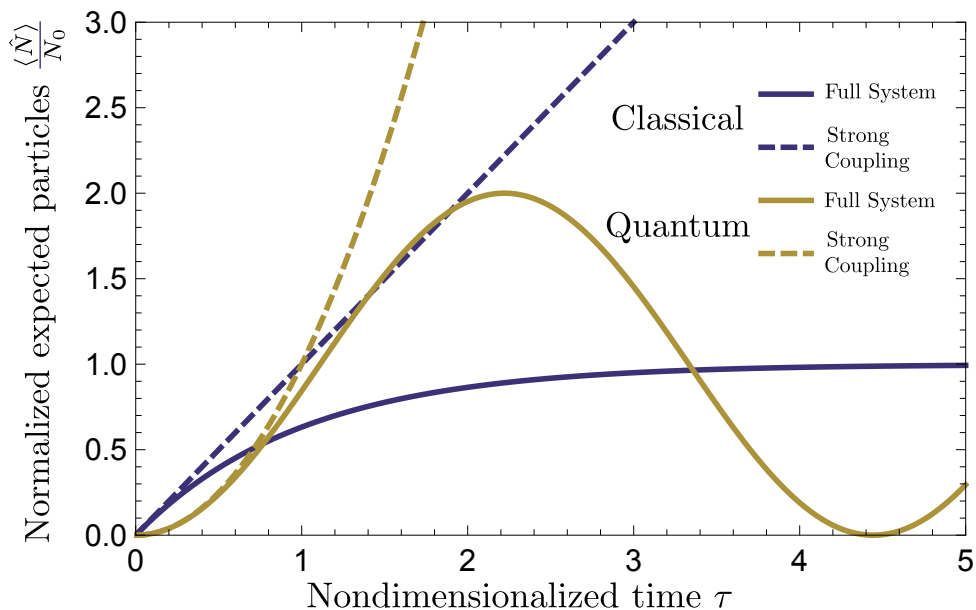


Figure 4.2: The temporal evolution of the classical high-temperature and the ultracold model of the first-order reaction (4.24). The quantum trajectories depict the occupation number of the ground state mode. For both models, we choose an initially depleted particle concentration/number. Using instructive parameters for the energies and reaction constants, we see the qualitatively different behaviour of the considered models. Whereas the full Hamiltonian of the quantum description generates an oscillating particle number between bath and species, the classical system relaxes to the fix point $[N] = N_0$. The approximated models also show different behaviour; the quantum interaction term causes a quadratic increase of the expectation value of the number operator, whereas in the case of the classical reaction the concentration grows linearly in time.

that this reaction is not coupled to a reservoir, the overall particle number \hat{N}_{tot} is a non-trivial constant of motion, making an unbounded growth of the particle number of any of the species impossible. The second set contains the type of reactions which are coupled to a bath. We expect the occurring dynamics to be qualitatively similar to the dynamics of the first-order reaction (4.24), that is, we expect an unbounded growth in the strong coupling regime.

Second-order reactions without bath

For the sake of completeness, we mention that formally



is a valid autocatalytic second-order reaction. Its dynamics are induced by

$$\begin{aligned}\hat{H} &= \int dx \left(\hat{\psi}_A^\dagger(x) \left(\hat{T}_A + V_A(x) \right) \hat{\psi}_A(x) \right) + k \int dx \left(\hat{\psi}_A(x) \hat{\psi}_A^\dagger(x) + \hat{\psi}_A^\dagger(x) \hat{\psi}_A(x) \right) \\ &= \sum_n E_n \hat{a}_n^\dagger \hat{a}_n + k \left(\hat{a}_n^\dagger \hat{a}_n + \hat{a}_n \hat{a}_n^\dagger \right),\end{aligned}\tag{4.46}$$

where the n labels the eigenmodes of the non-interacting part. Since (4.46) is entirely decoupled for any external potential, the particle number in each modes remains constant. Let us advance and consider the simplest of all ultracold chemical reactions, namely a simple particle conversion between two species.



According to our proposal this system is described by the Hamiltonian

$$\begin{aligned}\hat{H} &= \int dx \left(\hat{\psi}_A^\dagger(x) \left(\hat{T}_A + V_A(x) \right) \hat{\psi}_A(x) \right) + \int dx \left(\hat{\psi}_B^\dagger(x) \left(\hat{T}_B + V_B(x) \right) \hat{\psi}_B(x) \right) \\ &\quad + k \int dx \left(\hat{\psi}_A(x) \hat{\psi}_B^\dagger(x) + \hat{\psi}_A^\dagger(x) \hat{\psi}_B(x) \right)\end{aligned}\tag{4.48}$$

The first observation is that, since the reaction does not involve autocatalytic species and is not coupled to a bath, the overall particle number (4.4)

$$\hat{N}_{tot} = \hat{N}_A + \hat{N}_B,\tag{4.49}$$

with \hat{N}_A, \hat{N}_B as in 3.71, is conserved during the time evolution. Keeping this in mind we start our dynamical investigation of the strong coupling regime, that is, we focus on the dynamics induced by the interacting part of the Hamiltonian

$$\begin{aligned}\hat{H}_{\text{int}} &= k \int dx \left(\hat{\psi}_A(x) \hat{\psi}_B^\dagger(x) + \hat{\psi}_A^\dagger(x) \hat{\psi}_B(x) \right) \\ &= k \sum_n \left(\hat{a}_n^\dagger \hat{b}_n + \hat{a}_n \hat{b}_n^\dagger \right) = \sum_n \hat{H}_{\text{int}}^{(n)},\end{aligned}\tag{4.50}$$

which we already considered in (4.32). This Hamiltonian is entirely decoupled between the different modes of each species. It is therefore sufficient to study the

dynamics in the two-mode picture by choosing $n = 0$:

$$\hat{H}_{\text{int}}^{(0)} = k(\hat{a}^\dagger \hat{b} + \hat{a} \hat{b}^\dagger) = (\hat{a} \ \hat{b}) \begin{pmatrix} 0 & k \\ k & 0 \end{pmatrix} \begin{pmatrix} \hat{a}^\dagger \\ \hat{b}^\dagger \end{pmatrix}, \quad (4.51)$$

where we used $\hat{a} = \hat{a}_0$ and $\hat{b} = \hat{b}_0$ as abbreviated notation. Writing \hat{a}, \hat{b} as orthogonally transformed modes

$$\begin{pmatrix} \hat{a} \\ \hat{b} \end{pmatrix} = \frac{1}{\sqrt{2}} \begin{pmatrix} 1 & 1 \\ -1 & 1 \end{pmatrix} \begin{pmatrix} \hat{c}_1 \\ \hat{c}_2 \end{pmatrix} \quad (4.52)$$

yields a decoupled system:

$$\hat{H}_{\text{int}}^{(0)} = \lambda \left(\hat{c}_1^\dagger \hat{c}_1 - \hat{c}_2^\dagger \hat{c}_2 \right) \quad (4.53)$$

We find that this Hamiltonian does not have a well defined ground state as an infinite number particles in mode \hat{c}_2 corresponds to $E \rightarrow -\infty$. However, due to the conservation of N_{tot} , the solution of (4.53) amounts to a finite-dimensional problem. Therefore, the ground state is well-defined and represented by the state in which all particles are in mode \hat{c}_2 . Starting the system's evolution in a coherent state, we obtain the following dynamics for the ground state occupation number of each species:

$$\begin{aligned} \langle \hat{N}_A^{(0)}(t) \rangle &= \frac{N_A + N_B}{2} + \left(\frac{N_A - N_B}{2} \right) \cos(2kt) \\ \langle \hat{N}_B^{(0)}(t) \rangle &= \frac{N_A + N_B}{2} + \left(\frac{N_B - N_A}{2} \right) \cos(2kt), \end{aligned} \quad (4.54)$$

where N_A, N_B label the initial number of particles of the respective species. As already mentioned, this result applies to all other modes by adapting the initial occupation number.

After the investigation of the strong coupling regime we extend the model by incorporating the non-interacting part. Assuming a vanishing external potential for both species the plane wave expansion of (4.48) yields

$$\hat{H} = \sum_p \left(\frac{p^2}{2m_A} \hat{a}_p^\dagger \hat{a}_p + \frac{p^2}{2m_B} \hat{b}_p^\dagger \hat{b}_p + k \left(\hat{a}_p^\dagger \hat{b}_p + \hat{a}_p \hat{b}_p^\dagger \right) \right) = \sum_p \hat{H}^{(p)}. \quad (4.55)$$

This Hamiltonian is decoupled in terms of the modes of each species. We therefore

omit the index from the modes and find

$$\begin{aligned}\hat{H}^{(p)} &= E_A^{(p)} \hat{a}^\dagger \hat{a} + E_B^{(p)} \hat{b}^\dagger \hat{b} + k(\hat{a}^\dagger \hat{b} + \hat{a} \hat{b}^\dagger) \\ &= (\hat{a} \ \hat{b}) \underbrace{\begin{pmatrix} E_A^{(p)} & k \\ k & E_B^{(p)} \end{pmatrix}}_{A^{(p)} :=} \begin{pmatrix} \hat{a}^\dagger \\ \hat{b}^\dagger \end{pmatrix}.\end{aligned}\quad (4.56)$$

with $E_A^{(p)} = \frac{p^2}{2m_A}$ and $E_B^{(p)} = \frac{p^2}{2m_B}$ as eigenenergies. This model represents a linear interaction between two quantum fields (e.g. a beam-splitter in quantum optics [Mar08]). Let U denote the unitary transformation on the modes diagonalising $A^{(p)}$:

$$\begin{aligned}\hat{H}^{(p)} &= (\hat{a} \ \hat{b}) U \begin{pmatrix} \lambda_1^{(p)} & 0 \\ 0 & \lambda_2^{(p)} \end{pmatrix} U^\dagger \begin{pmatrix} \hat{a}^\dagger \\ \hat{b}^\dagger \end{pmatrix} \\ &= \lambda_1^{(p)} \hat{c}_1^\dagger \hat{c}_1 + \lambda_2^{(p)} \hat{c}_2^\dagger \hat{c}_2,\end{aligned}\quad (4.57)$$

where we already mentioned that \hat{c}_1, \hat{c}_2 satisfy the CCR and $\lambda_1, \lambda_2 \in \mathbb{R}$ are the eigenvalues of $A^{(p)}$. We see that the ground state of $\hat{H}^{(p)}$ has finite energy if and only if $\lambda_1^{(p)}, \lambda_2^{(p)} \geq 0$. This imposes the following conditions on the ground state energy and the coupling constant:

$$|E_A^{(p)} + E_B^{(p)}| \leq \underbrace{\sqrt{4k^2 + (E_A^{(p)} - E_B^{(p)})^2}}_{\Omega^{(p)} :=}, \quad (4.58)$$

where we introduced the characteristic frequency $\Omega^{(p)}$ of the system; assuming initially coherent states in the modes, $\Omega^{(p)}$ is the frequency of the oscillations in the p -th mode:

$$\begin{aligned}\langle \hat{N}_A^{(p)}(t) \rangle &\approx C_A^{(p)} (1 - \cos \Omega^{(p)} t) \\ \langle \hat{N}_B^{(p)}(t) \rangle &\approx C_B^{(p)} (1 - \cos \Omega^{(p)} t)\end{aligned}\quad (4.59)$$

The amplitudes $C_A^{(p)}, C_B^{(p)}$ of the oscillations are functions of the initial particle numbers and the eigenenergy difference. For $E_A^{(p)} - E_B^{(p)} = 0$ the trajectories coincide with (4.54).

Let us further consider the case, where the external potential is different from zero and not equal for both species, that is $V_A(x) \neq V_B(x)$. This introduces a coupling

between the modes in the plane wave basis

$$\hat{H} = \sum_{n,m} \langle n | \hat{H}_{0,A} | m \rangle \hat{a}_n^\dagger \hat{a}_m + \sum_{n,m} \langle n | \hat{H}_{0,B} | m \rangle \hat{b}_n^\dagger \hat{b}_m + k \left(\sum_n \hat{a}_n^\dagger \hat{b}_n + \hat{a}_n \hat{b}_n^\dagger \right). \quad (4.60)$$

However, due to the fact that unitary transformations preserve the canonical structure, we can transform this system to normal modes. Therefore, the time-evolution will be qualitatively equivalent to the case of no external potential.

Concerning the corresponding classical reactions, we notice that scheme (4.47) corresponds to two concurrent first-order reactions. The reaction kinetics is determined by

$$\begin{aligned} \frac{d[A]}{dt} &= -k[A] + k[B] \\ \frac{d[B]}{dt} &= -k[B] + k[A]. \end{aligned} \quad (4.61)$$

The concentrations, in contrast to the quantum behaviour, relax to a stationary state:

$$\begin{aligned} [A](t) &= \frac{[A]_0 + [B]_0}{2} - \left(\frac{[B]_0 - [A]_0}{2} \right) e^{-2kt} \\ [B](t) &= \frac{[A]_0 + [B]_0}{2} - \left(\frac{[A]_0 - [B]_0}{2} \right) e^{-2kt}. \end{aligned} \quad (4.62)$$

Fig. 4.3 shows typical trajectories for a single-mode in the strong coupling regime and the relaxation of the classical model. Whereas the ultracold reaction oscillates between the species, the classical trajectory relaxes to an equilibrium state. The reaction constant determines the frequency of the oscillations in the strong coupling limit. In contrast, in the classical case the reaction constant determines the time scale of relaxation.

Second-order reactions coupled to a bath

Second-order reactions coupled to a bath describe the production of ‘pairs’ from a bath:



Within our framework this corresponds to the Hamiltonian

$$\hat{H} = \int dx \left(\hat{\psi}_A^\dagger(x) \left(\hat{T}_A + V_A(x) \right) \hat{\psi}_A(x) \right) + k \int dx \left(\hat{\psi}_A^\dagger(x) \hat{\psi}_A^\dagger(x) + \hat{\psi}_A(x) \hat{\psi}_A(x) \right).$$

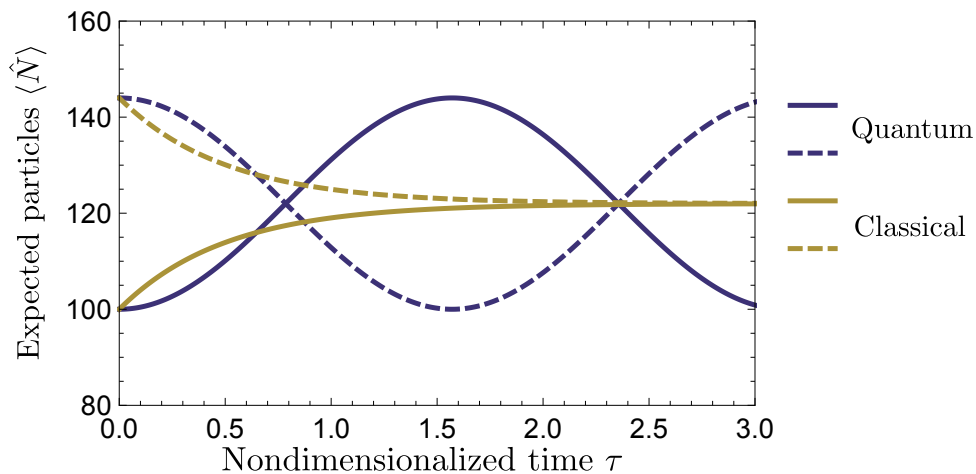


Figure 4.3: Comparison of the quantum and classical trajectories for the reaction (4.31). The quantum trajectory is plotted for the strong coupling regime. The plot shows the expected occupation number of species A as solid and species B as dashed lines. As initial state we choose both species to be in a coherent state with 100 particles of species A and 144 particles of species B . Whereas the overall particle number N_{tot} is conserved in both cases, the quantum reaction oscillates while the classical reaction equilibrates.

(4.64)

Let us start our consideration with the strong coupling regime. Expanding \hat{H}_{int} in the plane wave basis yields

$$\begin{aligned}
 \hat{H}_{\text{int}} &= k \int dx \left(\hat{\psi}_A^\dagger(x) \hat{\psi}_A^\dagger(x) + \hat{\psi}_A(x) \hat{\psi}_A(x) \right) \\
 &= \frac{k}{L} \int_0^L dx \left(\sum_{n,n'} e^{i(\omega_n + \omega_{n'})x} \hat{a}_n^\dagger \hat{a}_{n'}^\dagger + \sum_{m,m'} e^{-i(\omega_m + \omega_{m'})x} \hat{a}_m \hat{a}_{m'} \right) \\
 &= k \sum_n \left(\hat{a}_n^\dagger \hat{a}_{-n}^\dagger + \hat{a}_n \hat{a}_{-n} \right) = \sum_n \hat{H}_{\text{int}}^{(n)}.
 \end{aligned} \tag{4.65}$$

This term is quadratic in creation and annihilation operators. A similar Hamiltonian appears in the theory of the self-interacting Bose gas as an approximation to the two-body interaction potential [Sch05]. A standard technique to solve these kind of quadratic Hamiltonians is a Bogoliubov transformation [Bog47],

$$\begin{aligned}
 \hat{a}_n &= u_n \hat{b}_n + v_n \hat{b}_{-n}^\dagger \\
 \hat{a}_n^\dagger &= u_n \hat{b}_n^\dagger + v_n \hat{b}_{-n},
 \end{aligned} \tag{4.66}$$

with $u_n, v_n \in \mathbb{R}$. This transformation preserves the CCR if and only if the coefficients of the transformation satisfy

$$u_n^2 - v_n^2 = 1. \quad (4.67)$$

Substituting the Bogoliubov ansatz (4.66) into (4.65) yields

$$\hat{H}_{\text{int}} = k \left((u_n^2 + v_n^2) \hat{b}_n^\dagger \hat{b}_{-n}^\dagger + (u_n^2 + v_n^2) \hat{b}_n \hat{b}_{-n} + 2u_n v_n \left(\hat{b}_n^\dagger \hat{b}_n + \hat{b}_n \hat{b}_n^\dagger \right) \right). \quad (4.68)$$

Considering this expression we see that the system is only transformed to decoupled modes if

$$u_n^2 + v_n^2 = 0. \quad (4.69)$$

Solving the constraint (4.67) for u_n^2 and inserting into condition (4.69) results in

$$u_n^2 + v_n^2 = 0 \Leftrightarrow 1 + 2v_n^2 = 0 \Leftrightarrow v_n^2 = -\frac{1}{2}, \quad (4.70)$$

which has no solution in \mathbb{R} . While it seems that this system of coupled modes is too complex to solve exactly, we already get interesting insights considering the ground state mode approximation of the interaction Hamiltonian,

$$\hat{H}_{\text{int}}^{(0)} = k \left(\hat{a}_0^\dagger \hat{a}_0^\dagger + \hat{a}_0 \hat{a}_0 \right). \quad (4.71)$$

Note that this Hamiltonian surprisingly coincides up to a sign with the model we obtained from the canonical quantisation of a classical first order reaction $A \xrightarrow{k} B$ (see (3.27)). Actually, as (4.71) is an instance of a squeezing operator, it appears to better describe a pair of particles from a bath, like the generation of two squeezed photons in a crystal, than the particle conversion between two species. Assuming the vacuum as the initial state, we can infer from (3.35) that the expected particle number evolves according to

$$\left\langle \hat{N}_A^{(0)}(t) \right\rangle = \sinh^2(kt). \quad (4.72)$$

Now, let us go further and consider the full Hamiltonian in the case of no external potential. The resulting Hamiltonian in the plane wave expansion is

$$\hat{H} = \sum_p \left(\frac{p^2}{2m_A} \hat{a}_p^\dagger \hat{a}_p + k \left(\hat{a}_p^\dagger \hat{a}_{-p}^\dagger + \hat{a}_p \hat{a}_{-p} \right) \right). \quad (4.73)$$

Although we could not decouple the strong coupling regime with a Bogoliubov

transformation, we make another attempt for the full system. Substituting the Bogoliubov ansatz (4.66) into (4.73) yields

$$\begin{aligned} \hat{H} = & \frac{p^2}{2m_A} \left(u_p^2 \hat{b}_p^\dagger \hat{b}_p + v_p^2 \hat{b}_p \hat{b}_p^\dagger + u_p v_p \left(\hat{b}_p^\dagger \hat{b}_{-p}^\dagger + \hat{b}_p \hat{b}_{-p} \right) \right) \\ & + k \left((u_p^2 + v_p^2) \hat{b}_p^\dagger \hat{b}_{-p}^\dagger + (u_p^2 + v_p^2) \hat{b}_p \hat{b}_{-p} + 2u_p v_p \left(\hat{b}_p^\dagger \hat{b}_p + \hat{b}_p \hat{b}_p^\dagger \right) \right) \end{aligned} \quad (4.74)$$

Comparing the coefficients of the coupled terms yields the condition

$$k (u_p^2 + v_p^2) + \frac{p^2}{2m_A} u_p v_p = 0 \quad (4.75)$$

in order to decouple the modes. To see if this non-linear equation has a solution, we parametrise the solutions of (4.67) as

$$\begin{aligned} u_p &= \cosh \theta \\ v_p &= \sinh \theta, \end{aligned} \quad (4.76)$$

where we refer to θ as transformation angle. Inserting this parametrisation into (4.75) yields

$$\begin{aligned} 0 &= k (u_p^2 + v_p^2) + \frac{p^2}{2m_A} u_p v_p \\ &= k (\sinh^2(\theta) + \cosh^2(\theta)) + \frac{p^2}{2m_A} \cosh(\theta) \sinh(\theta) \\ &= k \cosh(2\theta) + \frac{p^2}{4m_A} \sinh(2\theta). \end{aligned} \quad (4.77)$$

This imposes the following constraint on the transformation angle

$$\tanh(2\theta) = -\frac{4m_A k}{p^2}, \quad (4.78)$$

which in turn imposes

$$p^2 > |4m_A k| \quad (4.79)$$

on the parameters of the system to be transformable to normal modes. This is an interesting result as it tells us that in the case vanishing external potential, the particle number in the ground state mode will always increase according to (4.72). Depending on the strength of the rate constant, the occupation number modes with higher momentum will grow unbounded as well, until the momentum of the mode is

large enough to satisfy (4.79). The particle number in these modes will oscillate as in a free system. To be more precise, the corresponding particle number for modes which satisfy (4.79) evolve in time according to

$$\begin{aligned} \langle \hat{N}_A^{(p)}(t) \rangle &= \langle 0 | (\hat{c}e^{-i\omega t} \sinh \theta + \hat{c}^\dagger e^{i\omega t} \cosh \theta) (\hat{c}e^{-i\omega t} \cosh \theta + \hat{c}e^{i\omega t} \sinh \theta) | 0 \rangle \\ &= 2 ((\cosh \theta \sinh \theta)^2 - (\cosh \theta \sinh \theta) \cos(2\omega t)), \end{aligned} \quad (4.80)$$

where we introduced

$$\omega = \sqrt{\left(\frac{p^2}{4m}\right)^2 - k^2}, \quad (4.81)$$

and assumed that the p -mode is initially in the vacuum state.

The equation of motion from classical kinetics for this reaction is given by

$$\frac{d[A]}{dt} = -k[A]^2 + kN_0, \quad (4.82)$$

where N_0 denotes the constant particle number of the bath. Assuming an initially depleted species A, the particle concentration converges towards the square root of the number of particles in the bath:

$$[A](t) = \sqrt{N_0} \tanh(k\sqrt{N_0}t) \quad (4.83)$$

In 4.4 we depicted trajectories of the classical and the quantum models. Comparing the trajectories with the first-order reaction we find that the behaviour is qualitatively similar. However, the exact shape of the trajectories differ and the classical trajectory converges to the stationary value $\sqrt{N_0}$ instead of N_0 . We close the discussion of this elementary reaction with the remark that the presence of an external potential will impede the investigations, due to the coupling between the modes of different momenta. It is not clear, how the generalisation of the Bogoliubov transformation should look in this case.

The last possible second order reaction is the creation of pairs of distinct species



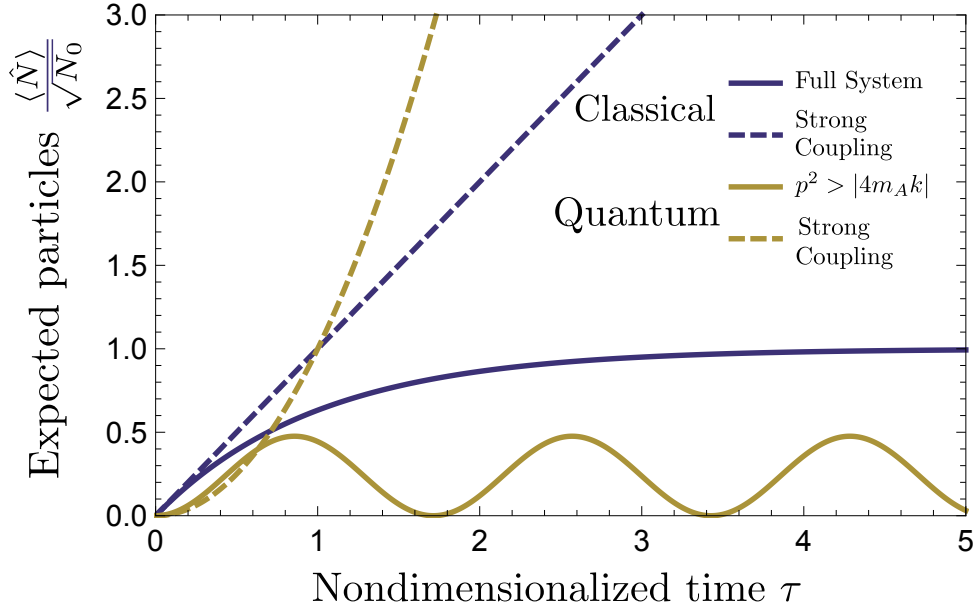


Figure 4.4: Classical and quantum trajectories of the reaction (4.63). As initial state we assumed completely depleted modes or particle concentrations. The modes which satisfy condition (4.79) oscillate periodically, while the number of particles in the ground state grows unbounded in the strong coupling limit. The classical model either relaxes to a stationary state $[N] = \sqrt{N_0}$ or grows linearly as in the case of a first-order reaction.

The Hamiltonian in ultracold kinetics is given by

$$\begin{aligned} \hat{H} = & \int dx \left(\hat{\psi}_A^\dagger(x) \left(\hat{T}_A + V_A(x) \right) \hat{\psi}_A(x) \right) + \int dx \left(\hat{\psi}_B^\dagger(x) \left(\hat{T}_B + V_B(x) \right) \hat{\psi}_B(x) \right) \\ & + k \int dx \left(\hat{\psi}_A^\dagger(x) \hat{\psi}_B^\dagger(x) + \hat{\psi}_A(x) \hat{\psi}_B(x) \right) \end{aligned} \quad (4.85)$$

Following our previous scheme by starting the investigations with the strong coupling regime in the plane wave basis results in

$$\begin{aligned} \hat{H}_{int} &= k \int dx \left(\hat{\psi}_A^\dagger(x) \hat{\psi}_B^\dagger(x) + \hat{\psi}_A(x) \hat{\psi}_B(x) \right) \\ &= \frac{k}{L} \int_0^L dx \left(\sum_{n,n'} e^{i(\omega_n + \omega_{n'})x} \hat{a}_n^\dagger \hat{b}_{n'}^\dagger + \sum_{m,m'} e^{-i(\omega_m + \omega_{m'})x} \hat{a}_m \hat{b}_{m'} \right) \\ &= k \sum_n \left(\hat{a}_n^\dagger \hat{b}_{-n}^\dagger + \hat{a}_n \hat{b}_{-n} \right) = \sum_n \hat{H}_{int}^{(n)} \end{aligned} \quad (4.86)$$

This Hamiltonian is, due to the coupling between the modes, too difficult to be solved in closed form. Similar to the previous reaction, we hope to gain insights from the ground state dynamics:

$$\begin{aligned}\hat{H}_{\text{int}}^{(0)} &= k \left(\hat{a}_0^\dagger \hat{b}_0^\dagger + \hat{a}_0 \hat{b}_0 \right) = \frac{k}{2} \left(\hat{a}_0^\dagger \hat{b}_0^\dagger + \hat{b}_0^\dagger \hat{a}_0^\dagger + \hat{a}_0 \hat{b}_0 + \hat{b}_0 \hat{a}_0 \right) \\ &= \frac{k}{2} \begin{pmatrix} \hat{a}_0 & \hat{b}_0 & \hat{a}_0^\dagger & \hat{b}_0^\dagger \end{pmatrix} \begin{pmatrix} 0 & 0 & 0 & 1 \\ 0 & 0 & 1 & 0 \\ 0 & 1 & 0 & 0 \\ 1 & 0 & 0 & 0 \end{pmatrix} \begin{pmatrix} \hat{a}_0^\dagger \\ \hat{b}_0^\dagger \\ \hat{b}_0 \\ \hat{a}_0 \end{pmatrix},\end{aligned}\tag{4.87}$$

Using the same transformation as in 4.52

$$\begin{pmatrix} \hat{a}_0 \\ \hat{b}_0 \end{pmatrix} = \frac{1}{\sqrt{2}} \begin{pmatrix} 1 & 1 \\ -1 & 1 \end{pmatrix} \begin{pmatrix} \hat{c}_1 \\ \hat{c}_2 \end{pmatrix}\tag{4.88}$$

yields

$$\hat{H}_{\text{int}}^{(0)} = \frac{k}{2} \left(\hat{c}_2^\dagger \hat{c}_2^\dagger + \hat{c}_2 \hat{c}_2 - \left(\hat{c}_1^\dagger \hat{c}_1^\dagger + \hat{c}_1 \hat{c}_1 \right) \right).\tag{4.89}$$

Therefore, the dynamics of the ground state mode is governed by two decoupled squeezing operators (4.71) leading to an unbounded increase of the particle number.

This similarity between the dynamics of the present system and the dynamics of the creation of pairs (4.63), lets us stop the investigations here. The second species makes the analytical treatment of the problem very hard and we do not see a way to generalise the Bogoliubov transformation to this setting. On the other hand, we do not expect fundamentally different behaviour from reaction(4.63), since we are still dealing with quadratic terms.

CHAPTER 5

Diatomic molecule formation

Since the first experimental realisation of a Bose-Einstein condensate (BEC) [Dav95], scientists began to investigate phenomena surrounding this new kind of quantum matter. It turns out that the theoretical models successfully explaining dynamical phenomena like solitons inside a BEC bear a resemblance to the models of non-linear quantum optics. Spurred by this insight, the first phenomenological proposal to describe diatomic molecule formation from a cloud of ultracold bosons was made in [Dru98]. The authors considered the formation of molecules within a BEC as the quantum atomic equivalent of second harmonic generation in quantum optics. The first experimental realisation of molecules in a BEC, achieved through coherent, stimulated recombination of atoms, was reported in [Wyn00].

Diatomic molecule formation is, within our framework, the simplest process which does not fall into the category of low-order reactions. As we saw in chapter 4, the dynamics of diatomic molecule formation are described by a non-linear field theory. This makes these reactions interesting, since we expect that, similarly to classical reaction kinetics, the non-linearity causes a range of new phenomena like entanglement [Wan07] in the quantum evolution or soliton solutions in the mean-field approximation [Hei00]. One of the reasons for these new phenomena is that the non-linearity makes a transformation to decoupled modes, and therefore a restriction to oscillatory behaviour of the system, a priori impossible. At the same time the non-linearity forces us to make approximations if we want to obtain analytical expressions for the resulting dynamics. An approximation which lends itself to obtaining qualitative insights is the mean-field approximation. This approximation is validated by its success in capturing complex many-body phenomena like phase transitions. Additionally, we employ numerical methods to study the phenomena.

This chapter is organised as follows. In section 5.1 we introduce the mean-field approximation as application of the time-dependent variational principle to coherent states. We illustrate by an instructive example the limitations of the approximation. In section 5.2 we introduce the two-mode model of diatomic molecule formation. This

model will be the basis for our approximative and perturbational investigations of the occurring dynamical phenomena. The two-mode model results in the mean-field approximation in an integrable system. The numerical study of the full quantum system shows that the oscillating behaviour predicted by the mean-field approximation breaks down due to the entanglement present in the system. After discussing the two-mode model we extend the reaction in section 5.3 by a concurrent coupling to a bath. The resulting mean-field equations describe a system non-linearly coupled oscillators. By employing perturbational methods we obtain analytic expressions of the trajectories for small couplings between the reactions. Progressive increase of the coupling causes perturbation theory to break down and finally results in Hamiltonian chaos. We point out that parts of this chapter haven been published in [Ric15].

5.1 Mean-field approximation

Since the early days of quantum mechanics physicists find themselves confronted with mathematical problems that, due to sheer complexity, can not be solved in compact form. In particular we only know a handful of many-body systems and non-linear interacting systems which are exactly solvable. For this reason one must often employ approximation or perturbation methods in order to gain insight into the physical structure of quantum systems. A widely used approximation is the *mean-field approximation* also called *mean-field theory*. Originating from the field of phase transitions in many-body systems, it was originally understood as a theory of vanishing fluctuations around the statistical mean value of operators [Lan37]. In this thesis we give a different account, considering (bosonic) mean-field theory as an application of the variational method to a product of coherent states [Osb11]. This provides us with clear intuition about the limitations of the mean-field approximation | whenever the actual dynamics of the considered quantum system leads it outside the manifold of coherent states, the approximation becomes inaccurate. This is in particular the case if entanglement plays an important role in the dynamics.

Ultracold chemical reactions beyond second order describe interacting field theories which support complex dynamics. Therefore, we must employ variational or perturbative methods to obtain less complicated systems which, as far as possible, still capture the most important physical aspects. In what follows, we quickly review the basic properties of the coherent states that form our variational manifold. This will lead us to the mean-field equations for bosonic systems.

5.1.1 Coherent states

Coherent states are an important class of states in quantum optics as they model the quantum state of a laser beam [Gla63]. Being in some sense the ‘most classical’ quantum states, they form a suitable set of initial states for comparison to classical dynamics.

We start by considering the Hilbert space of a single bosonic mode, that is

$\mathcal{H} = L^2(\mathbb{R})$. We define the coherent states $|\alpha\rangle$ within this space as eigenstates of the annihilation operator:

$$\{|\alpha\rangle\} := \{|\psi(\alpha)\rangle : \hat{a} |\psi(\alpha)\rangle = \alpha |\psi(\alpha)\rangle, \alpha \in \mathbb{C}\}. \quad (5.1)$$

The spectrum of the annihilation operator is indeed the entire complex plane. Alternatively, one can define the *displacement* operator

$$\hat{D}(\alpha) := e^{\alpha\hat{a}^\dagger - \bar{\alpha}\hat{a}}, \quad (5.2)$$

which creates coherent states by displacing the vacuum

$$|\alpha\rangle := \hat{D}(\alpha) |0\rangle. \quad (5.3)$$

Using the Baker-Campbell-Hausdorff formula, we can expand the coherent state in the Fock basis

$$\begin{aligned} |\alpha\rangle &= e^{\alpha\hat{a}^\dagger - \bar{\alpha}\hat{a}} |0\rangle = e^{-\frac{1}{2}|\alpha|^2} e^{\alpha\hat{a}^\dagger} e^{\bar{\alpha}\hat{a}} |0\rangle \\ &= e^{\frac{1}{2}|\alpha|^2} \sum_{n=0}^{\infty} \frac{(\alpha\hat{a}^\dagger)^n}{n!} |0\rangle = e^{\frac{1}{2}|\alpha|^2} \sum_{n=0}^{\infty} \frac{\alpha^n}{\sqrt{n!}} |n\rangle. \end{aligned} \quad (5.4)$$

We see that a coherent state is an infinite superposition of Fock states. However, the expectation value of particles in a coherent state is given by

$$\langle \hat{N} \rangle = \langle \alpha | \hat{a}^\dagger \hat{a} | \alpha \rangle = |\alpha|^2. \quad (5.5)$$

In quantum optics this equality is the central connection between the particle view and the wave view, as it relates the mean particle number to the complex amplitude squared. Notice that the displacement operator for $\alpha = it$ coincides with the operator which generates time evolution for a first-order ultracold chemical reaction. Let us now consider the expectation values of the quadratures \hat{x} and \hat{p} for a coherent state, that is

$$\begin{aligned} \langle \hat{x} \rangle &= \langle \alpha | \hat{x} | \alpha \rangle = \langle \alpha | \frac{1}{\sqrt{2}} (\hat{a}^\dagger + \hat{a}) | \alpha \rangle = \sqrt{2} \text{Re}(\alpha) \\ \langle \hat{p} \rangle &= \langle \alpha | \hat{p} | \alpha \rangle = \langle \alpha | \frac{i}{\sqrt{2}} (\hat{a}^\dagger - \hat{a}) | \alpha \rangle = \sqrt{2} \text{Im}(\alpha). \end{aligned} \quad (5.6)$$

The spread in the quadratures is given by

$$\begin{aligned}\langle \hat{x}^2 \rangle &= \langle \alpha | \hat{x}^2 | \alpha \rangle = \langle \alpha | \frac{1}{2} (\hat{a}^\dagger + \hat{a})^2 | \alpha \rangle = 2\text{Re}(\alpha) + \frac{1}{2} \\ \langle \hat{p}^2 \rangle &= \langle \alpha | \hat{p}^2 | \alpha \rangle = \langle \alpha | -\frac{1}{2} (\hat{a}^\dagger - \hat{a})^2 | \alpha \rangle = 2\text{Im}(\alpha) + \frac{1}{2}.\end{aligned}\tag{5.7}$$

Therefore, the \hat{x}, \hat{p} -uncertainty of a coherent state is independent of α :

$$\Delta \hat{x} \Delta \hat{p} = \sqrt{\langle \hat{x}^2 \rangle - \langle \hat{x} \rangle^2} \sqrt{\langle \hat{p}^2 \rangle - \langle \hat{p} \rangle^2} = \frac{1}{2}.\tag{5.8}$$

The generalisation of coherent states to multiple modes is straightforward. Suppose \hat{a}_j and \hat{a}_j^\dagger are the creation and annihilation operators of the j -th mode with $j \in \{1, 2, \dots, N\}$. Then we define a coherent state of the system to be of the following form

$$|\alpha\rangle = e^{\sum_{j=1}^N \alpha_j \hat{a}_j - \bar{\alpha}_j \hat{a}_j^\dagger} |\mathbf{0}\rangle,\tag{5.9}$$

where $\alpha \in \mathbb{C}^n$. According to this definition the multi-mode coherent state is a pure *product* state between the different modes and is therefore not capable of modelling quantum correlations between the modes.

5.1.2 Time-dependent variational principle

In this section we present aspects of the *time-dependent variational principle* (TDVP) [Dir30; Kra81]. This method reduces the complexity of given dynamical problem by restricting time evolution to a subspace referred to as the *variational manifold* \mathcal{V} . It is clear that, due to this restriction, the obtained dynamics will be an approximation of the actual dynamics, with the accuracy sensitively depending on the choice of manifold. Therefore, the key task in the application of the TDVP is to find a variational manifold which, on the one hand, is capable of capturing the important dynamical phenomena and, on the other hand, provides a significant simplification to the original problem. In what follows, we present one possible way to derive the equations of motion of the TDVP for a given variational class \mathcal{V} .

The principle of stationary action is one of the most important principles in modern physics as it is in most cases sufficient for deriving equations of motion, given a physical system. Schrödinger's equation in quantum mechanics is no exception, as we see by considering the action

$$S\{\bar{\psi}(t), \psi(t)\} = \int_{t_1}^{t_2} dt L(\bar{\psi}(t), \psi(t), t)\tag{5.10}$$

with the Lagrange function

$$L(\bar{\psi}(t), \psi(t), t) = \frac{i}{2} \langle \psi(t) | \frac{d\psi(t)}{dt} \rangle - \frac{i}{2} \langle \frac{d\psi(t)}{dt} | \psi(t) \rangle - \langle \psi(t) | \hat{H}(t) | \psi(t) \rangle. \quad (5.11)$$

To avoid cluttering the notation, we henceforth omit the explicit time dependence of each quantity. The principle of stationary action states that, for the physical trajectories, the variation of the action becomes zero or, equivalently, the trajectories solve the Euler-Lagrange equations. Assuming $|\psi\rangle$ and $\langle\psi|$ as independent coordinates and varying with respect to $\langle\psi|$ leads to

$$\frac{d}{dt} \frac{\partial L}{\partial \langle \frac{d\psi}{dt} |} - \frac{\partial L}{\partial \langle \psi |} = i \left| \frac{d\psi}{dt} \right\rangle - \hat{H} |\psi\rangle = 0, \quad (5.12)$$

which is the time-dependent Schrödinger equation (TDSE) on the full Hilbert space \mathcal{H} . Now we assume that the dynamics take place in a subspace $\mathcal{V} \subset \mathcal{H}$. Suppose this variational manifold is given by coherent states (5.1) of a single bosonic mode. The variational Lagrangian (5.11) then yields

$$L(\bar{\alpha}, \alpha) = \frac{i}{2} \langle \alpha | \frac{d\alpha}{dt} \rangle - \frac{i}{2} \langle \frac{d\alpha}{dt} | \alpha \rangle - \langle \alpha | \hat{H} | \alpha \rangle. \quad (5.13)$$

Let us consider the first term on the right-hand side of (5.13). We find

$$\begin{aligned} \langle \alpha | \frac{d\alpha}{dt} \rangle &= \langle \alpha | \frac{d}{dt} e^{-\frac{1}{2}|\alpha|^2} e^{\alpha \hat{a}^\dagger} | 0 \rangle \\ &= \langle \alpha | -\frac{1}{2} \left(\frac{d\bar{\alpha}}{dt} \alpha + \frac{d\alpha}{dt} \bar{\alpha} \right) e^{-\frac{1}{2}|\alpha|^2} e^{\alpha \hat{a}^\dagger} | 0 \rangle \\ &\quad + \langle \alpha | \frac{d\alpha}{dt} \hat{a}^\dagger e^{-\frac{1}{2}|\alpha|^2} e^{\alpha \hat{a}^\dagger} | 0 \rangle \\ &= \frac{1}{2} \left(\frac{d\alpha}{dt} \bar{\alpha} - \frac{d\bar{\alpha}}{dt} \alpha \right). \end{aligned} \quad (5.14)$$

Since the second term in (5.13) is the complex conjugate of the first one we obtain

$$L(\bar{\alpha}, \alpha) = \frac{i}{2} \left(\frac{d\alpha}{dt} \bar{\alpha} - \frac{d\bar{\alpha}}{dt} \alpha \right) - \langle \alpha | \hat{H} | \alpha \rangle. \quad (5.15)$$

We call this the mean-field Lagrangian of the original quantum problem. The Euler-Lagrange equations corresponding to a variation of $\bar{\alpha}$ in (5.15) yield

$$i \frac{d\alpha}{dt} = \frac{\partial}{\partial \bar{\alpha}} \langle \alpha | \hat{H} | \alpha \rangle = \frac{\partial}{\partial \bar{\alpha}} H(\bar{\alpha}, \alpha). \quad (5.16)$$

For a normal ordered quantum Hamiltonian, we obtain the mean-field Hamiltonian $H(\bar{\alpha}, \alpha)$ by simply replacing creation and annihilation operators by a single complex number and its complex conjugate, that is

$$\hat{a} \rightarrow \alpha \quad \text{and} \quad \hat{a}^\dagger \rightarrow \bar{\alpha}. \quad (5.17)$$

For the sake of completeness, we mention that instead of deriving (5.17) from the principle of stationary action, we can also understand the equations of motion as the result of an orthogonal projection of the actual dynamics onto the tangent plane of the variational manifold. For an overview of different interpretations of the TDVP, we refer the reader to [Hae11].

Comparing the full quantum formulation (5.12) with the mean-field approximation (5.16) shows that the complexity of the problem has drastically decreased. Indeed, considering the real and imaginary part of α as a conjugate variable pair $\alpha = x + ip$ transforms (5.16) into

$$\begin{aligned} i \frac{d\alpha}{dt} &= \frac{\partial}{\partial \bar{\alpha}} H(\bar{\alpha}, \alpha) \\ i \frac{d(x + ip)}{dt} &= \frac{\partial}{\partial x - ip} H(x, p) = \frac{\partial}{\partial x} H(x, p) + i \frac{\partial}{\partial x} H(x, p), \end{aligned} \quad (5.18)$$

which is equivalent to Hamilton's equations of motion

$$\begin{aligned} \frac{dx}{dt} &= \frac{\partial H(x, p)}{\partial p} \\ \frac{dp}{dt} &= -\frac{\partial H(x, p)}{\partial x}. \end{aligned} \quad (5.19)$$

of a one-dimensional system.

This scheme can be readily generalized to a scenario of N modes. The variational manifold in this case is

$$\mathcal{V} = \{ |\alpha_1, \alpha_2, \dots, \alpha_N\rangle = e^{\sum_{j=1}^N \alpha_j \hat{a}_j - \bar{\alpha}_j \hat{a}_j^\dagger} |0\rangle \}, \quad (5.20)$$

that is, a product of coherent states.

Although this method has an astonishing ability to qualitatively predict phase-transitions in many-body systems, its dynamical predictions can fail even for a single particle problem. To see this, we consider the Hamiltonian

$$\hat{H} = k (\hat{a}^\dagger \hat{a}^\dagger + \hat{a} \hat{a}), \quad (5.21)$$

which is part of our proposed model of creation of pairs from a bath. Replacing

operators by complex numbers, we readily obtain

$$i \frac{d\alpha}{dt} = 2k\bar{\alpha} \quad (5.22)$$

for the mean-field equations of motion. The mean-field approximation predicts the vacuum state $\alpha = 0$ to be a fixed point of the dynamics. This clearly contradicts the exact solution in (4.72), which shows a quadratic increase of particles at small times. Why does the mean-field approximation fail for an operator that is quadratic in creation and annihilation operators on a single mode? The answer is that (5.21) is an instance of a squeeze operator 3.31 and therefore generates dynamics that bring us immediately away from the manifold of coherent states.

To summarise, applying the TDVP with coherent states to a quantum problem on $\mathcal{H} = L^2(\mathbb{R})$ results in a one-dimensional phase space problem, which we call the mean-field approximation. Although greatly simplifying the problem, one should be aware of the limitations of this method. We have presented a simple example where the method fails to predict qualitatively correct dynamics.

5.2 Two-mode model

This section considers the dynamics of the most elementary second-order reaction, *diatomic molecule formation*:



The stoichiometric coefficient for the atomic species μ_A equals two and the molecular coefficient ν_M is one. According to our proposed framework this reaction is modelled by the Hamiltonian

$$\begin{aligned} \hat{H} = & \int dx \left(\hat{\psi}_A^\dagger(x) \left(\hat{T}_A + V_A(x) \right) \hat{\psi}_A(x) \right) + \int dx \left(\hat{\psi}_M^\dagger(x) \left(\hat{T}_M + V_M(x) \right) \hat{\psi}_M(x) \right) \\ & + k \int dx \left(\hat{\psi}_A(x) \hat{\psi}_A(x) \hat{\psi}_M^\dagger(x) + \hat{\psi}_M^\dagger(x) \hat{\psi}_A^\dagger(x) \hat{\psi}_M(x) \right). \end{aligned} \quad (5.24)$$

Since this reaction is not coupled to a bath, the overall particle number (4.4)

$$\hat{N}_{\text{tot}} = \hat{N}_A + 2\hat{N}_M \quad (5.25)$$

is a constant of motion. Let us follow our previous scheme from elementary reactions and start with the investigation of the interacting part, which dominates the reaction if the coupling constant is large compared to the other energies in the system.

Expanding the interacting part in the plane wave basis (4.23) yields

$$\begin{aligned}
\hat{H}_{\text{int}} &= k \int dx \left(\hat{\psi}_A(x) \hat{\psi}_A(x) \hat{\psi}_M^\dagger(x) + \hat{\psi}_A^\dagger(x) \hat{\psi}_A^\dagger(x) \hat{\psi}_M(x) \right) \\
&= \frac{k}{L^{\frac{3}{2}}} \int_0^L dx \left(\sum_{n,n',n''} e^{i(\omega_n + \omega_{n'} - \omega_{n''})x} \hat{a}_n^\dagger \hat{a}_{n'}^\dagger \hat{m}_{n''} + \sum_{l,l',l''} e^{-i(\omega_l + \omega_{l'} - \omega_{l''})x} \hat{a}_l \hat{a}_{l'} \hat{m}_{l''}^\dagger \right) \\
&= \frac{k}{\sqrt{L}} \sum_{n,n'} \left(\hat{a}_n^\dagger \hat{a}_{n'}^\dagger \hat{m}_{n+n'} + \hat{a}_n \hat{a}_{n'} \hat{m}_{n+n'}^\dagger \right)
\end{aligned} \tag{5.26}$$

This Hamiltonian annihilates two atoms with momentum n and n' and creates, due to momentum conservation, a molecule with wave number $n + n'$. A very similar Hamiltonian has been used to describe the chemical process of photoassociation in a BEC [Jav99]. The model of photoassociation differs by the fact that the momentum of the photon absorbed or emitted during molecule formation and dissociation is taken into account. A solution of the full system in (5.26) presents a very difficult task due to the coupling between the modes. Therefore, we restrict our considerations to the case where all atoms start out in the state $n = 0$. This yields the *two-mode model* of molecule formation

$$\hat{H}^{(0)} = E_A \hat{a}^\dagger \hat{a} + E_M \hat{m}^\dagger \hat{m} + \frac{k}{\sqrt{L}} (\hat{a}^\dagger \hat{a}^\dagger \hat{m} + \hat{a} \hat{a} \hat{m}^\dagger), \tag{5.27}$$

where $\hat{a} = \hat{a}_0$ and $\hat{m} = \hat{m}_0$ are ground-state modes. We add the ground-state energies E_A and E_M to the model to account for the fact that the different species still can have an energy offset in their zero momentum state. This Hamiltonian has been the subject of much recent research as it also models second harmonic generation [Wal72] and two-photon down conversion [Hil90]. Nonetheless, a comprehensive investigation of the dynamical regimes relevant for the reaction kinetics of ultracold chemistry is missing.

It is worth noting that strong doubts about the validity of the model as a description of photoassociation have been expressed in [Gór01], where the authors analyse the impact of the coupling to higher modes. This coupling arises, for example, if the initial condition of all particles having zero momentum is violated. The result of the coupling is to change the system dynamics dramatically, leading to a complete depletion of the ground state mode on short time scales. However, we should not forget that (5.26) is an effective Hamiltonian, where the exact local interaction results from the low-temperature approximation of an interaction potential. It may be possible, similarly to the case of Feshbach resonances in a Bose-Einstein condensate, to experimentally influence the interaction potential between the atoms

and molecules such that the modes decouple in (5.26), leaving

$$\hat{H}_{\text{int}} = \frac{k}{\sqrt{L}} \sum_n (\hat{a}_n^\dagger \hat{a}_n^\dagger \hat{m}_n + \hat{a}_n \hat{a}_n \hat{m}_n^\dagger). \quad (5.28)$$

In what follows we restrict our studies to the two-mode model (5.27).

5.2.1 Mean-field dynamics

Let us begin our studies of the two-mode model of diatomic molecule formation with the mean-field approximation of the system. As we mentioned when introducing our account of mean-field theory, this maps the quantum Hamiltonian onto a classical phase-space problem. Replacing the operators by complex numbers leads to the classical Hamiltonian

$$H(\alpha, \bar{\alpha}, \beta, \bar{\beta}) = E_A |\alpha|^2 + E_M |\beta|^2 + \frac{k}{\sqrt{L}} (\bar{\alpha}^2 \beta + \bar{\beta} \alpha^2), \quad (5.29)$$

where α labels the coherent state of the atomic mode and β the coherent state of the molecule. The conservation of the overall particle number (5.25) carries over to the mean-field approximation as the constant of motion

$$N_{\text{tot}} = |\alpha|^2 + 2|\beta|^2. \quad (5.30)$$

This is already enough to make some qualitative statements about the type of dynamics that occur in the mean-field approximation. The dynamics of the mean-field approximation take place in a two-dimensional phase space. Since the energy and overall particle number are independent constants of motion, the Hamiltonian (5.29) describes an integrable system. Hence the trajectories in phase-space are lines on a two-dimensional torus. The equations of motion follow from (5.16) as

$$\begin{aligned} i\dot{\alpha} &= E_A \alpha + 2\tilde{k} \bar{\alpha} \beta \quad \text{and} \\ i\dot{\beta} &= E_M \beta + \tilde{k} \alpha^2, \end{aligned} \quad (5.31)$$

where we set $\tilde{k} = \frac{k}{\sqrt{L}}$. A straightforward analysis shows that the fixed points of this system are at

$$\begin{aligned} (\alpha_0, \beta_0) &= (0, 0) \quad \text{and} \\ (\alpha_\phi, \beta_\phi) &= \left(\sqrt{\frac{E_A E_M}{2\tilde{k}^2}} e^{i\phi}, -\frac{E_A}{2\tilde{k}} e^{2i\phi} \right) \quad \text{with } \phi \in [0, 2\pi). \end{aligned} \quad (5.32)$$

In Fig. 5.1 we plot two trajectories of the expected atom number $|\alpha|^2$ for slightly different initial conditions. The number of molecules can be easily inferred from the

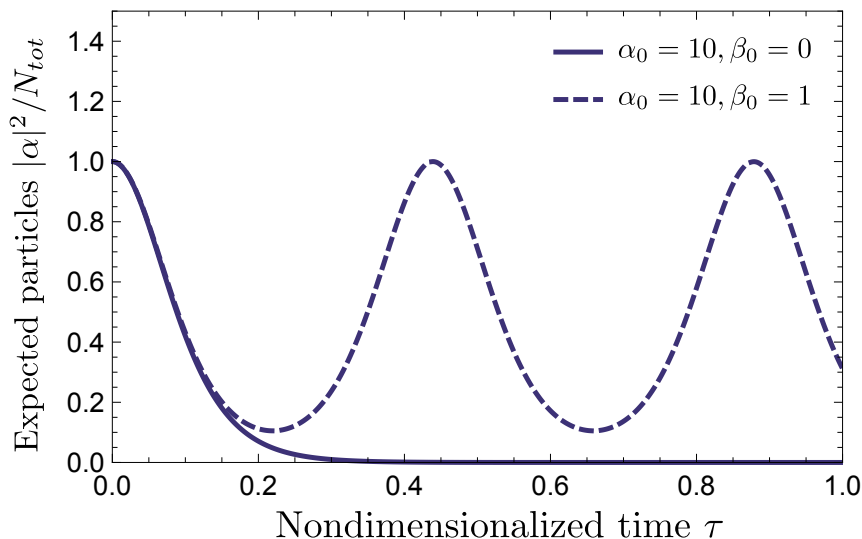


Figure 5.1: Two mean-field trajectories predicted by (5.31). The plot shows the expected number of atoms for slightly different initial conditions. The dynamical parameters are set to $E_A = 1, E_M = 2, k = 1$. While the atomic mode completely depletes if there are no molecules present initially, a single initial molecule suffices to drastically change the dynamics of the system.

number of atoms due to the conservation of N_{tot} . The mean-field approximation predicts a complete inversion of the population if the eigenenergies are coupled through $E_A = 2E_M$, given an initially depleted molecular mode. However, this fixed point for the dynamics of the absolute square $|\alpha|^2$ is not stable. A tiny change in the initial condition brings the trajectory away from the fixed point and leads to an oscillation of the system.

What can we say at this point about the validity of the mean-field approximation in the present case? Due to the fact that the Hamiltonian resembles a squeezing operator on the atomic system, we already learned from example (5.22) that the mean-field prediction can not be entirely correct. However, we still can hope for a qualitative approximation away from the fixed points. A more detailed analysis of the mean-field system of the two-mode approximation can be found in [San06]. A recent article presenting a nice illustration of the mean-field dynamics as a trajectory on a tear-drop deformed Bloch sphere can be found in [Gra15].

5.2.2 Quantum phenomena

We are interested in studying the role that entanglement plays in the kinetics of the two-mode model of reaction (5.23). The overall particle number operator is a conserved quantity for the dynamics, hence we can restrict our study to the reduced dynamics of the atomic mode, writing $N \equiv N_A$. The behaviour of the molecular mode can be deduced straightforwardly. In Fig. 5.2 we plot the full quantum time

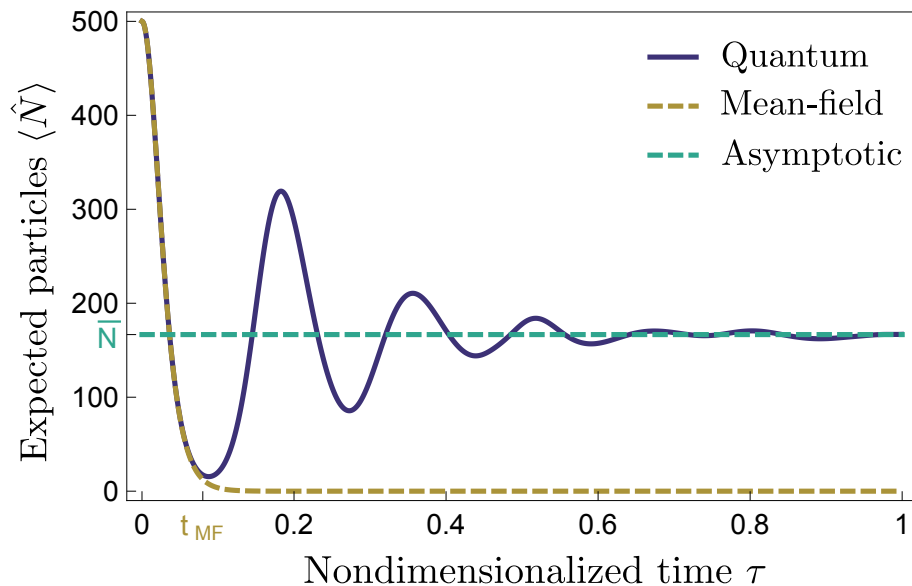


Figure 5.2: The dynamics of the atomic occupation number expectation value $\langle \hat{N} \rangle$ with respect to the rescaled time $\tau = tk/\hbar$ for the diatomic molecular reaction (5.23), with $N = 500$ particles. The quantum and mean field trajectories coincide until they separate at τ_{MF} . From then on, the quantum trajectory approaches a stationary value \bar{N} via entanglement-induced damped oscillations.

evolution of the expectation value of \hat{N} (obtained via exact diagonalisation) together with the mean field prediction for the dynamics of the reaction. The system is initially in a product state of a coherent atomic state and a completely depleted molecular state. As we discussed in section 5.2.1, mean-field theory predicts a complete inversion of the population, where the system is driven to an unstable fixed point [Var01b]. However, in the full quantum solution we can identify three different dynamical regimes. First, there is a *semi-classical* regime where the quantum and mean field dynamics coincide. At the *breakdown time* τ_{MF} the full solution drifts away from the mean field approximation [Var01a] and the semi-classical regime transitions to an intermediate *evanescent regime*, where the quantum trajectory oscillates with an increasingly damped amplitude. Eventually, the system reaches the *asymptotic* regime where the expectation value of the population imbalance relaxes to a stationary value \bar{N} .

We can understand the three different dynamical regimes by studying the time evolution of the quantum entanglement between the atomic and molecular modes. These results are shown in 5.3. In the semi-classical regime we see a rapid increase of the entanglement at the beginning of the reaction, which is necessary for the formation of molecules. It is initially rather surprising that the mean field approximation works as well as it does in the semi-classical regime given that the state rapidly becomes

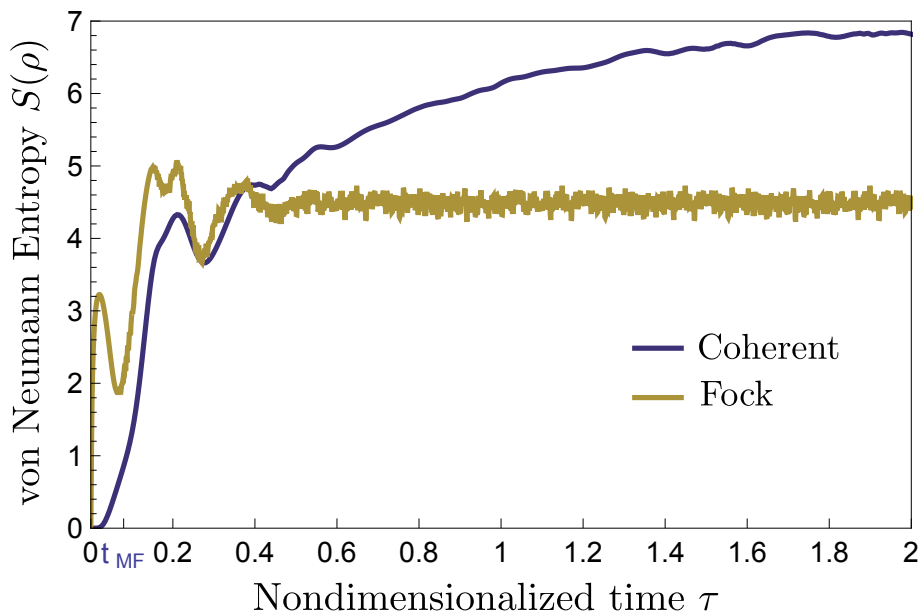


Figure 5.3: Evolution of the quantum entanglement (in terms of the von Neumann entropy of the atomic reduced density operator ρ_A) between the atomic and molecular modes for the reaction (5.23) with respect to rescaled time $\tau = tk/\hbar$. For an initially coherent atomic state the amount of entanglement is close to zero for short times. For an initial Fock state, however, the entanglement grows considerably for small times. In the vicinity of the breakdown time t_{MF} the entanglement in the coherent case rapidly increases. At large times, both initial states lead to a roughly constant level of entanglement.

entangled and is not well-modelled by a product state. A possible explanation is that the entanglement evolution in the semi-classical regime is typical of that produced by *integrable interactions* [Hin03], at least until the breakdown time τ_{MF} . After the breakdown time, in the evanescent regime, the system rapidly reaches the maximum available entanglement and begins to explore the full Hilbert space. Soon after, it enters the asymptotic regime where it ergodically evolves through highly entangled states. It remains in the asymptotic regime until it experiences a quantum revival.

The dynamical behaviour exhibited by the reaction (5.23) is reminiscent of the local relaxation observed in quenched many-particle quantum systems [Cra08]. That relaxation indeed takes place is supported by studying the time-averaged fluctuations $\Delta N^2 = \lim_{\tau \rightarrow \infty} \frac{1}{\tau} \int_0^\tau dt \left(\langle \hat{N}(t) \rangle - \bar{N} \right)^2$ relative to the mean value $\bar{N} = \lim_{\tau \rightarrow \infty} \frac{1}{\tau} \int_0^\tau dt \langle \hat{N}(t) \rangle$, which we plot in 5.4. We find that the fluctuations decrease as the particle number N is increased. However, the mechanism leading to the local relaxation observed in quenched dynamics is slightly different to that found here. In quenched many-particle systems the incoherent interference of localised excitations

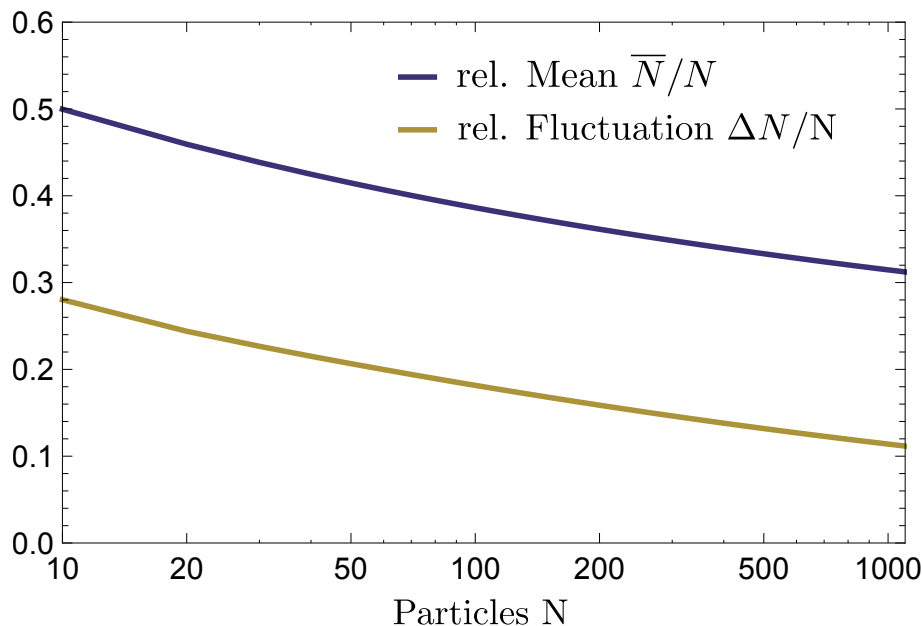


Figure 5.4: The time-averaged relative mean value of atoms, and the fluctuations around it, plotted against the overall particle number for the reaction (5.23). As the particle number is increased, the fraction of atoms in the asymptotic regime and the relative temporal fluctuations decrease.

travelling at different velocities leads to a cumulative effect of relaxation. However, in our case we have an interaction between just two modes and the relaxation we observe is directly related to the growth of entanglement between them or, equivalently, the loss of coherence, or purity, of the reduced density operators. Interestingly, the relaxation behaviour in the asymptotic regime is remarkably similar to the classical high temperature kinetics of (5.23), which relaxes to the fixed point $[A]^2 = [A_2]$ even though our system is always in a global pure state.

We obtained \bar{N} and ΔN^2 via exact diagonalisation. Although the full Hamiltonian has degenerate eigenvalues, the dynamical problem, due to the conservation of \hat{N}_{tot} , can be separated into finite-dimensional problems with no degeneracy. Exploiting this we find that the time-averaged expectation value of the atoms and the molecules coincides with the predictions given by the diagonal ensemble $\bar{N}_{\text{ens}} := \sum_{\alpha} |c_{\alpha}|^2 N_{\alpha,\alpha}$, where $c_{\alpha} = \langle \psi_{\text{in}} | \alpha \rangle$ and $N_{\alpha,\beta} = \langle \alpha | \hat{N} | \beta \rangle$ [Neu29; Rig08] are the coefficients in the complete energy eigenbasis. Moreover, the time-averaged fluctuations around this mean value can be obtained via $\Delta N_t^2 = \sum_{\alpha \neq \beta} |c_{\alpha}|^2 |c_{\beta}|^2 |N_{\alpha,\beta}|^2$ [Sre99]. However, the system *does not thermalise* as the predicted expectation values do not coincide with those of the microcanonical ensemble.

5.3 Molecule formation coupled to a bath

In classical high-temperature kinetics we need to consider complex reactions involving numerous reactants in order to obtain oscillating or irregular dynamics. However, we will see that when we add a simple first-order reaction to the ultracold diatomic molecule formation, we already encounter Hamiltonian chaos within the mean-field approximation. We first consider the chemical reaction



Applying the proposed rules and assuming an energy offset between the ground states, we obtain the Hamiltonian

$$\hat{H} = E_A \hat{n}_A + E_M \hat{n}_M + k_1 (\hat{a}^\dagger \hat{a}^\dagger \hat{m} + \hat{a} \hat{a} \hat{m}^\dagger) + k_2 (\hat{a}^\dagger + \hat{a}),
 \tag{5.34}$$

where E_A and E_M denote the ground state energies of the atomic and molecular species, respectively. The concurrent first-order reaction (5.33) breaks the conservation of the overall particle number \hat{N}_{tot} and impedes a full quantum mechanical treatment. Consequently, we investigate the dynamics of the system in the mean-field approximation by replacing the creation and annihilation operators in (5.34) with complex numbers (α, β) labelling the coherent states of the atomic and molecular modes respectively. Note that within this approximation we obtain the average particle number of a certain species $\langle \hat{N}_i \rangle$ by considering the absolute square of the corresponding complex number ($|\alpha|^2$ or $|\beta|^2$).

In the previous section we saw that diatomic molecule formation amounts involves deviations from mean field dynamics because of the occurrence of quantum effects. Therefore, we need to keep the coupling parameter k_1 as small as possible compared to some relevant energies to consider the mean-field approximation as an appropriate description of the actual dynamics. Keeping this in mind, we obtain the equations of motion from the variational principle:

$$\begin{aligned}
 i\dot{\alpha} &= E_A \alpha + 2k_1 \bar{\alpha} \beta + k_2 \\
 i\dot{\beta} &= E_M \beta + k_1 \alpha^2.
 \end{aligned}
 \tag{5.35}$$

To reduce the number of parameters in the system, we remove unnecessary degrees of freedom by replacing the dynamical variables with the non-dimensionalised quantities

$$\tilde{\alpha} = \frac{\alpha}{\alpha_0}, \quad \tilde{\beta} = \frac{\beta}{\beta_0}, \quad \text{and} \quad \tau = \frac{t}{t_0}.
 \tag{5.36}$$

Substituting this into (5.35) results in the coupled equations

$$\begin{aligned} i\frac{d\tilde{\alpha}}{d\tau} - \tilde{\alpha} &= 1 + c_1 2\tilde{\alpha}\tilde{\beta} \\ i\frac{d\tilde{\beta}}{d\tau} - c_2\tilde{\beta} &= c_1\tilde{\alpha}^2. \end{aligned} \quad (5.37)$$

The non-dimensionalised Hamiltonian is given by

$$\tilde{H} := \frac{H}{k_2^2/E_A} = |\tilde{\alpha}|^2 + c_2|\tilde{\beta}|^2 + c_1(\tilde{\alpha}\tilde{\alpha}\tilde{\beta} + c.c.) + (\tilde{\alpha} + c.c.), \quad (5.38)$$

with parameters

$$t_0 = \frac{1}{E_A}, \quad \alpha_0 = \frac{k_2}{E_A}, \quad c_1 = \frac{k_1 k_2}{E_M}, \quad c_2 = \frac{E_M}{E_A}. \quad (5.39)$$

The dynamics of the system is completely determined by the choice of the two parameters $c_1, c_2 \in \mathbb{R}$ and its initial conditions. Note that due to our choice of parameters $c_1 = 0$ implies $k_1 = 0$, i.e. no molecule formation, and arbitrary k_2 . Moreover, the constraint stemming from the validity of the mean field approximation can now be precisely expressed as $c_1 \ll 1$, where the constraint on the molecular reaction constant becomes $k_1 \ll \frac{E_M}{k_2}$.

5.3.1 Perturbation theory

The dynamical system (5.37) is, due to the non-linear terms, too difficult to be solved analytically. In such situations, perturbation theory often provides useful analytical approximations of the full solution. However, a naive application of perturbation theory may lead to qualitatively wrong results [Hin91]. Therefore, we first need some physical intuition of the considered chemical system. To this end, we examine again the structure of the non-dimensionalised equations of motion (5.37)

$$\begin{aligned} i\frac{d\tilde{\alpha}}{d\tau} - \tilde{\alpha} &= 1 + c_1 2\tilde{\alpha}\tilde{\beta} \\ i\frac{d\tilde{\beta}}{d\tau} - c_2\tilde{\beta} &= c_1\tilde{\alpha}^2. \end{aligned} \quad (5.40)$$

What is the physical meaning of the two parameters c_1 and c_2 ? The ODE system (5.40) is equivalent to a pair of non-linearly coupled harmonic oscillators. Whereas the oscillator describing the atoms has eigenfrequency one, c_2 determines the eigenfrequency of the molecular oscillator. We see that c_1 is the coupling strength between the two oscillators and represents the only non-linear term in the system. We therefore expect a regular behaviour for small values of c_1 . Moreover, we see from

(5.38) that if $c_1 \gg 1$ the system is also integrable due to the conservation of the overall particle number $N_{tot} = |\tilde{\alpha}|^2 + 2|\tilde{\beta}|^2$. Altogether, we decide to employ perturbation theory for anharmonic oscillators by expanding the functions in terms of c_1 , and fix c_2 to an experimentally realistic value. The method we use is called the Poincaré-Lindsted method [Lin82]. It dates back to the time when physicists tried to find approximations to the exact trajectory of the moon. Let us first expand the quantities considered into a perturbation series. This means expanding dynamical quantities in (5.40) as

$$\begin{aligned}\tilde{\alpha}(\tau) &= \tilde{\alpha}_0(\tau) + c_1\tilde{\alpha}_1(\tau) + c_1^2\tilde{\alpha}_2(\tau) + \dots \\ \tilde{\beta}(\tau) &= \tilde{\beta}_0(\tau) + c_1\tilde{\beta}_1(\tau) + c_1^2\tilde{\beta}_2(\tau) + \dots\end{aligned}\quad (5.41)$$

The Poincaré-Lindsted method modifies this expansion by rescaling the argument τ of each dynamical quantity differently, that is, we evaluate

$$\begin{aligned}\tilde{\alpha}(\phi_1 = \omega_1\tau) \quad \text{and} \\ \tilde{\beta}(\phi_2 = \omega_2\tau),\end{aligned}\quad (5.42)$$

yielding the system

$$\begin{aligned}i\omega_1 \frac{d\tilde{\alpha}(\phi_1)}{d\phi_1} - \tilde{\alpha}(\phi_1) &= 1 + c_1 2\overline{\tilde{\alpha}(\phi_1)}\tilde{\beta}(\phi_2) \\ i\omega_2 \frac{d\tilde{\beta}(\phi_2)}{d\phi_2} - c_2\tilde{\beta}(\phi_2) &= c_1\tilde{\alpha}(\phi_1)^2.\end{aligned}\quad (5.43)$$

The key of the method is now to not only expand the dynamical quantities but also expand the frequencies as perturbed quantities

$$\begin{aligned}\omega_1 &= \omega_1^{(0)} + c_1\omega_1^{(1)} + c_1^2\omega_1^{(2)} + \dots \\ \omega_2 &= \omega_2^{(0)} + c_1\omega_2^{(1)} + c_1^2\omega_2^{(2)} + \dots\end{aligned}\quad (5.44)$$

This additional degree of freedom compared to the regular perturbation ansatz is used to remove secular terms from the perturbational solution. Before we proceed to discuss the terms of perturbation expansion, we simplify ansatz (5.44) by coupling the frequencies as

$$\omega_2 = c_2\omega_1.\quad (5.45)$$

This coupling is justified if we consider the solution of the unperturbed system, where we find $\omega_1^{(0)} = 1$ and $\omega_2^{(0)} = c_2$. Substituting (5.45) into (5.44) and expanding the frequencies and dynamical quantities into the perturbation series yields at zeroth-

order the system

$$\begin{aligned} i \frac{d\tilde{\alpha}_0(\phi_1)}{d\phi_1} - \tilde{\alpha}_0 &= 1 \\ ic_2 \frac{d\tilde{\beta}_0(\phi_2)}{d\phi_2} - c_2 \tilde{\beta}_0 &= 0. \end{aligned} \quad (5.46)$$

This system is the unperturbed system, having only a constant shift as an inhomogeneous part. It is solved by

$$\begin{aligned} \alpha_0(\phi_1) &= (1 + A_0)e^{i\phi_1} - 1 \\ \beta_0(\phi_2) &= B_0e^{i\phi_2}. \end{aligned} \quad (5.47)$$

Using this solution of the zeroth-order terms, first-order perturbation theory yields

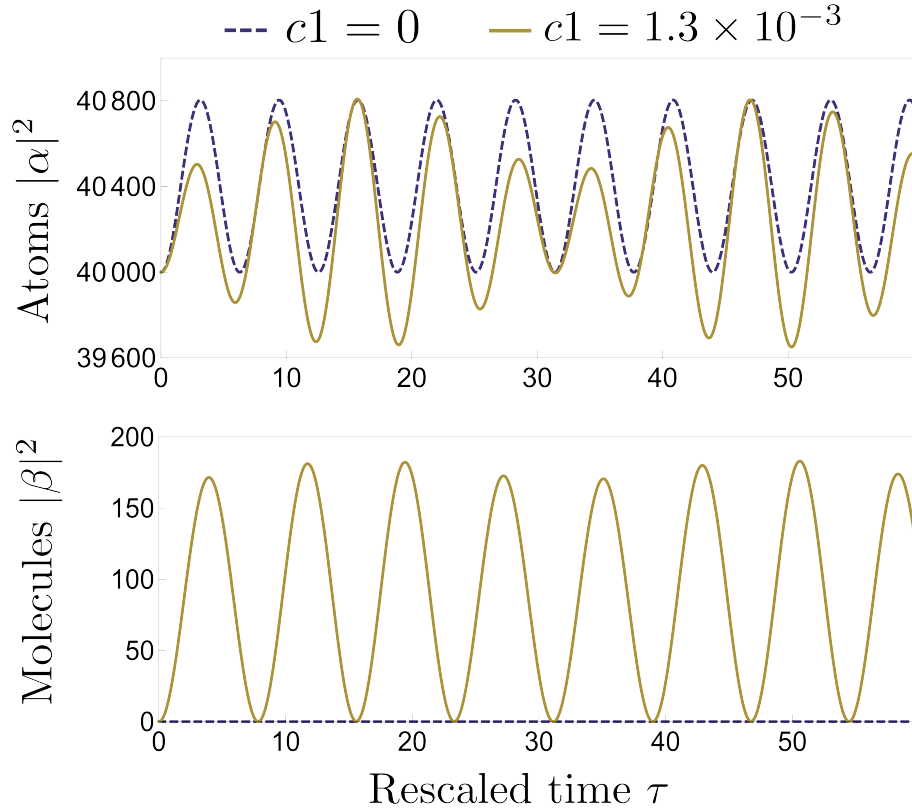


Figure 5.5: Time evolution of the rescaled average number of atoms and molecules in mean field approximation. The relative energy of the ground states is $c_2 = 1.1$ and the initial number of atoms is 40000. The oscillation becomes more and more strongly modulated with increasing molecule formation c_1 . Perturbation theory determines an amplitude $A_{mod} \approx 320$ atoms for $c_1 = 13 \times 10^{-5}$ (see (5.49)).

the equations

$$\begin{aligned} i \frac{d\tilde{\alpha}_1(\phi_1)}{d\phi_1} - \tilde{\alpha}_0 &= -\omega_1(1 + A_0)e^{i\phi_1} + 2B_0e^{ic_2\phi_1} \\ ic_2 \frac{d\tilde{\beta}_1(\phi_2)}{d\phi_2} - c_2\tilde{\beta}_0 &= -1 + (1 + A_0)e^{i\frac{\phi_2}{c_2}} - \omega_1c_1B_0e^{-i\phi_2}. \end{aligned} \quad (5.48)$$

Considering the right-hand side of the equations, we can understand schematically the motivation for expanding the frequency into a perturbation series. The inhomogeneous terms that are oscillating with the eigenfrequency of the respective oscillators cause a resonance in the perturbative solution. This leads to a breakdown of perturbation theory in time even for small values of c_1 . Thanks to the freedom of choosing ω_1 , we can avoid the resonance in the terms on the right-hand side of (5.48). In the present system this is achieved by setting $\omega_1 = 0$. We content ourselves at this point by considering first-order perturbation theory. At higher order, the terms occurring become more complex and do not provide new insights regarding the application of the method. Let us in the following compare the result of the Poincaré-Lindstedt to numerical results.

The trajectories depicted in Figure 5.5 show the expectation value of atoms $|\tilde{\alpha}|^2$ and molecules $|\tilde{\beta}|^2$ for an initially depleted molecular mode and 40000 atoms. In case of no coupling at all, i.e. $c_1 = 0$, the molecular mode remains completely depleted whereas the atomic mode oscillates due to the coupling to the bath. However, as we increase c_1 the system progressively enters a *modulation regime*, in which the molecular site oscillates and the amplitude of the free oscillation on the atomic site is modulated. Let $A_0 = \tilde{\alpha}(0)$ denote the square root of the initial rescaled number of atoms, we then obtain from perturbation theory (5.48) the following analytical expressions for the amplitude A_{mod} and frequency ω_{mod} of this modulation:

$$\begin{aligned} A_{mod} &= \frac{4(A_0 + 1)A_0^3c_1^2}{(c_2 - 2)^2} + \mathcal{O}(c_1^4), \\ \omega_{mod} &= c_2 - 1 + \mathcal{O}(A_0^2c_1^2). \end{aligned} \quad (5.49)$$

This means increasing c_1 causes a quadratic increase of A_{mod} whereas the frequency of modulation ω_{mod} remains approximately unchanged. The restrictions on the parameters for perturbation theory to be valid are $c_1^2A_0^2 \ll 1 \ll A_0$ and $c_2 \in (1, 2)$.

5.3.2 Chaos

What happens to the system if we increase c_1 beyond the regime of perturbation theory? We already mentioned that c_1 interpolates between integrable systems. But does the system remain integrable for all choices of c_1 ? Chaos in Hamiltonian systems is an interesting phenomenon which has been extensively studied in the context of

the validation of statistical mechanics. A well-known tool to characterize irregular behaviour of a system is to consider its Poincaré sections [Ott02]. In our case, we choose the quadratures of the atomic species

$$\begin{aligned} X_A &= \frac{1}{2}(\alpha + \bar{\alpha}) \\ P_A &= \frac{1}{2i}(\alpha - \bar{\alpha}), \end{aligned} \tag{5.50}$$

and the quadratures of the molecular species

$$\begin{aligned} X_M &= \frac{1}{2}(\beta + \bar{\beta}) \\ P_M &= \frac{1}{2i}(\beta - \bar{\beta}) \end{aligned} \tag{5.51}$$

as dynamical variables. We choose the surface $X_M = 0$ as the intersection surface. Poincaré sections with X_A and P_A on the (x,y)-axes are shown from Fig. 5.6 to Fig. 5.11. We set $c_2 = 1.1$ and the energy $E = 100$. Note that in contrast to usual Poincaré sections in the literature, we plotted P_M on the z-axis to get an better impression of the projected energy hypersurface. The sections are plotted for 25 long-time trajectories with arbitrary initial conditions. We find that, for a certain range of c_1 , the system shows behaviour which is typical for Hamiltonian chaos. As long as the system remains integrable, the Poincaré section consists of closed curves corresponding to sections of two-dimensional tori. However, increasing c_1 deforms and finally destroys some of the closed curves. Some of the sampled trajectories start to densely fill out parts of the energy hypersurface. We call this the *chaotic regime* of the reaction. Finally, further increase of c_1 leads to deformation of the energy hypersurface and eventually restores the integrability of the system.

To summarise, we have seen that chaos plays an important role in the mean-field approximation of ultracold chemical reactions. In contrast to classical reactions, where one needs a very complex multi-species reaction to obtain dynamical chaos, the ultracold reaction (5.33) consists of two concurrent reactions, where one is a simple coupling to a reservoir. This looks a promising route to follow from experimental point of view. The diatomic molecule formation could be implemented by Raman photoassociation, whereas the coupling to a bath coupling to a reservoir could be realised by coherent interaction to a second BEC, containing much more particles than the molecule forming BEC.

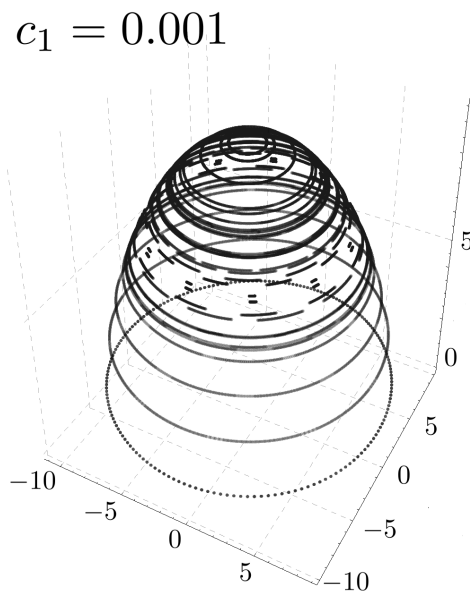


Figure 5.6: Poincaré section of the mean-field approximation of the reaction network (5.33) for parameter $c = 0.001$. For this small perturbation the system remains integrable, which is consistent with the observation of perturbation theory.

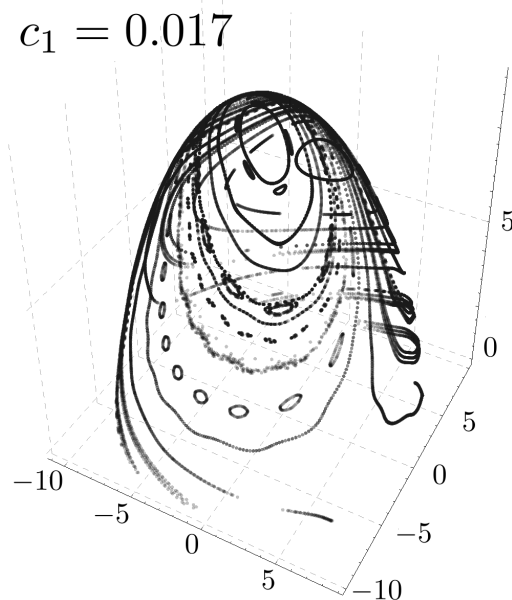


Figure 5.7: Poincaré section with $c_1 = 0.017$. The increase of the perturbation leads to splitting of the first orbits into little islands in accordance with the predictions of the Poincaré-Birkhoff theorem [Poi12]

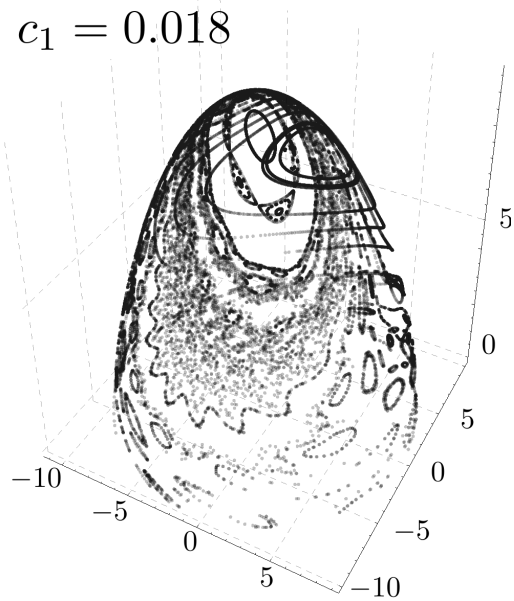


Figure 5.8: Poincaré section of the mean-field approximation of the reaction network (5.33) for parameter $c_1 = 0.018$. The irregular trajectories begin to spread out and densely fill out the energy hypersurface

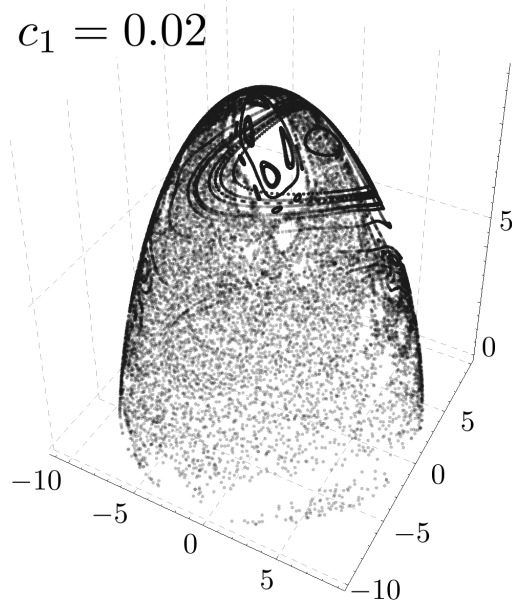


Figure 5.9: Poincaré section with $c_1 = 0.02$. Most of the energy hypersurface is covered by irregular trajectories.

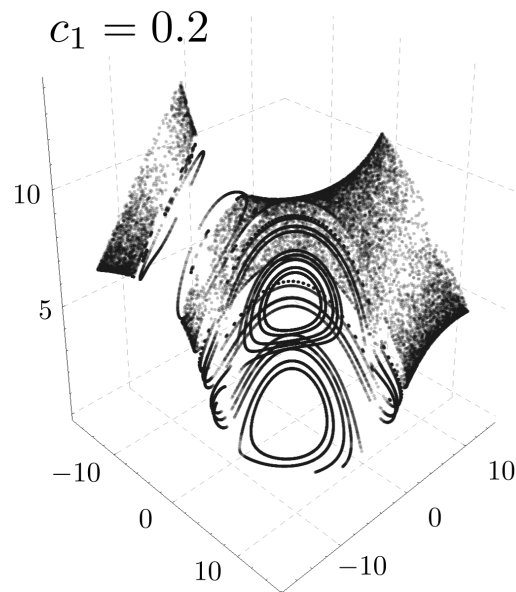


Figure 5.10: Poincaré section with $c_1 = 0.2$. The energy hypersurface shows a significant deformation.

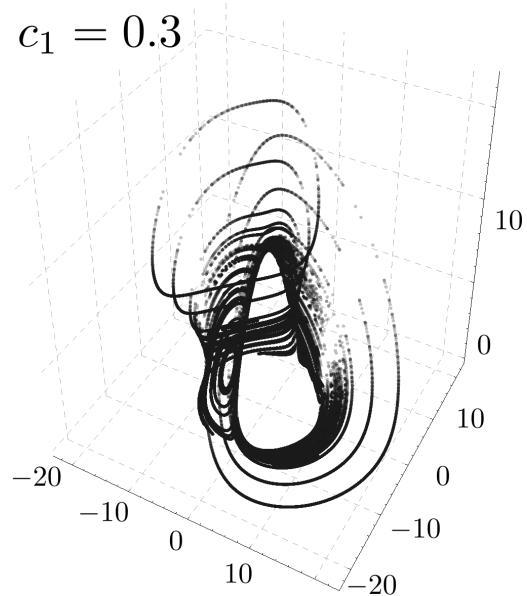


Figure 5.11: Poincaré section with $c_1 = 0.3$. All of the plotted trajectories are on closed curves. Therefore, the system is eventually integrable again.

CHAPTER 6

Solitons in ultracold chemistry

Solitons are wave-like solutions to non-linear equations which appear in many areas of physics. They fascinate scientists since their discovery in the middle of the 19th century, not only for their remarkable experimental properties, but also for new insights that they provide to physical systems. In the context of ultracold atoms, solitons were first observed in Sodium BECs [Bur99; Den00]. This observation was a remarkable confirmation for the non-linear model of a self-interacting Bose gas. Moreover, solitary solutions are a central theoretical aspect in coupled atomic-molecular Bose-Einstein condensates [Das13; Dru98; Ole07; Vau04]. However, the experimental proof of the predicted solitons is, to the best knowledge of the author, still missing.

In addition to the field of ultracold atoms, solitary solutions have been extensively studied in the realm of reaction-diffusion models [Pur05]. Reaction-diffusion models combine classical reaction kinetics and the theory of diffusion to describe the time-evolution of a spatially inhomogeneous classical chemical reaction. Motivated by the resemblance we observed between the ultracold reactions and high-temperature reactions so far, we study if the solitary solutions in reaction-diffusion systems carry over into the ultracold setting.

This chapter is organised as follows: In section 6.1 we study solitary solutions to the Gross-Pitaevskii equation. This equation describes the mean-field approximation of a self-interacting Bose gas. We introduce phase space methods as central tool to show the existence of solitons. The material presented in section 6.1 is well known and can be found in many textbooks. We follow here in particular [Dau06]. In section 6.2, we apply phase space methods to the diatomic molecule formation. We discuss the stability of bright solitons in this reaction.

6.1 Gross-Pitaevskii equation

The phenomenon of Bose-Einstein condensation can be explained by considering an ideal non-interacting Bose gas. However, for any temperature that is not exactly

zero there will be an atom-atom interaction inside a condensate. As we discussed in section 3.2, a natural approach to formulate interactions inside a condensate of indistinguishable particles is to use the formalism of second quantisation. A general Hamiltonian with self-interaction is given by

$$\hat{H} = \int dx \hat{\psi}^\dagger(x) \left(\hat{T} + V_{\text{ext}}(x) \right) \hat{\psi}(x) + \int dx dy \hat{\psi}^\dagger(x) \hat{\psi}^\dagger(y) V(x,y) \hat{\psi}(x) \hat{\psi}(y), \quad (6.1)$$

where $V(x,y)$ denotes the two-body interaction potential. All prominent examples of two-body interactions are translationally invariant, that is $V(x,y) = V(x-y)$. The resulting scattering problem can be solved in the center-of-mass frame (see section 2.2.2). If the potential in relative coordinates decays faster than r^{-3} , the s-wave scattering contribution becomes dominant for bosons at small temperatures [Dau02]. Additionally, for most potentials the s-wave scattering amplitude (2.46) converges for small momenta towards a constant value

$$\lim_{k \rightarrow 0} f_{n',n}(\vec{r}, \vec{k}) = -a, \quad (6.2)$$

which is called the scattering length. The exact calculation of a depends on the parameters of the problem. As a result of this dependence it is possible, for example by crossing a Feshbach resonance, to tune the scattering length from a large and positive value, meaning strong repulsive interaction, to a large negative value resulting in strong attractive interaction. Using the fact that in case of low-energy scattering two potentials with the same scattering length lead to the same physics, we replace $V(x,y)$ by a contact potential

$$W(x-y) \rightarrow g\delta(x-y) \quad (6.3)$$

with effective interaction constant $g = \frac{4\pi a}{m}$. Substituting this into (6.1) yields

$$\hat{H} = \int dx \hat{\psi}^\dagger(x) \left(\hat{T} + V_{\text{ext}}(x) \right) \hat{\psi}(x) + \frac{g}{2} \int dx \hat{\psi}^\dagger(x) \hat{\psi}^\dagger(x) \hat{\psi}(x) \hat{\psi}(x). \quad (6.4)$$

Due to the high order of the self-interaction term, we can not hope to find an exact solution. Therefore we apply the variational method to decrease the difficulty of the problem.

6.1.1 Derivation as mean-field approximation

To this end, we try to find a suitable variational class. A natural generalisation of coherent states to infinitely many modes are the *field coherent states*. They are

defined as eigenfunctions of the field operator

$$\hat{\psi}(x) |\phi(x,t)\rangle = \phi(x,t) |\phi(x,t)\rangle. \quad (6.5)$$

Note, that in contrast to the optical coherent states, which are labelled by a complex number $\alpha(t)$, we have

$$\phi : \mathbb{R}^2 \mapsto \mathbb{C}, \quad (6.6)$$

that is a classical field. Alternatively, the states can be generated by the unitary displacement operator

$$D(\hat{\psi}, \phi) = e^{\int dx \phi(x,t) \hat{\psi}^\dagger(x) - \bar{\phi}(x,t) \hat{\psi}(x)}, \quad (6.7)$$

which displaces the vacuum to a field coherent state

$$|\phi(x,t)\rangle = D(\hat{\psi}, \phi) |0\rangle. \quad (6.8)$$

Using the field coherent states as variational class in (5.11) yields

$$\begin{aligned} L(\bar{\phi}(x,t), \phi(x,t), x, t) &= \frac{i}{2} \langle \phi(x,t) | \frac{\partial \phi(x,t)}{\partial t} \rangle - \frac{i}{2} \langle \frac{\partial \bar{\phi}(x,t)}{\partial t} | \phi(x,t) \rangle \\ &\quad - \langle \phi(x,t) | \hat{H}(t) | \phi(x,t) \rangle, \end{aligned} \quad (6.9)$$

with (6.4) as $\hat{H}(t)$. Performing calculations analogous to (5.14), we can rewrite the first two terms in terms of the classical field $\phi(x,t)$ as

$$\begin{aligned} L(\bar{\phi}(x,t), \phi(x,t), x, t) &= \frac{i}{2} \int dx \bar{\phi}(x,t) \frac{\partial \phi(x,t)}{\partial t} - \frac{i}{2} \int dx \frac{\partial \bar{\phi}(x,t)}{\partial t} \phi(x,t) \\ &\quad - \langle \phi(x,t) | \hat{H}(t) | \phi(x,t) \rangle. \end{aligned} \quad (6.10)$$

Let us now evaluate the expectation value of the Hamiltonian. To this end, we consider the potential, kinetic and interaction parts separately. Using the definition of the field coherent states as eigenvectors of the field operator (6.5), we obtain for the potential energy term

$$\langle \phi(x,t) | \int dx \hat{\psi}^\dagger(x) V_{\text{ext}}(x) \hat{\psi}(x) | \phi(x,t) \rangle = \int dx V_{\text{ext}}(x) |\phi(x,t)|^2. \quad (6.11)$$

For the kinetic energy term we use the fact that the field is contained in some finite volume. Therefore we obtain by partial integration

$$\begin{aligned} \langle \phi(x,t) | \int dx \hat{\psi}^\dagger(x) \frac{-1}{2m} \frac{\partial^2}{\partial x^2} \hat{\psi} | \phi(x,t) \rangle &= \frac{-1}{2m} \int dx \bar{\phi}(x,t) \frac{\partial^2 \phi(x,t)}{\partial x^2} \\ &= \frac{1}{2m} \int dx \frac{\partial \bar{\phi}(x,t)}{\partial x} \frac{\partial \phi(x,t)}{\partial x}. \end{aligned} \quad (6.12)$$

Finally, we evaluate the interaction term

$$\langle \phi(x,t) | \frac{g}{2} \int dx \hat{\psi}^\dagger(x) \hat{\psi}^\dagger(x) \hat{\psi}(x) \hat{\psi}(x) | \phi(x,t) \rangle = \frac{g}{2} \int dx |\phi(x,t)|^4. \quad (6.13)$$

This amounts to an overall Lagrangian

$$\begin{aligned} L(\bar{\phi}(x,t), \phi(x,t), x, t) &= \int dx \left(\frac{i}{2} \bar{\phi}(x,t) \frac{\partial \phi(x,t)}{\partial t} - \frac{i}{2} \frac{\partial \bar{\phi}(x,t)}{\partial t} \phi(x,t) \right. \\ &\quad \left. - \frac{1}{2m} \frac{\partial \bar{\phi}(x,t)}{\partial x} \frac{\partial \phi(x,t)}{\partial x} - V_{\text{ext}}(x) |\phi(x,t)|^2 - \frac{g}{2} \int dx |\phi(x,t)|^4 \right). \end{aligned} \quad (6.14)$$

Note that this Lagrangian is of the form $L = \int dx \mathcal{L}$, where \mathcal{L} is called Lagrangian density. The corresponding Euler-Lagrange equations are in this case [Gol65]

$$\frac{d}{dt} \frac{\partial \mathcal{L}}{\partial [\partial_t \bar{\phi}]} + \frac{d}{dx} \frac{\partial \mathcal{L}}{\partial [\partial_x \bar{\phi}]} = \frac{\partial \mathcal{L}}{\partial \bar{\phi}}, \quad (6.15)$$

and its complex conjugate. Evaluated with the Lagrangian density in (6.14) we obtain the equations of motion for $\phi(x,t)$ as

$$i \frac{\partial}{\partial t} \phi(x,t) = \left(-\frac{1}{2m} \frac{\partial^2}{\partial x^2} + V_{\text{ext}}(x) + g |\phi(x,t)|^2 \right) \phi(x,t) \quad (6.16)$$

This equation is called the time-dependent Gross-Pitaevskii equation (GPE) [Gro61; Pit61]. We refer to (6.16) as mean-field approximation of (6.4) by the same reasoning as for coherent states of a single bosonic mode. Note, that similar to the single-mode case (5.17), the mean-field equations can be obtained via the simple replacement

$$\hat{\psi}(x) \rightarrow \psi(x) \quad \text{and} \quad \hat{\psi}^\dagger(x) \rightarrow \overline{\psi(x)}, \quad (6.17)$$

for a normal ordered Hamiltonian.

6.1.2 Bright and dark solitons

In what follows, we consider solutions to the GPE referred to as *bright* solitons. In a first step, we neglect the external potential term in (6.16). This is a valid assumption for real experimental implementations of BECs [Bur99]. Furthermore, we assume the coupling constant to be smaller than zero, that is, attractive interaction between the particles. With these assumption (6.16) can be rewritten as

$$i\frac{\partial}{\partial t}\phi(x,t) = \left(-\frac{1}{2m}\frac{\partial^2}{\partial x^2} - g|\phi(x,t)|^2\right)\phi(x,t) \quad \text{with } g > 0 \quad (6.18)$$

This equation is also known as *nonlinear Schrödinger equation* (NLSE). The denomination is due to obvious reasons: Equation (6.18) has exactly the form of the classical Schrödinger equation, where the 'potential' term is proportional to the squared of the wave function. The NLSE has a wide field of applications outside quantum optics. For example, it is used to model the evolution of the envelope of modulated water waves [Zak68]. It is exactly solvable by the use of the inverse scattering transform [Sha72]. Due to the fact that this analytical method is restricted to a very special class of equations, we like to follow another route to solve the NLSE. This method can be understood as instance of a *phase space method*.

To this end, we rewrite the complex NLSE in terms of the modulus and phase of the complex wave function

$$\phi(x,t) = R(x,t)e^{i\theta(x,t)}, \quad (6.19)$$

which are real functions. Substituting this into (6.18) and separating the real and imaginary part yields the coupled equations

$$\begin{aligned} -R\frac{\partial\theta}{\partial t} + \frac{1}{2m}\frac{\partial^2 R}{\partial x^2} - \frac{1}{2m}R\left(\frac{\partial\theta}{\partial x}\right)^2 + gR^3 &= 0 \\ \frac{\partial R}{\partial t} + \frac{1}{m}\frac{\partial\theta}{\partial x}\frac{\partial R}{\partial x} + \frac{1}{2m}\frac{\partial^2\theta}{\partial x^2}R &= 0 \end{aligned} \quad (6.20)$$

The next important step to reduce the complexity of the problem is to assume that phase and modulus are translationally invariant functions with respect to position and a scaled time. We introduce the variable $z_i = (x - u_i t)$ and write

$$\begin{aligned} R(x,t) &= R(x - u_R t) = R(z_R) \\ \theta(x,t) &= \theta(x - u_\theta t) = \theta(z_\theta), \end{aligned} \quad (6.21)$$

where we emphasize that $u_R \neq u_\theta$. This assumption turns (6.20) into a coupled ODE

system

$$u_\theta R\theta' + \frac{1}{2m}R'' - \frac{1}{2m}(\theta')^2 R + gR^3 = 0 \quad (6.22)$$

$$-u_R R' + \frac{1}{m}\theta' R' + \frac{1}{2m}R\theta'' = 0, \quad (6.23)$$

where the dash denotes the derivative with respect to the inner variable. Multiplying (6.23) with R and subsequent integration results in

$$-\frac{u_R}{2}R^2 + \frac{1}{2m}R^2\theta' = C, \quad (6.24)$$

where C is an integration constant. Up to now we have not specified what kind of solutions we are looking for. We now make the further assumption that our solution should be spatially localized, that is

$$\lim_{|x| \rightarrow \infty} \phi(x,t) = \lim_{|x| \rightarrow \infty} \frac{\partial \phi(x,t)}{\partial x} = 0. \quad (6.25)$$

This restriction requires that C is zero. Therefore we can easily determine the phase function from (6.24) to be

$$\theta' = u_R m \quad (6.26)$$

Excluding constant solutions for θ and subsequent integration of this equation yields the expression

$$\theta(x,t) = u_R m(x - u_\theta t) + C', \quad (6.27)$$

where we can set $C' = 0$ due to the boundary conditions. Putting this solution into (6.22) yields

$$u_\theta u_R m R + \frac{1}{2m}R'' - \frac{m}{2}u_R^2 R + gR^3 = 0. \quad (6.28)$$

This is a second-order differential equation for the modulus of the wave function. The idea of the phase space method is to rewrite (6.28) as a first-order ODE system via the introduction of the variables $x_1 = R$ and $x_2 = R'$

$$\begin{aligned} x_1' &= x_2 \\ x_2' &= -2mgx_1^3 + m^2(u_R^2 - 2u_\theta u_R)x_1 = -2mgx_1^3 + m^2\Delta_u x_1, \end{aligned} \quad (6.29)$$

where we defined $\Delta_u = u_R^2 - 2u_\theta u_R$. Solutions to this system can now be visualized

as trajectories in the phase space. Assuming the function to become stationary for $|x| \rightarrow \infty$, the fixed points in the phase space plot indicate the possible values the function can take for $|x| \rightarrow \infty$. Since we were interested in spatially localized solutions, we need to find a closed trajectory that starts at the origin. Figure 6.1 shows two examples of the phase space for different values of Δ_u with distinct sign. We see that in the case $\Delta_u > 0$ we find a closed curve starting at the origin. Indeed, this trajectory is a separatrix, that is, a curve which separates two different regimes of motion in phase space. This solutions corresponds to a soliton. Due to the simple form of the NLSE, we can give the exact form of the solution as

$$R(z) = \sqrt{\frac{mg}{\Delta_u}} \operatorname{sech}\left(\sqrt{m^2 \Delta_u} z\right). \quad (6.30)$$

This can be obtained via directly solving (6.28) by the ansatz $R(z) = A \operatorname{sech}(Bz)$. The overall wave function is then given by

$$\phi(x,t) = \sqrt{\frac{mg}{u_R^2 - 2u_\theta u_R}} \operatorname{sech}\left(\sqrt{m^2 (u_R^2 - 2u_\theta u_R)} (x - u_R t)\right) e^{iu_R m(x - u_\theta t)} \quad (6.31)$$

These sech-shaped solutions are referred to as *bright* solitons. However, we see from (6.30) that the solution is spatially localized if and only if $\Delta_u > 0$. To see what happens if Δ_u becomes smaller than zero, we consider again figure 6.1. We find that in this case the trajectory starting from the origin diverges to infinity, making it impossible to find spatially localized soliton solutions. Finally, we remark that if we choose the velocities u_R and u_θ to be equal, this results in $\Delta_u < 0$ and therefore corresponds to the case where no soliton solution exists. This a posteriori justifies ansatz (6.21).

Let us now proceed by looking for solutions with a constant but nonvanishing modulus at large distances. As we have seen in the previous calculations, such solutions to the NLSE do not exist in case of attractive interaction. Let us therefore revise the NLSE and assume repulsive interaction

$$i \frac{\partial}{\partial t} \phi(x,t) = \left(-\frac{1}{2m} \frac{\partial^2}{\partial x^2} + g |\phi(x,t)|^2 \right) \phi(x,t) \quad \text{with } g > 0. \quad (6.32)$$

Similar to the case of the attractive NLSE, we split the wave function into amplitude and phase

$$\phi(x,t) = R(x,t) e^{i\theta(x,t)}. \quad (6.33)$$

This time we have to choose a slightly modified ansatz for modulus and phase due

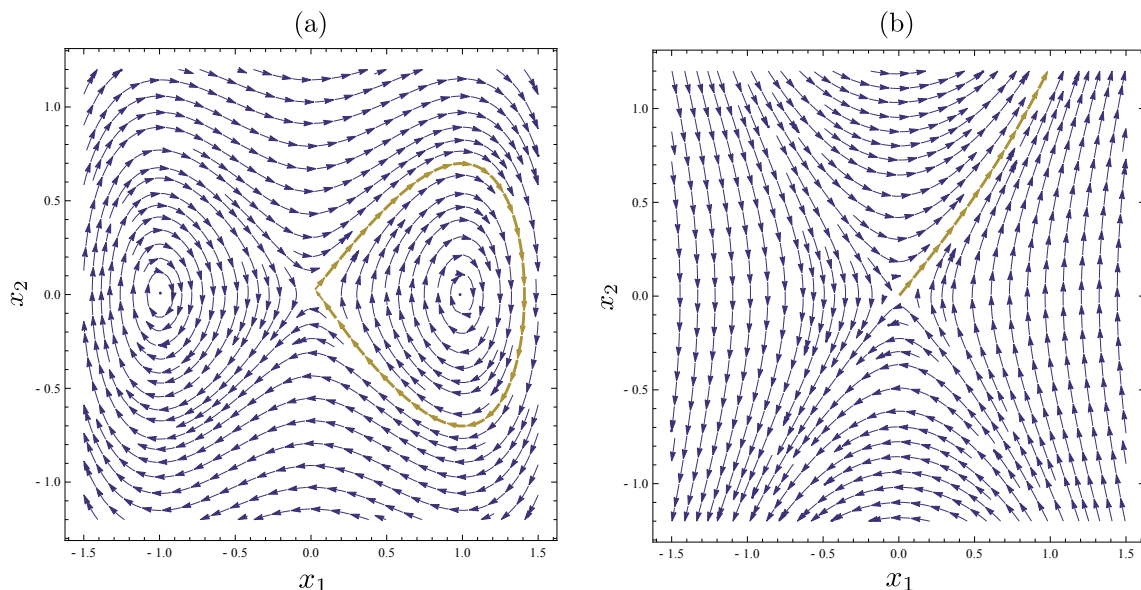


Figure 6.1: Two phase space plots of (6.29) for $\Delta_u = 1$ in (a) and $\Delta_u = -1$ in (b). The other parameters are equal and set to $(m = 1, g = \frac{1}{2})$. In the first case, the phase space is divided by a separatrix which starts and ends at the origin. This corresponds to a soliton. However, the topology of the phase space plot entirely changes for the second case. The divergence of the trajectories makes it impossible to find a spatially restricted solution.

to the nonvanishing amplitude at large distances,

$$\lim_{|x| \rightarrow \infty} R(x, t) = R_0 \quad \text{and} \quad \lim_{|x| \rightarrow \infty} \theta(x, t) = 0. \quad (6.34)$$

Using the previous approach of the attractive NLSE only admits the trivial solution $\psi(x, t) = 0$. We therefore extend (6.21) to

$$\begin{aligned} R(x, t) &= R(x - u_R t) \\ \theta(x, t) &= \alpha(x - u_\theta t) + \beta t. \end{aligned} \quad (6.35)$$

With this ansatz, the wave function becomes

$$\phi(x, t) = R_0 e^{i\beta t} \quad (6.36)$$

at the boundaries. Substituting (6.36) into the asymptotic form of (6.32) fixes the phase factor to

$$\beta = -gR_0^2 \quad (6.37)$$

for nontrivial solutions. Therefore the phase factor vanishes if we demand $R_0 = 0$ when $|x|$ goes to infinity, which is consistent with ansatz (6.21). Substituting (6.35) into (6.32) and separating real and imaginary parts leads to the coupled ODE system

$$Ru_\theta\alpha' + gR_0^2R + \frac{1}{2m}R'' - \frac{1}{2m}R(\alpha')^2 - R^3 = 0 \quad (6.38)$$

$$-u_RR' + \frac{1}{m}R'\alpha' + \frac{1}{2m}\alpha''R = 0. \quad (6.39)$$

Multiplication of (6.39) with $2R$ and subsequent integration yields

$$-u_RR^2 + \frac{1}{m}R^2\alpha' = C. \quad (6.40)$$

This can be solved for α' , yielding

$$\alpha' = \frac{Cm}{R^2} + u_Rm, \quad (6.41)$$

where C is a constant. Substituting this into (6.38) and introducing phase space coordinates $x_1 = R$ and $x_2 = R'$ yields the first-order system

$$\begin{aligned} x_1' &= x_2 \\ \frac{1}{2m}x_2' &= - \left(u_\theta m u_R + gR_0^2 - \frac{m}{2}u_R^2 \right) x_1 - ((u_\theta - u_r)mC) \frac{1}{x_1} \\ &\quad + \frac{m}{2}C^2 \frac{1}{x_1^3} + x_1^3. \end{aligned} \quad (6.42)$$

This system has various parameters involved. However, contrary to the case of the attracting NLSE, we can choose $v = u_\theta = u_R$ simplifying (6.42) to

$$\begin{aligned} x_1' &= x_2 \\ \frac{1}{2m}x_2' &= - \left(\frac{mv^2}{2} + gR_0^2 \right) x_1 + \frac{m}{2}C^2 \frac{1}{x_1^3} + x_1^3. \end{aligned} \quad (6.43)$$

The phase space plot is shown in Fig. 6.2. We see that the shape of soliton solutions depends sensitively on the choice of the integration constant C . The trajectory of the solitons for $C = 0$ crosses the x_2 -axis, which means that at some point the amplitude vanishes. However, for boundary conditions with $C \neq 0$ we find the class of grey solitons, as the modulus decreases but never vanishes. For the sake of completeness, we mention that system (6.43) can be solved analytically for a

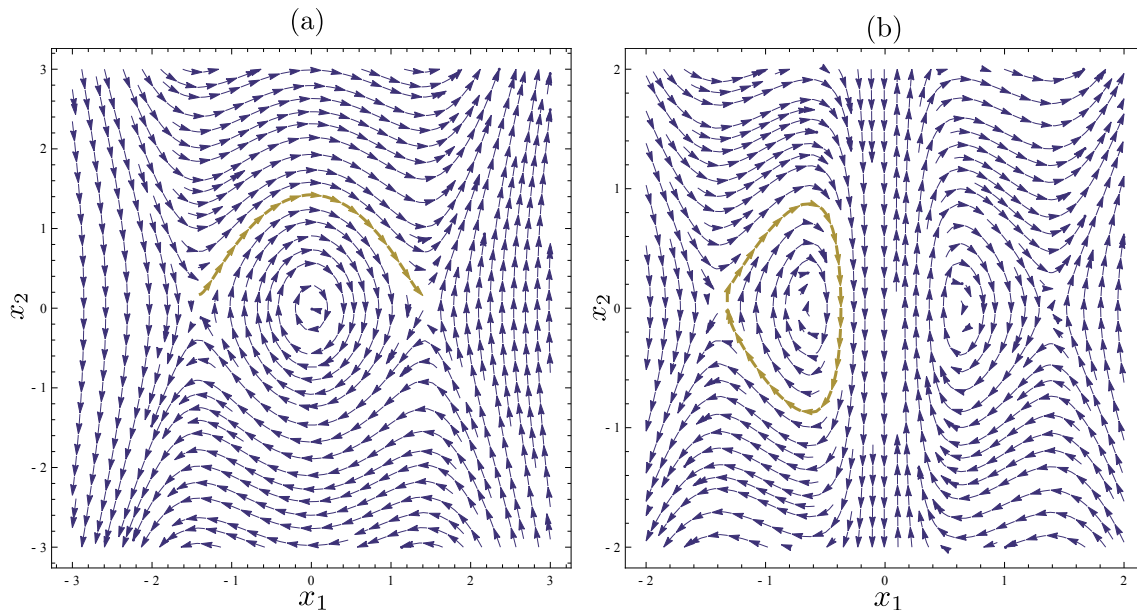


Figure 6.2: Two phase space plots of (6.43) for $C = 0$ in (a) and $C = \frac{1}{2}$ in (b). The other parameters are equal and set to ($R_0 = \sqrt{2}, m = 2, g = 1, v = 1$). The left plot shows the phase trajectory of a dark soliton with different starting and end point and therefore vanishing amplitude at some position. The right soliton, however, starts at the unstable fix point with negative x_1 value and returns to the start without crossing the line $x_1 = 0$. Due to the remaining amplitude at the turning point, these solutions are referred to as *grey* solitons.

vanishing velocity [Dau06]

$$\phi(x,t) = R_0 \tanh\left(R_0 \sqrt{2}x\right) e^{-2iR_0 t}. \quad (6.44)$$

To summarise, we have introduced phase space methods to identify soliton solutions to the attractive and repulsive GPE. Although the GPE is analytical solvable, we hope that the phase space method carries over to more complex systems arising from interacting quantum fields in ultracold chemical reactions.

6.2 Solitons in diatomic molecule formation

The possibility of soliton-like solutions to the chemical reaction of diatomic molecule formation was first considered in [Dru98]. Using a gaussian variational ansatz in three dimensions, the authors find a stable solution the coupled GPEs. In what follows, we consider soliton-like solutions for the diatomic molecule formation in one-dimension, using phase space methods. We a couple of bright solitons and argue that it is unstable against small perturbations.

Solitons are inherently phenomena of non-linear equations. Therefore, we begin to consider the lowest-order reaction with non-linear interaction term, that is the diatomic molecule formation



According to our proposal the describing Hamiltonian can be written as sum of an interacting part,

$$\hat{H}_{\text{int}} = k \int dx \left(\hat{\psi}_A(x) \hat{\psi}_A(x) \hat{\psi}_M^\dagger(x) + \hat{\psi}_A^\dagger(x) \hat{\psi}_A^\dagger(x) \hat{\psi}_M(x) \right), \quad (6.46)$$

and a non-interacting part,

$$\hat{H}_0 = \int dx \hat{\psi}_A(x) \frac{-1}{2m_A} \frac{\partial^2}{\partial x^2} \hat{\psi}_A^\dagger(x) + \hat{\psi}_M(x) \frac{-1}{4m_A} \frac{\partial^2}{\partial x^2} \hat{\psi}_M^\dagger(x). \quad (6.47)$$

Here we assumed that the mass of the diatomic molecule is twice the mass of the atom. For the sake of simplicity, we neglected the potential term in (6.47). In what follows, we consider the mean-field approximation of $\hat{H} = \hat{H}_0 + \hat{H}_{\text{int}}$, by replacing the operators with a classical field. The corresponding Euler-Lagrange equations result in the coupled partial differential equations

$$\begin{aligned} i \frac{\partial \psi_A}{\partial t} &= \frac{-1}{2m_A} \frac{\partial^2 \psi_A}{\partial x^2} + 2k \bar{\psi}_A \psi_M \\ i \frac{\partial \psi_M}{\partial t} &= \frac{-1}{4m_A} \frac{\partial^2 \psi_M}{\partial x^2} + k \psi_A^2, \end{aligned} \quad (6.48)$$

where we omitted the time and position dependence for a clearer notation. Furthermore, we introduce the dimensionless variable

$$\xi = x \sqrt{2m_A}. \quad (6.49)$$

In terms of this variable we can rewrite (6.48) as

$$\begin{aligned} i \frac{\partial \psi_A}{\partial t} &= -\frac{\partial^2 \psi_A}{\partial \xi^2} + 2k \bar{\psi}_A \psi_M \\ i \frac{\partial \psi_M}{\partial t} &= -\frac{1}{2} \frac{\partial^2 \psi_M}{\partial \xi^2} + k \psi_A^2. \end{aligned} \quad (6.50)$$

Note, that (6.50) is not a system of coupled NLSE, due to the absence of the self-interaction term. Nevertheless, due to the nonlinear coupling we are hopeful to find soliton solutions. Taking guidance from the treatment of the GPE, we look for

solutions of the form

$$\begin{aligned}\psi_A(x,t) &= f(\xi - \omega_M t) e^{i(\xi - \omega_P t)} \\ \psi_M(x,t) &= g(\xi - \omega_M t) e^{2i(\xi - \omega_P t)}.\end{aligned}\tag{6.51}$$

This particularly assumes that the phase of the molecular field rotates with twice the frequency of the atomic field. This idea is inspired by the quantum optic analogue of the diatomic molecule formation, namely the second harmonic generation. The molecular field corresponds to a laser field of double frequency. Substituting (6.51) into (6.50) yields the equations for modulus and amplitude of both fields

$$\begin{aligned}-i\omega_M f' + \omega_P f &= -\left[f'' + 2if' - f\right] + 2k\bar{f}g \\ -i\omega_M g' + 2\omega_P g &= -\frac{1}{2}\left[g'' + 4ig' - 4g\right] + kf^2\end{aligned}\tag{6.52}$$

Fixing $\omega_M = 2$ removes the terms proportional to i from (6.52). Therefore we can assume the amplitudes f and g to be real. Setting $\omega_P = 0$ and $k = -1$ results in the the following ODE-system:

$$f'' = f - 2fg\tag{6.53}$$

$$\frac{g''}{2} = 2g - f^2.\tag{6.54}$$

This coupled system of two second-order equations can be transformed to a four-dimensional state space, where we could apply phase space methods to look for soliton-like solutions. However, we follow a slightly different way. After rescaling the inner variable of g , we see that this coupled system can be understood as a particle moving in the two-dimensional potential

$$V(f,g) = -\frac{f^2}{2} - g^2 + f^2g.\tag{6.55}$$

This potential is depicted in Fig. 6.3. Due to the fact that a soliton becomes a stationary solution at the boundaries, we look for trajectories where the particle is initially and at the end of the motion at rest. Therefore, soliton-like solutions correspond in this picture to a bounded motion of the particle between extremal points. We see that this potential allows for solitary solutions: Starting with zero initial energy at the origin, the particle moves along the gradient of the potential. After passing a minimum, the particle reaches a turning point and rolls back to the origin. The corresponding solution is a pair of bright solitons. We can also see by the potential that the bright soliton solution is highly unstable. A small perturbation will cause the particle to drift away from the trajectory. The exact shape of the

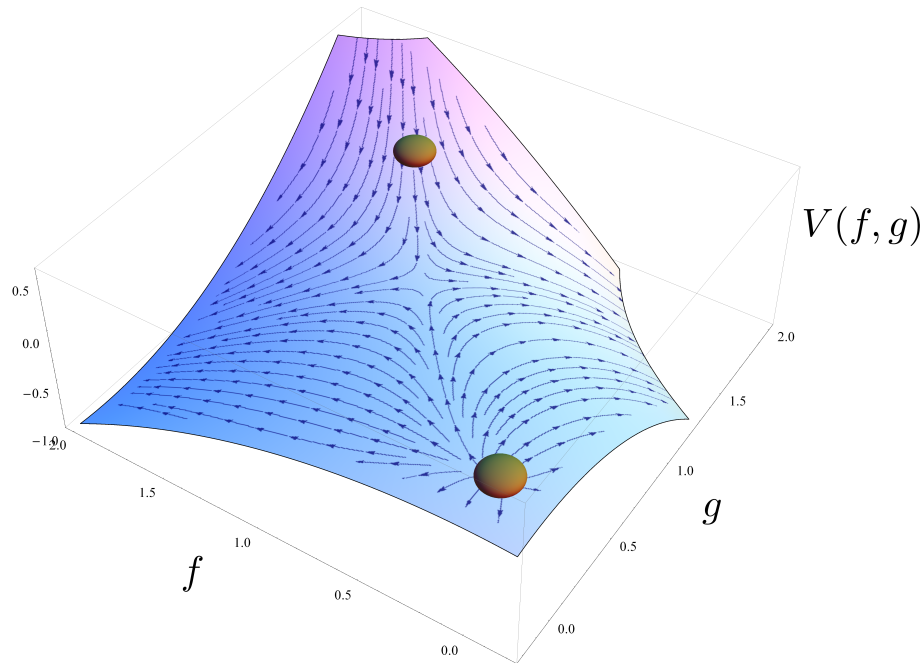


Figure 6.3: Landscape of the potential (6.55). Bright soliton solutions correspond to the particle moving between both points indicated by the spheres. Starting at the origin with zero potential energy the particle follows the gradient, passes a minimum and comes back to the starting point. Note, that the potential is indeed negative for all the range of the trajectory. Note that the soliton solution is highly unstable. A little perturbation will bring the particle away from the trajectory.

soliton couple can numerically be obtained and is depicted in Fig. 6.4. Since the potential is a smooth function of f and g a small change in the coupling strength will just shift the extrema of the potential a little and hence also have soliton solutions. This means that the diatomic molecule with the coupling strength as parameter has a whole class of bright soliton solutions. This class of solutions was found in the context of second harmonic generation in [Bur95]. However, the parameters in the system of second harmonic generation have a different physical meaning. Let us close the discussion with the remark that further research at this point is needed. An interesting question arises when we ask, how the diatomic molecule formation can be embedded into an ultracold reaction network, such that the bright solitons become a stable solution to the system. If we couple a certain class of reactions to the molecule formation, the equations resulting from the ansatz (6.51) can still be interpreted as the motion of a particle in a potential. For example, the reaction



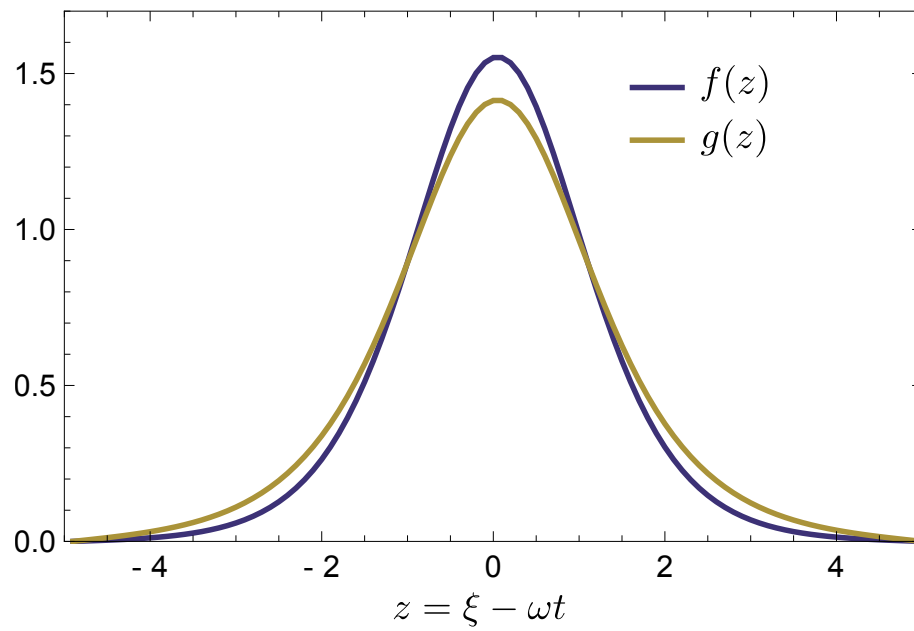


Figure 6.4: The exact shape of the bright soliton solution of the potential landscape depicted in Fig. 6.3. According to the starting and end point of the motion the function f and g vanish at the boundaries.

adds the linear term in $k_1 f$ in (6.55). ‘Stabilizing’ the soliton solution would correspond in this picture to constructing a potential shape that has different stability properties at its extrema.

CHAPTER 7

Conclusion and outlook

This thesis presented a framework for the description of the kinetics of ultracold chemical reactions. Inspired by the success in describing non-linear phenomena in ultracold gases, we formulate the framework in the language of second quantisation. The resulting dynamical equations are described by quantum field theories, which implies a classification of ultracold reactions into two groups. The first consists of reactions in which the interaction of the quantum fields is linear. These reactions allow for an analytical and compact form of solutions. The second class of reactions is described by non-linear interacting quantum fields such that the ensuing dynamics can only be obtained approximately. Using variational and perturbational methods, we systematically investigated the dynamics of ultracold chemical reactions and obtained the following results:

In chapter 4 we proved that within our framework, elementary bosonic reactions have a non-trivial constant of motion. This quantity can be thought of as quantum analogue of the classical principle of the conservation of mass. Moreover, we carried out a systematic analysis of bosonic low-order reactions. By employing standard techniques of quantum optics we obtained analytical expressions for the time-evolution of the particle number of each participating species. Comparing the results to the dynamics of classical low-order reactions allowed us to identify fundamental differences between these two frameworks. Whereas in classical low-order reactions a quantitative change in the reaction constant has no qualitative consequences to the reaction, the coupling strength in second-order ultracold reactions can change the dynamical regime.

In chapter 5 we studied the simplest non-trivial example of a reaction that amounts to an interacting field theory: the diatomic molecule formation. After discussing the validity of the two-mode model of this reaction, we found that the mean-field approximation predicts a complete depletion of the atomic mode. However, by numerical investigation of the full quantum dynamics, we found that entanglement between the molecular and atomic mode plays a major role in the formation of

ultracold molecules. The large amount of entanglement in the system causes a breakdown of the mean-field prediction and a relaxation of the atoms and molecules to a stationary state. The relative fluctuations around the stationary state are found to become smaller with increasing particle number. Extending the system by a coupling of the atoms to a particle reservoir changed the mean-field dynamics drastically. If the coupling strength increases beyond a certain threshold, the system evolves chaotically in phase space.

In chapter 6 we investigated soliton-like solutions to the mean-field approximation of diatomic molecule formation. By adapting an ansatz from second harmonic generation, we were able to describe solutions of the coupled mean-field equations as motion of a particle in a two dimensional potential. Using this method provided us with a way to characterise the stability of the emerging solitons.

We conclude with a list of possible next steps for future research:

- Although we compared the dynamics of high-temperature kinetics to our proposed framework, it is not clear how exactly classical kinetics appears as classical limit of our theory. A first step towards the dissipative dynamics of classical kinetics could be the incorporation of particle loss into our framework. This could be modelled, for example, by giving up condition (3.75) on the reaction constants. This would result in a non-hermitian Hamiltonian similar to the introduction of a complex valued potential in standard quantum mechanics. Subsequent application of the mean-field approximation may result in equations of motion that are similar to classical kinetics.
- Within this thesis we focused on the dynamics of chemical reactions of bosonic species. However, we expect fundamentally different behaviour for fermionic or mixed systems, which play an important role in the context of experimental implementations. Since these reactions can already be described by our framework, the extension of the analysis should be straightforward.
- The important role of entanglement in the dynamical evolution of two-mode model of molecule formation shows that entanglement may also play a major role in the formation of solitons. Therefore, employing matrix-product states as variational manifold for the interacting field Hamiltonian should provide new insights. A numerical simulator which uses matrix-product states as variational class and which is able to capture a spatially discretised model of diatomic molecule formation can be found in [Mil13].
- The coupling of the atomic species within the diatomic molecule formation to a larger particle reservoir discussed in 5.3 has, to the best of the authors knowledge, never been experimentally realised. An actual experimental proposal to measure the predicted modulations of the particle number or even the chaotic regime would be the next natural step.

Bibliography

- [Arr89] Arrhenius, S.: *Über die Dissociationswärme und den Einfluss der Temperatur auf den Dissociationsgrad der Elektrolyte*. Wilhelm Engelmann, 1889.
- [Bae15] Baez, J. C. and B. Fong: ‘[Quantum techniques for studying equilibrium in reaction networks](#)’. *Journal of Complex Networks* (2015), vol. 3(1): pp. 22–34.
- [Bag87] Bagnato, V., D. E. Pritchard, and D. Kleppner: ‘[Bose–Einstein condensation in an external potential](#)’. *Phys. Rev. A* (10 1987), vol. 35: pp. 4354–4358.
- [Bar57] Bardeen, J., L. N. Cooper, and J. R. Schrieffer: ‘[Theory of Superconductivity](#)’. *Phys. Rev.* (5 1957), vol. 108: pp. 1175–1204.
- [Bel59] Belousov, B. P.: ‘A periodic reaction and its mechanism’. *Ref. Radiats. Med.* (1959), vol. 1958: p. 145.
- [Bog47] Bogolyubov, N.: ‘On the theory of superfluidity’. *J.Phys.(USSR)* (1947), vol. 11: pp. 23–32.
- [Bro10] Brouard, M. and C. Vallance, eds.: *Tutorials in molecular reaction dynamics*. Royal Society of Chemistry, 2010.
- [Bur99] Burger, S., K. Bongs, S. Dettmer, W. Ertmer, K. Sengstock, A. Sanpera, G. V. Shlyapnikov, and M. Lewenstein: ‘[Dark Solitons in Bose–Einstein Condensates](#)’. *Phys. Rev. Lett.* (25 1999), vol. 83: pp. 5198–5201.
- [Bur70] Burnham, D. C. and D. L. Weinberg: ‘[Observation of Simultaneity in Parametric Production of Optical Photon Pairs](#)’. *Phys. Rev. Lett.* (2 1970), vol. 25: pp. 84–87.
- [Bur95] Buryak, A. V. and Y. S. Kivshar: ‘[Solitons due to second harmonic generation](#)’. *Physics Letters A* (1995), vol. 197(5): pp. 407–412.
- [Con90] Connors, K. A.: *Chemical Kinetics: The Study of Reaction Rates in Solution*. John Wiley & Sons, 1990.

- [Cou66] Courant, R. and D. Hilbert: *Methods of mathematical physics*. Vol. 1. CUP Archive, 1966.
- [Cra08] Cramer, M., A. Flesch, I. P. McCulloch, U. Schollwöck, and J. Eisert: ‘Exploring Local Quantum Many-Body Relaxation by Atoms in Optical Superlattices’. *Phys. Rev. Lett.* (2008), vol. 101(6): p. 063001.
- [Das93] Das, A.: *Field theory: a path integral approach*. Vol. 52. World Scientific, 1993.
- [Das13] Dastidar, K. and D. Ray: ‘Generation of bright atomic and molecular solitons in hybrid atom-molecular Bose-Einstein condensates coupled through raman photoassociation’. *The European Physical Journal D* (2013), vol. 67(12), 249.
- [Dau06] Dauxois, T. and M. Peyrard: *Physics of solitons*. Cambridge University Press, 2006.
- [Dau02] Dauxois, T., S. Ruffo, E. Arimondo, and M. Wilkens: *Dynamics and thermodynamics of systems with long-range interactions: An introduction*. Springer, 2002: pp. 1–22.
- [Dav95] Davis, K. B., M. O. Mewes, M. R. Andrews, N. J. van Druten, D. S. Durfee, D. M. Kurn, and W. Ketterle: ‘Bose-Einstein Condensation in a Gas of Sodium Atoms’. *Phys. Rev. Lett.* (1995), vol. 75: pp. 3969–3973.
- [Den00] Denschlag, J., J. Simsarian, D. Feder, C. W. Clark, L. Collins, J. Cubizolles, L. Deng, E. Hagley, K. Helmerson, W. Reinhardt, et al.: ‘Generating solitons by phase engineering of a Bose-Einstein condensate’. *Science* (2000), vol. 287(5450): pp. 97–101.
- [Dir30] Dirac, P. A. M.: ‘Note on Exchange Phenomena in the Thomas Atom’. *Mathematical Proceedings of the Cambridge Philosophical Society* (03 1930), vol. 26: pp. 376–385.
- [Dir25] Dirac, P. A. M.: ‘The Fundamental Equations of Quantum Mechanics’. *Proceedings of the Royal Society of London A: Mathematical, Physical and Engineering Sciences* (1925), vol. 109(752): pp. 642–653.
- [Don02] Donley, E. A., N. R. Claussen, S. T. Thompson, and C. E. Wieman: ‘Atom-molecule coherence in a Bose-Einstein condensate’. *Nature* (2002), vol. 417(6888): pp. 529–533.
- [Dru98] Drummond, P. D., K. V. Kheruntsyan, and H. He: ‘Coherent Molecular Solitons in Bose-Einstein Condensates’. *Phys. Rev. Lett.* (15 1998), vol. 81: pp. 3055–3058.
- [Dru14] Drummond, P. D. and M. Hillery: *The quantum theory of nonlinear optics*. Cambridge University Press, 2014.

- [Eps96] Epstein, I. R. and K. Showalter: ‘[Nonlinear Chemical Dynamics: Oscillations, Patterns, and Chaos](#)’. *J. Phys. Chem.* (1996), vol. 100(31): pp. 13132–13147.
- [Ger05] Gerry, C. and P. Knight: *Introductory quantum optics*. Cambridge university press, 2005.
- [Gla63] Glauber, R. J.: ‘[Coherent and Incoherent States of the Radiation Field](#)’. *Phys. Rev.* (6 1963), vol. 131: pp. 2766–2788.
- [Gol65] Goldstein, H.: *Classical mechanics*. Pearson Education India, 1965.
- [Gór01] Góral, K., M. Gajda, and K. Rzażewski: ‘[Multimode Dynamics of a Coupled Ultracold Atomic–Molecular System](#)’. *Phys. Rev. Lett.* (8 2001), vol. 86: pp. 1397–1401.
- [Gra15] Graefe, E.-M., M. Graney, and A. Rush: *Semiclassical quantisation for a bosonic atom–molecule conversion system*. 2015. arXiv: [1505.03351 \[quant-ph\]](#).
- [Gro61] Gross, E.: ‘[Structure of a quantized vortex in boson systems](#)’. *Il Nuovo Cimento Series 10* (1961), vol. 20(3): pp. 454–477.
- [Gul64] Guldberg, C. M. and P. Waage: ‘[Studies concerning affinity](#)’. *CM Forhandlinger: Videnskabs-Selskabet i Christiania* (1864), vol. 35(1864): p. 1864.
- [Hae11] Haegeman, J.: ‘[Variational Renormalization Group methods for extended quantum systems](#)’. PhD thesis. Ghent University, 2011.
- [Hei00] Heinzen, D. J., R. Wynar, P. D. Drummond, and K. V. Kheruntsyan: ‘[Superchemistry: Dynamics of Coupled Atomic and Molecular Bose–Einstein Condensates](#)’. *Phys. Rev. Lett.* (22 2000), vol. 84: pp. 5029–5033.
- [Hil90] Hillery, M.: ‘[Photon number divergence in the quantum theory of n–photon down conversion](#)’. *Phys. Rev. A* (1990), vol. 42(1): pp. 498–502.
- [Hin91] Hinch, E. J.: *Perturbation methods*. Cambridge university press, 1991.
- [Hin03] Hines, A. P., R. H. McKenzie, and G. J. Milburn: ‘[Entanglement of two–mode Bose–Einstein condensates](#)’. *Phys. Rev. A* (2003), vol. 67(1): p. 013609.
- [Hop01] Hope, J. J. and M. K. Olsen: ‘[Quantum Superchemistry: Dynamical Quantum Effects in Coupled Atomic and Molecular Bose–Einstein Condensates](#)’. *Phys. Rev. Lett.* (15 2001), vol. 86: pp. 3220–3223.
- [Hu06] Hu, W. and G. C. Schatz: ‘[Theories of reactive scattering](#)’. *The Journal of chemical physics* (2006), vol. 125(13): p. 132301.
- [Hut10] Hutson, J. M.: ‘[Ultracold Chemistry](#)’. *Science* (2010), vol. 327(5967): pp. 788–789.

- [Jav99] Javanainen, J. and M. Mackie: ‘Coherent photoassociation of a Bose–Einstein condensate’. *Phys. Rev. A* (5 1999), vol. 59: R3186–R3189.
- [Jin11] Jing, H., Y.-j. Jiang, and Y.-g. Deng: ‘Quantum superchemistry of de Broglie waves: New wonderland at ultracold temperature’. *Frontiers of Physics in China* (2011), vol. 6: pp. 15–45.
- [Kam92] Kampen, N. G. van: *Stochastic processes in physics and chemistry*. Vol. 1. Elsevier, 1992.
- [Kos00] Kostrun, M., M. Mackie, R. Côté, and J. Javanainen: ‘Theory of coherent photoassociation of a Bose–Einstein condensate’. *Physical Review A* (2000), vol. 62(6): p. 063616.
- [Kra81] Kramer, P. and M. Saraceno: *Geometry of the Time–Dependent Variational Principle in Quantum Mechanics*. Springer–Verlag, 1981.
- [Kup68] Kuppermann, A. and E. F. Greene: ‘Chemical reaction cross sections and rate constants’. *Journal of Chemical Education* (1968), vol. 45(6): p. 361. eprint: <http://dx.doi.org/10.1021/ed045p361>.
- [Lan37] Landau, L. D.: ‘On the theory of phase transitions. I.’ *Zh. Eksp. Teor. Fiz.* (1937), vol. 11: p. 19.
- [Lie05] Lieb, E. H.: *The mathematics of the Bose gas and its condensation*. Vol. 34. Springer, 2005.
- [Lin82] Linstedt, A.: ‘Beitrag zur Integration der Differentialgleichungen der Störungstheorie, Abh. K’. *Akad. Wiss. st. Petersbourg* (1882), vol. 31.
- [Lou00] Loudon, R.: *The quantum theory of light*. Oxford university press, 2000.
- [Mar08] Mar-Sarao, R. and H. Moya-Cessa: ‘Optical realization of a quantum beam splitter’. *Opt. Lett.* (2008), vol. 33(17): pp. 1966–1968.
- [Mil13] Milsted, A., J. Haegeman, and T. J. Osborne: ‘Matrix product states and variational methods applied to critical quantum field theory’. *Phys. Rev. D* (8 Oct. 2013), vol. 88: p. 085030.
- [Moo02] Moore, M. G. and A. Vardi: ‘Bose–Enhanced Chemistry: Amplification of Selectivity in the Dissociation of Molecular Bose–Einstein Condensates’. *Phys. Rev. Lett.* (16 2002), vol. 88: p. 160402.
- [Neu29] Neumann, J.: ‘Beweis des Ergodensatzes und des H–Theorems in der neuen Mechanik’. *Z. Phys.* (1929), vol. 57(1–2): pp. 30–70.
- [Nic77] Nicolis, G., I. Prigogine, et al.: *Self–organization in nonequilibrium systems*. Vol. 191977. Wiley, New York, 1977.

- [Ole07] Oleś, B. and K. Sacha: ‘Solitons in coupled atomic–molecular Bose–Einstein condensates’. *Journal of Physics B: Atomic, Molecular and Optical Physics* (2007), vol. 40(6): p. 1103.
- [Oli04] Oliveira, F. D. de and M. Olsen: ‘Mean field dynamics of Bose–Einstein superchemistry’. *Optics communications* (2004), vol. 234(1): pp. 235–243.
- [Osb11] Osborne, T.: *The time-dependent variational principle in quantum mechanics*. 2011. URL: <https://tjoresearchnotes.wordpress.com/2011/05/05/the-variational-principle-in-quantum-mechanics-lecture-4/>.
- [Osp10] Ospelkaus, S., K.-K. Ni, D. Wang, M. H. G. de Miranda, B. Neyenhuis, G. Quéméner, P. S. Julienne, J. L. Bohn, D. S. Jin, and J. Ye: ‘Quantum–State Controlled Chemical Reactions of Ultracold Potassium–Rubidium Molecules’. *Science* (2010), vol. 327(5967): pp. 853–857.
- [Ott02] Ott, E.: *Chaos in dynamical systems*. Cambridge university press, 2002.
- [Pit61] Pitaevskii, L.: ‘Vortex lines in an imperfect Bose gas’. *Sov. Phys. JETP* (1961), vol. 13(2): pp. 451–454.
- [Poi12] Poincaré, H.: ‘Sur un théorème de géometrie’. *Rend. Circ. Mat. Palermo* (1912), vol. 33: pp. 375–407.
- [Pri68] Prigogine, I. and R. Lefever: ‘Symmetry Breaking Instabilities in Dissipative Systems. II’. *The Journal of Chemical Physics* (1968), vol. 48(4): pp. 1695–1700.
- [Pur05] Purwins, H.-G., H. Bödeker, and A. Liehr: ‘Dissipative solitons in reaction–diffusion systems’. *Dissipative solitons*. Springer, 2005: pp. 267–308.
- [Qué10] Quéméner, G. and J. L. Bohn: ‘Strong dependence of ultracold chemical rates on electric dipole moments’. *Phys. Rev. A* (2 2010), vol. 81: p. 022702.
- [Reg03] Regal, C. A., C. Ticknor, J. L. Bohn, and D. S. Jin: ‘Creation of ultracold molecules from a Fermi gas of atoms’. *Nature* (2003), vol. 424(6944): pp. 47–50.
- [Ric15] Richter, F., D. Becker, C. Bény, T. A. Schulze, S. Ospelkaus, and T. J. Osborne: ‘Ultracold chemistry and its reaction kinetics’. *New Journal of Physics* (2015), vol. 17(5): pp. 55005–55014.
- [Rig08] Rigol, M., V. Dunjko, and M. Olshanii: ‘Thermalization and its mechanism for generic isolated quantum systems’. *Nature* (2008), vol. 452(7189): pp. 854–858.
- [San06] Santos, G., A. Tonel, A. Foerster, and J. Links: ‘Classical and quantum dynamics of a model for atomic–molecular Bose–Einstein condensates’. *Phys. Rev. A* (2 2006), vol. 73: p. 023609.

- [Sch13] Schachenmayer, J., B. P. Lanyon, C. F. Roos, and A. J. Daley: ‘[Entanglement Growth in Quench Dynamics with Variable Range Interactions](#)’. *Phys. Rev. X* (3 2013), vol. 3: p. 031015.
- [Sch06] Schwabl, F.: *Statistical Mechanics*. Advanced Texts in Physics. Springer, 2006.
- [Sch05] Schwabl, F., R. Hilton, and A. Lahee: *Advanced quantum mechanics*. Springer Science & Business Media, 2005.
- [Sha72] Shabat, A. and V. Zakharov: ‘Exact theory of two-dimensional self-focusing and one-dimensional self-modulation of waves in nonlinear media’. *Soviet Physics JETP* (1972), vol. 34(1): p. 62.
- [Sre99] Srednicki, M.: ‘[The approach to thermal equilibrium in quantized chaotic systems](#)’. *J. Phys. A* (1999), vol. 32(7): p. 1163.
- [Upa07] Upadhyay, S. K.: *Chemical kinetics and reaction dynamics*. Springer Science & Business Media, 2007.
- [Var01a] Vardi, A. and J. R. Anglin: ‘[Bose–Einstein Condensates beyond Mean Field Theory: Quantum Backreaction as Decoherence](#)’. *Phys. Rev. Lett.* (4 2001), vol. 86: pp. 568–571.
- [Var01b] Vardi, A., V. A. Yurovsky, and J. R. Anglin: ‘[Quantum effects on the dynamics of a two-mode atom–molecule Bose–Einstein condensate](#)’. *Phys. Rev. A* (6 2001), vol. 64: p. 063611.
- [Vau04] Vaughan, T. G., K. V. Kheruntsyan, and P. D. Drummond: ‘[Three-dimensional solitons in coupled atomic–molecular Bose–Einstein condensates](#)’. *Phys. Rev. A* (6 2004), vol. 70: p. 063611.
- [Wal72] Walls, D. F. and C. T. Tindle: ‘Nonlinear quantum effects in optics’. *J. Phys. A: Gen. Phys.* (1972), vol. 5(4): p. 534.
- [Wal07] Walls, D. F. and G. J. Milburn: *Quantum optics*. Springer Science & Business Media, 2007.
- [Wan07] Wang, H. and S. Kais: ‘Quantum entanglement and electron correlation in molecular systems’. *Israel Journal of Chemistry* (2007), vol. 47(1): pp. 59–65.
- [Wig48] Wigner, E. P.: ‘[On the Behavior of Cross Sections Near Thresholds](#)’. *Phys. Rev.* (9 1948), vol. 73: pp. 1002–1009.
- [Wu86] Wu, L.-A., H. J. Kimble, J. L. Hall, and H. Wu: ‘[Generation of Squeezed States by Parametric Down Conversion](#)’. *Phys. Rev. Lett.* (20 1986), vol. 57: pp. 2520–2523.

-
- [Wyn00] Wynar, R., R. S. Freeland, D. J. Han, C. Ryu, and D. J. Heinzen: ‘[Molecules in a Bose–Einstein Condensate](#)’. *Science* (2000), vol. 287(5455): pp. 1016–1019.
- [Zak68] Zakharov, V.: ‘[Stability of periodic waves of finite amplitude on the surface of a deep fluid](#)’. *Journal of Applied Mechanics and Technical Physics* (1968), vol. 9(2): pp. 190–194.
- [Zha64] Zhabotinsky, A. M.: ‘Periodical oxidation of malonic acid in solution (a study of the Belousov reaction kinetics)’. *Biofizika* (1964), vol. 9: pp. 306–311.

Publications

Scientific publications

1. Ahlbrecht, A., F. Richter, and R. F. Werner: ‘[How long can it take for a quantum channel to forget everything?](#)’ *International Journal of Quantum Information* (2012), vol. 10(05): p. 1250057.
2. Bény, C. and F. Richter: *Algebraic approach to quantum theory: a finite-dimensional guide*. 2015. arXiv: [1505.03106 \[quant-ph\]](#).
3. Richter, F., D. Becker, C. Bény, T. A. Schulze, S. Ospelkaus, and T. J. Osborne: ‘[Ultracold chemistry and its reaction kinetics](#)’. *New Journal of Physics* (2015), vol. 17(5): pp. 55005–55014.

Curriculum Vitae

Personalien

Name Florian Richter
geboren am 02.05.1983 in Emden
verheiratet, deutsch

Schulbildung

2002 Abitur, Hölty-Gymnasium Wunstorf

Wehrdienst

07/02 - 04/03 2. Schnellbootgeschwader, Marinestützpunkt Rostock-Warnemünde

Studium

WS/03 - SS/11 Universität Hannover, Studium der Elektrotechnik
Thema der Diplomarbeit: 'Rauschmodellierung in elektronischen Oszillatoren unter Betrachtung kanonisch-dissipativer Systeme', durchgeführt am Institut für Theoretische Elektrotechnik

Oktober 2011 Abschluss: Diplom-Ingenieur

WS/05 - WS/10 Universität Hannover, Studium der Physik
Thema der Diplomarbeit: 'Finite Roots of Completely Depolarizing Channels', durchgeführt am Institut für Theoretische Physik

Oktober 2010 Abschluss: Diplom-Physiker

Promotion

11/2011 - heute Wissenschaftlicher Mitarbeiter am Institut für Theoretische Physik, Leibniz Universität Hannover

Acknowledgments

I would like to thank my supervisor Prof. Dr. Tobias J. Osborne for his help and guidance. Furthermore, I am grateful to my former office mate Cédric Bény with whom I had many fruitful discussions and exchange of ideas. I also wish to thank Prof. Dr. Silke Ospelkaus, who kindly agreed to review this thesis as second examiner.

Furthermore, I like to thank my collaborators Daniel Becker and Torben Schulze for many interesting discussions around ultracold atoms.

I was fortunate to spend a most enjoyable and productive period of time in the group of Prof. Reinhard Werner at the Institut für Theoretische Physik, Leibniz Universität Hannover. I extend my deepest gratitude to Reinhard and the entire group for their hospitality, generosity and kindness. In particular I like to thank Ashley Milsted, Christoph Stahl and Emil Schreiber for proofreading this thesis.

My final thanks go to my wife for her unwavering support.